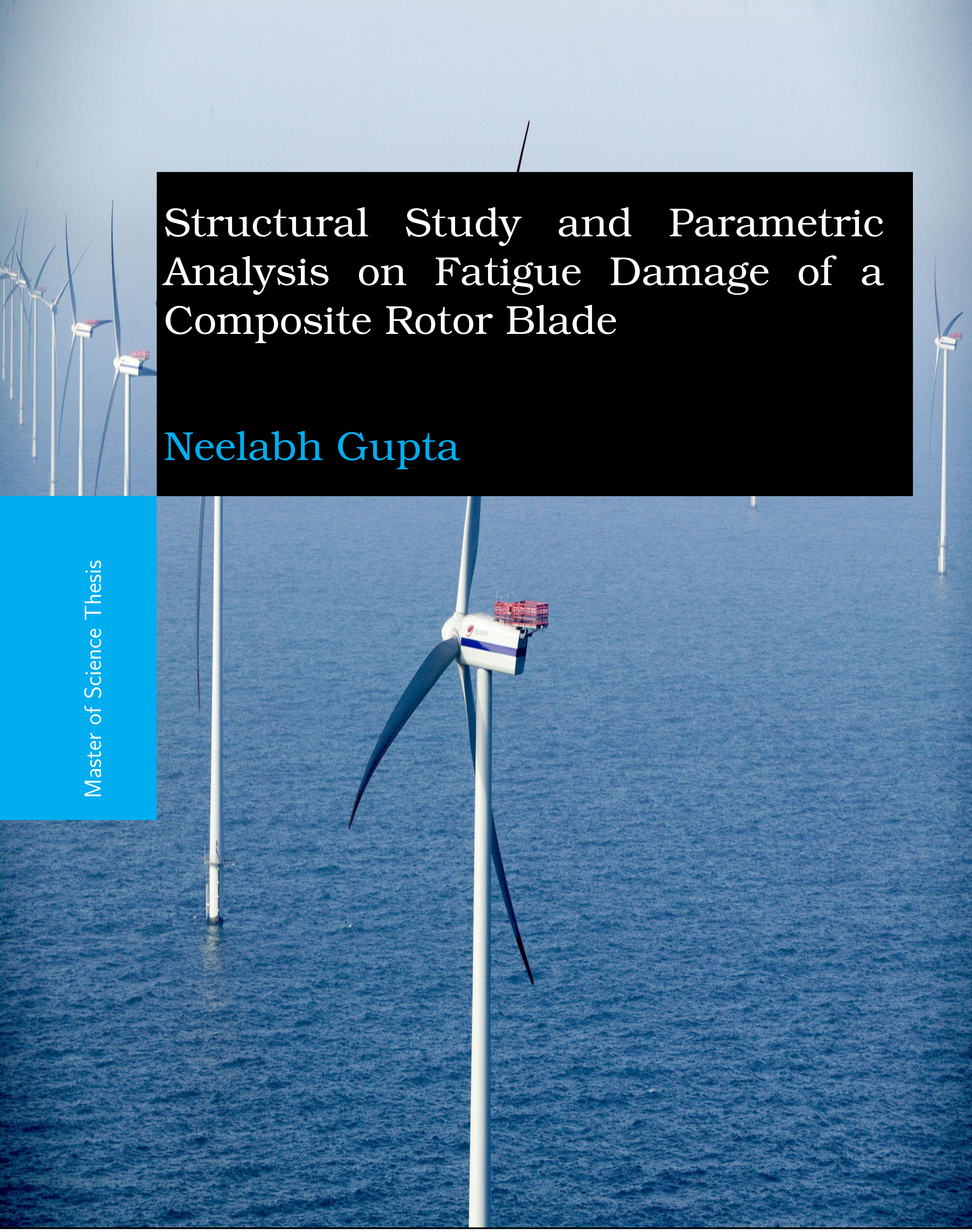

Structural Study and Parametric Analysis on Fatigue Damage of a Composite Rotor Blade

Neelabh Gupta

Master of Science Thesis

Fraunhofer IWES: Competence Center Rotor Blade
TU Delft: Mechanical Engineering

Structural Study and Parametric Analysis on Fatigue Damage of a Composite Rotor Blade

Master of Science Thesis

For the degree of Master of Science in Sustainable Process and Energy Technology at TU Delft

Neelabh Gupta

July 14, 2013

Faculty of Mechanical, Maritime and Materials Engineering (3mE) · Delft University of Technology

The work in this thesis was supported and supervised by department of Competence Center Rotor Blade: Courtesy of Fraunhofer Institute for Wind Energy and Energy System Technology (Fraunhofer IWES). Their cooperation is hereby gratefully acknowledged.

Delft University of Technology
Department of
Mechanical Engineering

The undersigned hereby certify that they have read and recommend to the Faculty of Mechanical, Maritime and Materials Engineering (3mE) for acceptance a thesis entitled

Structural Study and Parametric Analysis on Fatigue Damage of a Composite Rotor Blade

by

Neelabh Gupta

in partial fulfillment of the requirements for the degree of

Master of Science Sustainable Process and Energy Technology

Dated: July 14, 2013

Supervisor(s):

Dr.Ing. A. Antoniou

Prof.Dr.Ir. B. J. Boersma

Reader(s):

Ir. W. Bierbooms

Abstract

Fatigue damage calculations are conducted as state-of-art design process for wind turbines. Fatigue analysis is performed on spar caps and trailing edge tape (UD material) considering uni-axial stress state. The main objective of the research project is to analyze the effect of various parameters like yaw errors, wind turbine design load cases and blade mass imbalances on fatigue damage of blade. Also, an overall structural study of the blade has been performed based on the guidelines of International Electro-technical Commission (IEC) 61400-1 Ed. 3 to understand the structural robustness of blade in terms of stiffness and strength.

Loads based on an onshore site have been generated using aero-(servo)-elastic code, Fatigue Aerodynamics Structural and Turbulence (FAST). Based on these loads and predominantly linear Finite Element Model (FEM) calculations on a blade model in ANSYS (except for flapwise loading on spar caps), stress time series are calculated. Finally, using these stress time series, the fatigue damage at different blade sections are calculated in 'Octave' environment using rain-flow cycle counting method and Miner's rule.

Results show that blade is stiff enough from blade-tower interference and resonance perspective, but buckling is observed in the trailing edge close to the tip, with flapwise buckling mode coming out as the most critical one. Fatigue is not a structural issue based on state-of-art calculations and design load cases, even in the critical transition region (from circular to DU airfoil along the span of the blade). It was found that positive yaw errors are more detrimental to fatigue life than negative ones for an anti-clockwise rotating turbine. Trailing edge tape is more affected by blade mass imbalance while spar caps are sensitive to changes in yaw errors in terms of fatigue life. Power production design load case is completely dominating fatigue life when compared to start up and shutdown load cases.

All the results that have been presented here are based on a particular wind site conditions, a specific blade and a wind turbine model. The idea has been to give a qualitative and relative overview of different trends in the structural analysis, rather than coming to a conclusion in an absolute sense.

Due to the presence of considerable cone angle, shaft tilt and rotor overhang, blade-tower interference is not an issue for the analyzed blade design. It should be, however, considered to increase the trailing edge tape length towards the tip region to prevent buckling issues. Also, extra core materials could be provided (thus increasing bending stiffness and thickness) to prevent buckling problems. Operation of turbine under other significant loading conditions like icing and heavy leading edge erosion should be incorporated to study fatigue in more detail. Fatigue life should be evaluated and validated with models other than Miner's sum (for example, residual strength degradation model) along with full blade test (for an existent blade) for precise results. An aero-elastic stability analysis of full wind turbine model should be performed to understand the dynamics of whole system on blades. Finally, fatigue damage in bond lines between different components of blade is also a critical consideration for future work.

Table of Contents

List of Figures

List of Tables

Acknowledgment

This thesis interest was a result of my internship in Fraunhofer IWES in the area of aero-elastic loads analysis. That work motivated me to pursue the structural analysis based on the calculated loads and use the results of internship as inputs for this thesis project.

During the last nine months of this thesis work, I would like to acknowledge and extend my heartfelt gratitude to the following persons for their continuous support, guidance, motivation and making the completion of this thesis project possible in a timely manner:

Firstly, my thesis supervisor in Fraunhofer IWES, Dr. Alexandros Antoniou who provoked inquisitive and insightful thoughts on the topic and hence helped in better understanding of structural aspects of wind turbine blade, especially fatigue.

My department head in TU Delft, Prof. Bendiks Boersma, for being very open and supportive about pursuing a thesis in this domain of energy technology. Then, I would like to convey my since gratitude to Ir. W. Bierbooms for his assistance during the writing of this thesis. He was instrumental in directing me to experts in different field of wind turbine and getting their guidance as and when required.

My colleagues Oliver Kranke, Roman Braun, Eric Putnam, Malo Rosemeier and Matthias Saathoff for their help and support in different phases of the project which really brought all the aspects of the work together.

Finally, I would like to thank Fraunhofer IWES, for providing me this exciting and learning opportunity in the field of wind energy and thus, extending my horizons in this domain.

Delft University of Technology
July 14, 2013

Neelabh Gupta

Basic Terminologies

1. Aeroelasticity: Phenomenon which exhibits appreciable reciprocal interactions (static or dynamic) between aerodynamic forces and the deformations induced in the structure (wind turbine blade, for example).
2. Applied Loads: General term for inertial, gravitational, operational and/or aerodynamic forces acting on wind turbine blade.
3. Design Load Case (DLC): For design purpose, the life of a wind turbine is represented by a certain set of load scenarios covering the most significant part of their operation.
4. IEC 61400-1 and GL 2010: Standards that define the design requirement for land-based onshore wind turbines.
5. FAST: Aero-Elastic Wind Turbine Simulation Tool.
6. Fibre Reinforced Plastic (FRP): A generic term for a composite material consisting of a polymeric matrix, and a reinforcing fibre.
7. Fibre: A single homogeneous strand of material used as a principal constituent in FRP materials due to its high axial strength and modulus.
8. GNU Octave: It is a high-level interpreted language, primarily intended for numerical computations (used for fatigue calculations in current project).
9. Lamina: A single ply or layer (in a particular fibre direction) in a laminate made up of a series of layers.
10. Laminae: The plural of lamina.
11. Laminate: A product made by the bonding of individual laminae together.
12. Loads (Reaction): General term for bending moment, torsion, shear forces and/or axial forces (longitudinal: along the span of blade) occurring in a wind turbine blade as a result of applied loads.
13. Limit State: A state beyond which the structure no longer satisfies the requirements. The following categories of limit states are of relevance for structures: ultimate limit state, fatigue limit state, and serviceability limit state.
14. Matrix: The essentially homogeneous constituent of an FRP material that binds and protects the fibres.
15. Ply: The layers (lamina) that make up a stack (laminate).
16. Unidirectional laminate: A composite laminate in which substantially all of the fibres are oriented in the same direction.
17. Sectional Blade Loads: Blade loads occurring at a particular span or cross section.

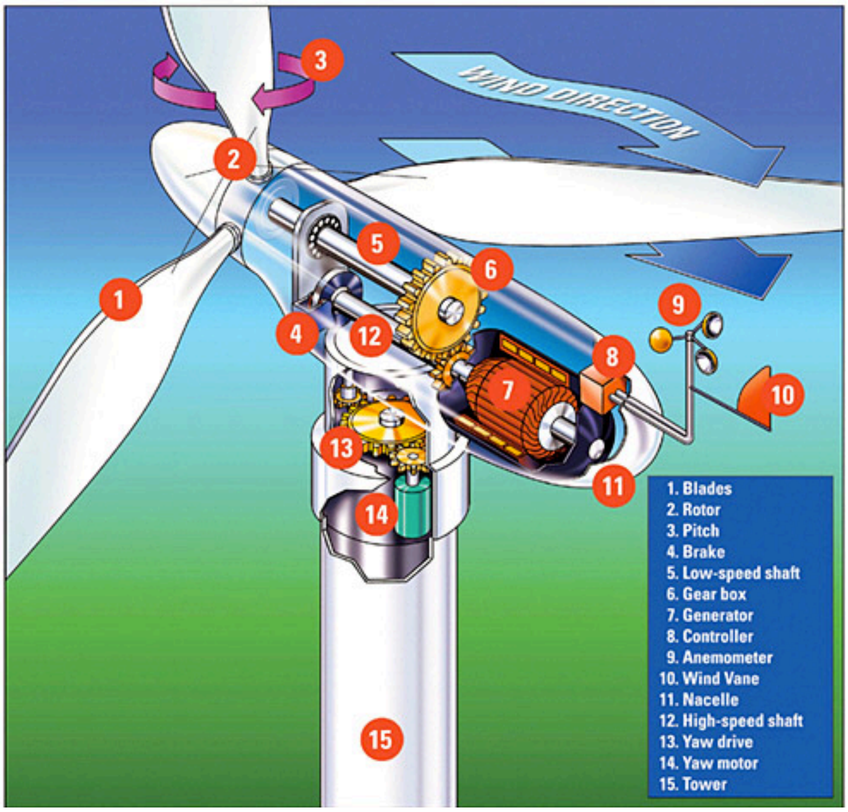

Figure 1: Basic Components in Wind Turbine [1]

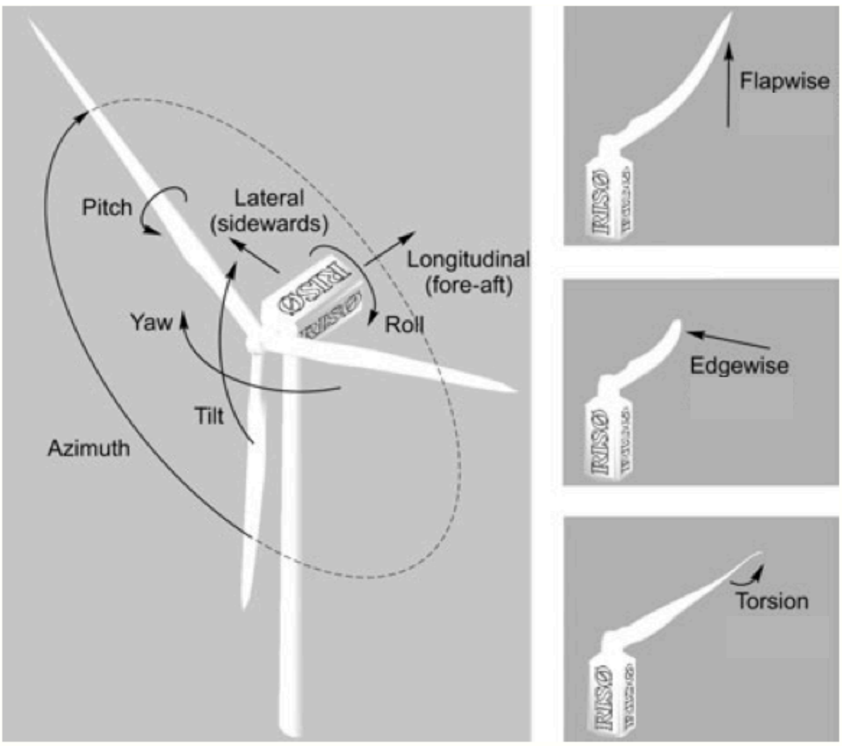

Figure 2: Terminology for Degree of Freedom in Wind Turbines [2]

Chapter 1

Introduction

1-1 Wind Turbine Design: Considerations

In today's world energy scenario, solar, wind, biomass and hydro power have become the major renewable segments that are playing a pivotal role in trying to find a right balance between growing energy demands and making it as 'green' as possible. No wonder, they have got so much attention and thrust over the past years that countries are trying to shift their energy profile from conventional resources to renewables.

Wind power is growing at the rate of 30 % annually [3] and, hence with this evolution, the design of a wind turbine and its implications needs to be well understood. Annual energy production (AEP) and cost are the two pivotal drivers governing the overall design of a wind turbine. The design should be reliable enough to prevent any unwanted maintenance or downtime and structurally stable enough to bear all the loads acting on it through its expected lifetime of around 20 years.

To get a building permit for the wind turbine, a certificate for its design is required. This certificate is delivered when the design requirements with respect to standards and guidelines used in wind energy are fulfilled. IEC 61400-1 and Germanischer Lloyd (GL) 2010 are two of such guidelines which are widely accepted and referred, while designing a wind turbine or any of its component for onshore (land-based) applications. In this project, most of the load calculations and design criteria are assessed using IEC-61400-1 Ed. 3 [4] (unless stated otherwise).

The design of a wind turbine components starts with an integrated loads analysis in the structure so as to have a check on its engineering solidarity. Its purpose is to assess and prevent against any physical damage occurring in a wind turbine and its components during the entire lifetime. Before a loads analysis can be performed, a wind turbine site and its conditions need to be defined based on the place where it's going to be installed. Once this is known, the set of wind conditions are applied (simulated) on a wind turbine during its planned lifetime and checked for its integrity.

Aerodynamics, structures, materials and production methods form four major pillars in wind turbine design. In the context of structure and aerodynamics, a wind turbine blade can be considered a crucial component in a wind turbine package, governing its cost and energy production. Primarily, its design is driven by the aerodynamic requirements (due to its direct impact on efficiency and power production), but economics (and mass) mean that the blade shape is a compromise to keep the structure robust, materials cheaper and lighter, and cost of construction (production) reasonable. In the nutshell, the choice of materials and manufacturing process will also have an influence on how thin (hence aerodynamically ideal) and complex the blade can be built. For example, carbon fiber material is stiffer and stronger than infused glass fiber along fiber direction but manufacturing and cost constraints might prevent it from being used in actual application. Hence it is important to consider an integrated approach while designing wind turbine blades.

The blade design process begins with a "best-guess" compromise between aerodynamic and structural efficiency. The wind conditions based on chosen aerodynamic shape gives rise to loads, which are fed into the structural design. Problems identified at this stage can then be used to modify the shape if necessary and recalculate the aerodynamic performance. The structural engineering process has a critical role in bringing all the disciplines of design and manufacture together and producing the optimum solution in terms of robust performance and cost.

1-2 Blade Structural Design

Imagine there is a flexible cornstalk in the corn field bending under the influence of the wind as depicted in figure 1-1. When the corn stalk is cut and looked inside, one comes across a cylindrical thin-walled, hollow structure. Evolution decided the stalk to become as it is, because in this way it could withstand the wind, and thus large displacements. The corn stalk can be compared with a blade of a wind turbine as shown in figure 1-1. They have certain structural similarities: Wind turbine blades are slender and have to be light and thus flexible, thin-walled, and hollow. Both structures underly large displacements caused by wind forces, where the cornstalk and the blade bend due to drag and lift force respectively. The structural difference to the stalk is, that the shape is not cylindrical, but rather a rectangular hollow beam encased with an airfoil shape. In any case, this similarity and evolution convey the importance of a structural design [5].

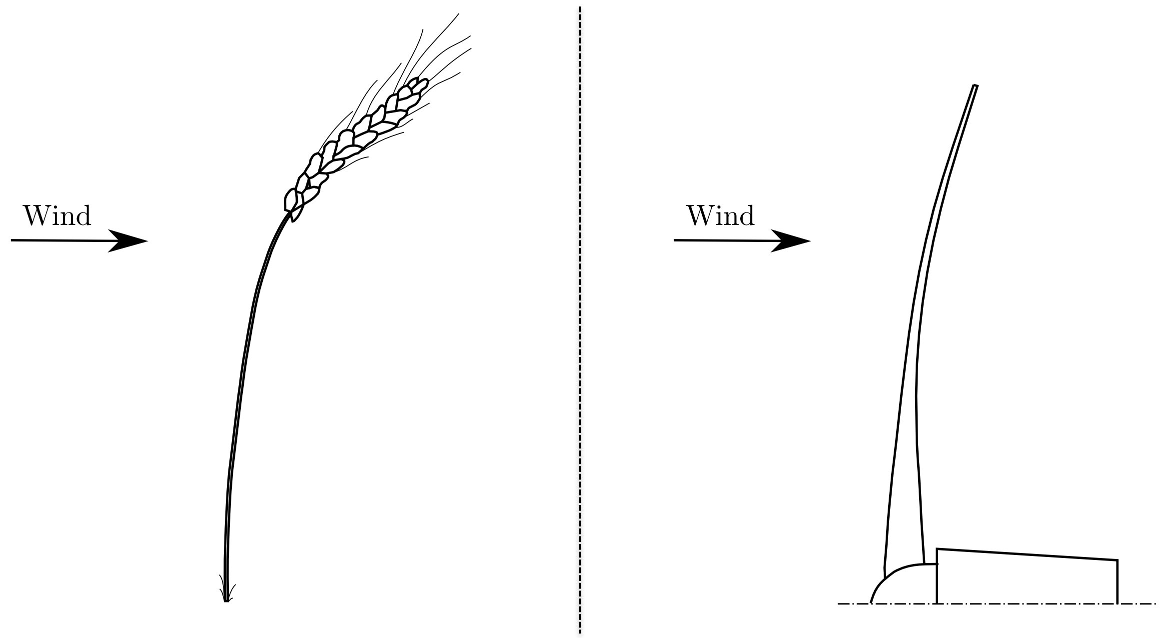

Figure 1-1: Analogy between a Corn Stalk and a Wind Turbine Blade with Cut Section of Nacelle and Hub [5]

Structural design of blade determines the cost of manufacturing a blade, load bearing capacity and hence performance of the overall structure (in terms of reliability and robustness). There is always an optimization required between the aerodynamic and structural design (which again, should be evaluated in terms of manufacturing capabilities). For example the aerodynamic design would want the design to be as light and thin as possible where as structural considerations might want it to be strengthened at certain regions due to large loads (for example at the root section of blade).

Figure 1-2 gives an overview of the typical structural analysis required during the design of wind turbine blade [5].

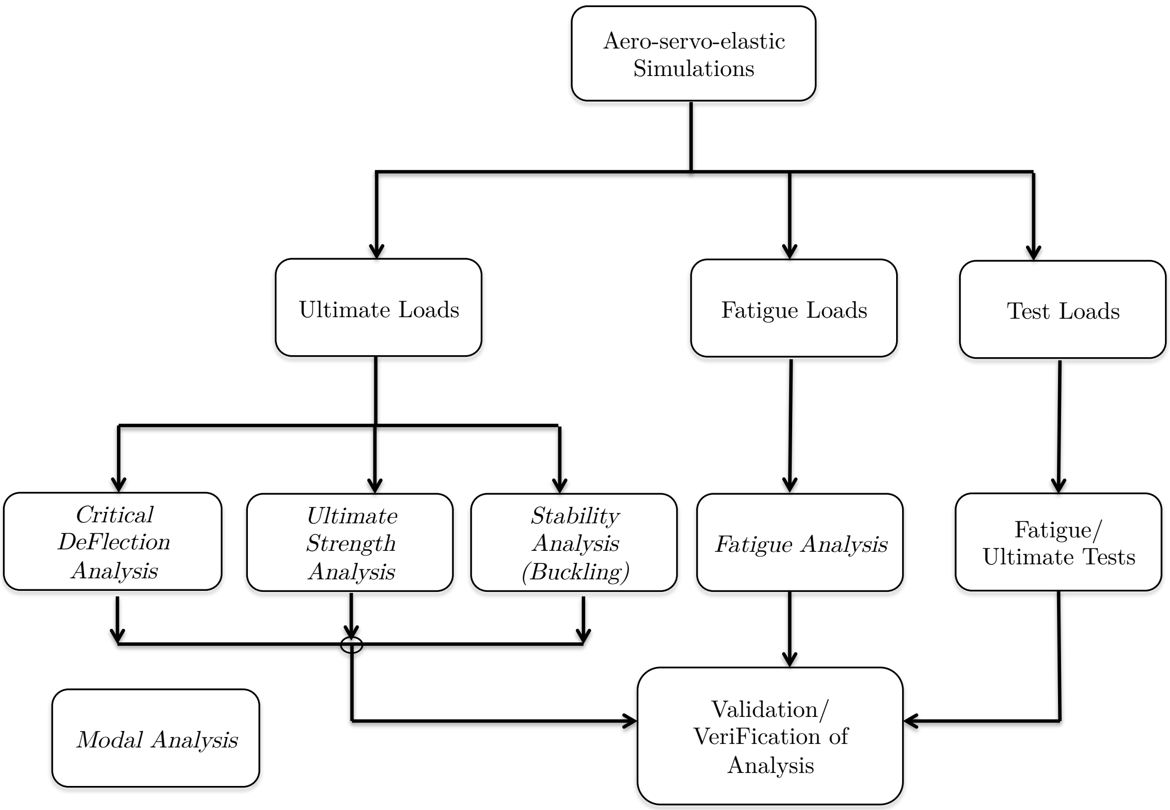

Figure 1-2: Structural Analysis Breakdown for Wind Turbine Blade Design

It has to be understood that blade deflection, buckling and modal analysis are stiffness (and mass) driven issues while ultimate strength and fatigue analysis are strength driven. The strength of a blade material is its ability to withstand an applied stress without failure. The field of strength of materials deals with loads, deformations and the forces acting on a wind turbine blade during its lifetime. It is the inherent property of the material of the blade and does not depend on shape, size and geometry of the blade. Stiffness, on the other hand, is the measure of resistance of elastic blade to deflections and deformations. It is also called rigidity and is dependent of the geometrical properties (chord, thickness and span) of the blade.

Current state of art for structural blade design in terms of criticality is extreme loading analysis (i.e. tip deflections and buckling) followed by fatigue and modal analysis. Fabric (laminate) and inter-fiber failure (static strength analysis) along with aero-elastic stability (like flutter) play a secondary role in blade design process. Laminates consist of different ply layers of fibers stacked on the top of one-another along a particular direction. But with long and slender blades, the issues related to stability (related to stiffness, damping and mass), resonance (eigen value problems) and deflections need to be understood fairly well in order to design a wind turbine blade. For the same reason, an integrated structural analysis has been performed in this project.

Generally speaking, for relatively smaller wind turbine blades (i.e. radius $\approx <$ 30-35 m), strength per unit mass should be as high as possible, but as blades grow bigger in radius, stiffness per unit cost play a vital role in the structural design.

Objective of the Project: The present study encompasses the analysis pertaining to structural discipline of wind turbine blade design. Here, ultimate (blade deflection towards the tower, strength and stability) and fatigue loads have been evaluated to check the structural integrity of a wind turbine blade. In addition, modal analysis is performed to check the possibility of resonance occurring in a blade. Resonance occurs when the blade's natural frequency (due to its structural and inertial properties) matches the frequency of external excitation. The same have been highlighted in *italics* in Figure 1-2. This study is done in based on specifications of three-bladed NREL 5MW machine [1] and the blade properties are taken from UpWind Project [2].

Apart from understanding of structural design of wind turbine blade, the main research and scientific objective of the project is to understand fatigue in wind turbine blade in a more elaborate way. This is done with the help of parametric studies i.e. analyzing the effect of yaw errors (due to difference in the direction of wind and rotor blades plane as shown in figure 1-3), rotor mass imbalances (due to difference in masses of blades during manufacturing) and load case operations (for example, when a turbine is producing power vs. when it is shutting down) on fatigue damage.

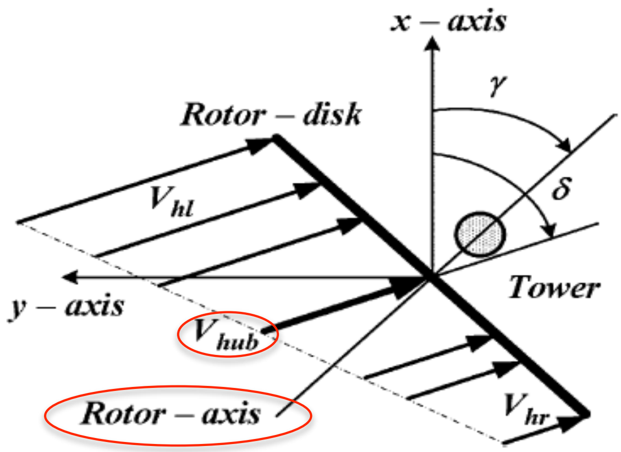

Figure 1-3: Yaw Error Visualization for a Wind Turbine Blade When Looking from the Top [6]

`Note:` The wind direction (δ) and yaw angle (γ) are both defined with respect to the x-axis (global direction indicating zero yaw and wind direction angles). All directions and shear are shown in their positive sense. The value $\delta - \gamma$ is called the yaw error and is positive when it is greater than zero and negative for values less than zero. When $\delta = \gamma$, there is no yaw error.

Chapter 2

Analysis and Methodology

This part of the report deals with procedure and approach used for calculation of aero-elastic loads (briefly), blade layout for Finite Element Analysis (FEA) and various branches of structural analysis for a rotor blade with special emphasis on Fatigue.

2-1 Load Calculations Overview

The required Design Load Case/s (DLC) cover essential design-driving situations such as normal operating conditions, start-up events, shut-down events, extreme and abnormal events like 50 year gust, parked or idling states, together with appropriate normal and extreme external conditions and likely fault scenarios. All the possible load case scenarios have been mentioned in IEC 61400-1 Ed. 3 [4].

The time series of wind velocity (turbulent) is generated in 'TurbSim' (Turbulent Simulation) [7] based on the onshore wind site data of IJmuiden in Netherlands. 'TurbSim' is a stochastic, full field, turbulent wind simulator. This wind field is like a cuboid with certain dimensions along the three directions and covers the entire rotor volume of turbine. Turbulent wind fields are, then, used for power production DLC and steady wind flow for startup and shutdown conditions during simulation. FAST [8] with AeroDyn (tool that caters to aerodynamics of a wind turbine) [6] accounts for the applied aerodynamic and gravitational loads, the behavior of the control system, and the structural dynamics of the wind turbine. Hence, FAST is an aero-servo-elastic code. FAST incorporates the elasticity of the rotor, drivetrain, tower, and the dynamic coupling between the motions of the tower and wind turbine. It employs a combined modal and multi-body structural dynamics formulation and has been interfaced with AeroDyn to enable the full aero-servo-elastic modeling of wind turbines. AeroDyn calculates the aerodynamic forces for each of the blades and models almost all aerodynamic aspects of a wind energy conversion system (WECS) including tower effect, vertical wind shear etc. Figure 2-1 represents a block diagram on calculation of aero-servo-elastic loads.

It was not considered necessary for this loads analysis to run all the DLCs prescribed by the design standards; instead, a subset of DLCs were used. The final aim of this analysis was to perform extreme static strength and stiffness calculations along with fatigue damage prediction, and hence, only extreme 50 year gust event for ultimate load case (2.3) was considered. For fatigue, the load cases that were considered are: power production (1.2), start-up (3.1) and normal shutdown (4.1) due to generic nature of reference wind turbine and significant impact, these fatigue load cases, have, on the lifetime of a turbine (no certification of wind turbine involved here). Also, power production load case covers, a major part wind turbine life during its operation as the mean wind speed has maximum probability at around 8 m/s for the defined onshore site. Wind speeds below 3 m/s (very low) and above 25 m/s (very high) are very rare. Startups and shut downs produce transient loads with significant amplitude and gradient and have a major impact on reliability and availability of turbine. This means, turbine with a realistic availability passes most of its lifetime of its operations

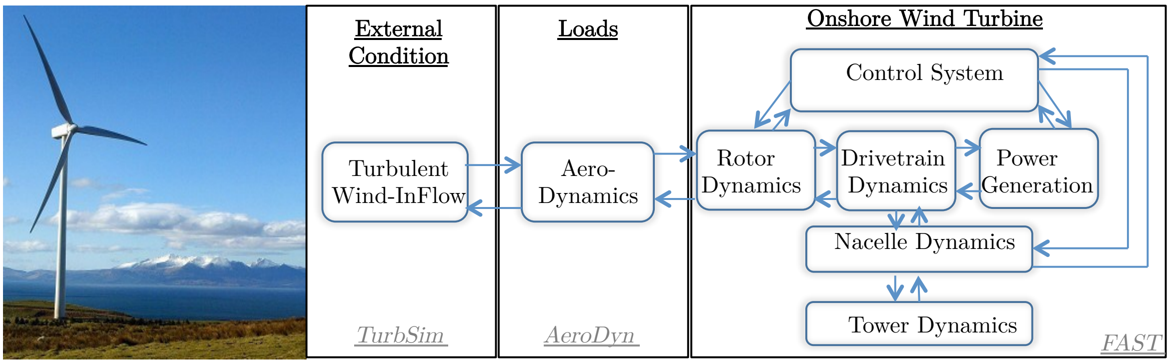

Figure 2-1: Integrated Approach to Modeling Onshore Wind Turbine: Aero-Servo-Elastic Simulation [9]

covered by these three load cases [10].

A small summary of the load cases under consideration from the IEC standard [4] has been put up in Table 2-1. For detailed loads analysis procedure, refer to [9].

Table 2-1: Design Load Cases (DLC) Under Consideration

Design Situation	DLC	Wind Condition	Type of Analysis	General Remarks
Power Production	1.2	NTM, Vin<Vhub<Vout	Fatigue	Stochastic Seeds, Yaw Errors, Rotor Mass Imbalance.
Startup	3.1	NWP, Vin<Vhub<Vout	Fatigue	Steady Deterministic Wind.
Normal Shut Down	4.1	NWP, Vin<Vhub<Vout	Fatigue	Steady Deterministic Wind.
Power production plus occurrence of fault	2.3	EOG, Vhub = Vr$\pm$ 2 m/s and Vout m/s	Ultimate Load	External or internal electrical fault including loss of electrical network.

NTM: Normal Turbulence Model
NWP: Normal Wind Profile
EOG: Extreme Operating Gust

Based on Table 2-1, a total of 294 load cases (288+3+3; respectively for power production, startup and shutdown) are considered for fatigue analysis. Also, DLC 1.2 includes three yaw errors (For Benchmark case: 0^o, $+8^o$ and -8^o), rotor mass imbalance among three blades (For Benchmark case: blade 1 is 3 % heavier while blade 3 is 3 % lighter than blade 2). The detailed loads analysis has already been performed as a prelude to this project and can be found in [9]. To sum up the relation between design load cases and structural analysis, one can view static strength, buckling and critical deflection analysis based on design load case of 50 years extreme operating gust (DLC 2.3), while fatigue analysis is based on three predominant design load cases namely: Power production (DLC 1.2), Start up(DLC 3.1) and Normal Shutdown (DLC 4.1).

Figure 2-2 and 2-3 represent some of the results from loads analysis [9]. It can be seen that negative yaw error cause more loading amplitude in a blade where as mass imbalance of blades cause more loads fluctuations in a tower. These results give an insight to loads occurring in rotating and stationary reference frame for different scenarios and would be useful for fatigue analysis, going forward. Note that these results are for a clockwise rotating turbine and 'Vxi' represents longitudinal wind velocity at hub height.

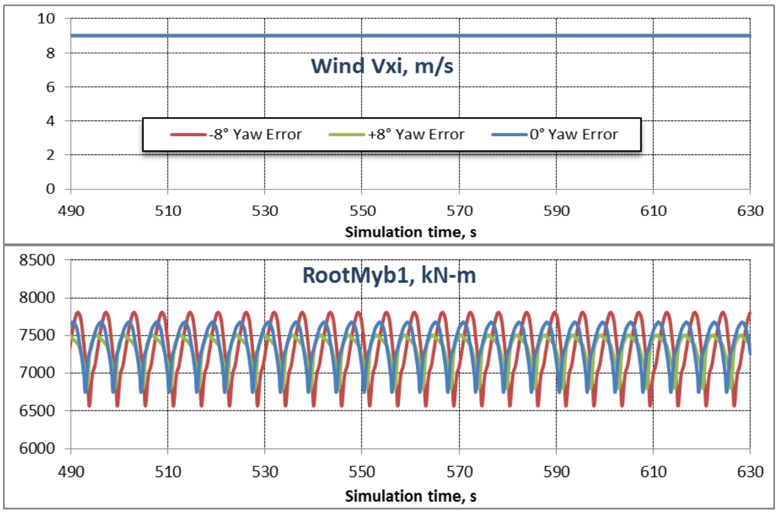

Figure 2-2: Flapwise Root Bending Moment (RootMyb1) for Different Yaw Error Scenarios [9]

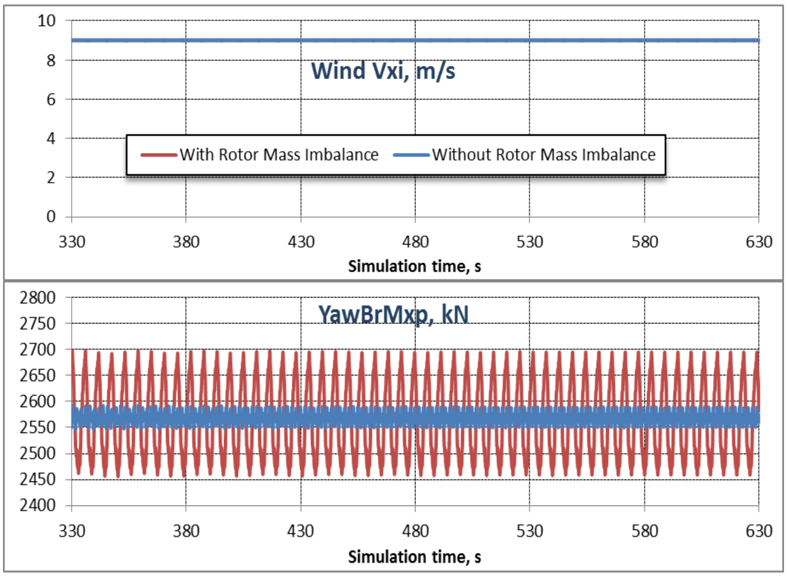

Figure 2-3: Tower Top Fore-Aft Shear Force (YawBrFxp) for a Balanced/Unbalanced Rotor [9]

2-2 Structural Layout, Material Properties and Safety Factors

The current state-of-art wind turbine rotor blades are constructed from fibre reinforced polymers (FRP). The reason for this is the high strength, high stiffness, high stiffness-to-density ratio and high strength-to-density ratio. Typically, continuous glass-fibre composites are used, but as blades become longer and slender, designers are also going for carbon fibres because these stiffer fibres are becoming affordable for large wind turbine blade structure (trade-off between cost and stiffness).

The fibres are embedded in a polymer matrix, which provides some resistance to compression loads, but mainly serves to align and fix the fibres geometrically. Polyester and epoxy are typical resins, used in the manufacture of wind turbine blades. The density is very similar, but better fatigue performance is attributed to composites with epoxy matrices, enabling lighter design. Essentially all blades are made with these thermoset resins [11].

A wind turbine blade is predominantly loaded in flapwise and edgewise direction (refer appendix A for coordinate system and direction). A wind turbine blade cross section can be divided into load carrying parts, and parts, that are geometrically optimized for aerodynamic shape. This is a kind of compromise between the structural integrity and aerodynamic performance in a wind turbine blade. The flapwise loads are carried by the main spar (or girders) where as edgewise loads are taken partially by spar and partially, if present, by reinforcement in the leading and trailing edge. Shear webs (made of bi-axial fibre laminate with core in the middle: sandwich structure) is present between the two spar caps and provides shear strength to the blade. The remainder of the blade is constructed from multi-axial skin material and sandwich structure (fibre layers with core material like foam or balsa wood in between) ensuring aerodynamics geometry, low mass, resistance to torsion and high buckling resistance. It should be observed (Figure 2-4) that, the foam core is omitted (present in sandwich structures) where the spar caps support the shell, indeed it is advantageous to do this as it allows the spar caps to be better separated to carry the bending loads and hence is beneficial from both, cost and strength perspective. Figure 2-4 indicates this load bearing cross section of a typical wind turbine blade [11].

Just to point out here, that flapwise loads are mainly generated from stochastic nature of wind (hence strongly irregular in amplitude and mean) where as edgewise loads are mainly due to the weight of the blade (gravity forces) and the torque loads that drives the turbine (hence regular and periodic in nature). Also, a point to consider here is, flapwise and edgewise directions are local in terms of blade section where as out-of-plane and in-plane directions are with respect to the whole rotor.

Before discussing the actual layout of the blade, lets look into a brief overview of the composites. A composite material is a heterogeneous and anisotropic material made up of two or more materials (continuous fibres embedded in a polymeric matrix called resin). Fibres can be either carbon, glass, boron, aramid etc. (common industry practice is glass and carbon) and resins can be either thermoset or thermoplastic (common practice in industry is thermoset).

The main function of the reinforcing fibres is to carry the load and provide strength, stiffness, thermal stability and other structural properties to the composite blade. The prime purpose of matrix (composed of resin, hardener and might be, some additives) is to bind

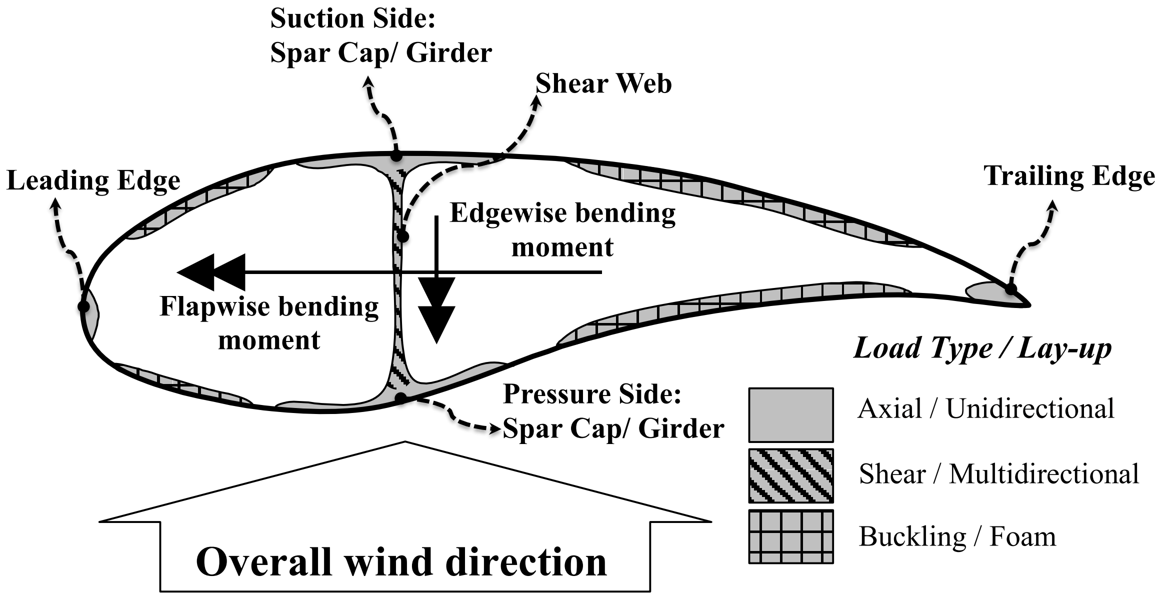

Figure 2-4: Typical Cross Section of a Wind Turbine Rotor Blade [11]

the fibres together and transfer the load to fibres providing rigidity and shape to the blade structure. The failure mode during structural analysis is strongly affected by the type of matrix material used in the composites.

Material properties of blade (mass, stiffness, strength) are taken from UpWind Project [12] [13] [14]. The properties used for the material in the current design of UpWind blades is given in Table 2-2 and 2-3.

Partial safety factors for loads, materials and consequence of failure have been considered in the analysis unless stated otherwise. Partial safety factors account for the uncertainties and variability in loads, materials, the uncertainties in the analysis methods and the importance of structural components with respect to the consequences of failure. These values are mostly based on IEC 61400-1 ed. 3 guidelines [4], but wherever the information was not found to be sufficient, GL 2010 guidelines [15] where used.

- Partial safety factor for loads was taken to be 1.10 (except for strength analysis as this is used to evaluate inter fiber failure and GL guidelines mandates to use the characteristic load values for such an analysis) as the design load case under consideration is an abnormal event and IEC 61400-1 stipulates the usage of this factor for the same (Section 7.6.2.1, Table 3).
- Material partial safety factor for deflection analysis is taken to be 1.10 based on IEC 61400-1 guidelines (Section 7.6.5)
- Material partial safety factors for buckling analysis have been derived from GL guidelines (section 5.5.3.2.3) as no concrete values have been mentioned in IEC standard. Material factor for laminates (considering temperature effect, linear computation and scattering

Table 2-2: In-Plane Stiffness Related Properties of UpWind Blade

Material	E_l, MPa	E_t, MPa	G, MPa	**Poisson's Ratio**	**Density,** kg/m^3
Uni-directional Laminate (SC and TE Tape)	38887	9000	3600	0.249	1869
Triaxial Laminate (Skin)	24800	11500	4861	0.416	1826
Biaxial Laminate (Shear Web, $\pm 45^o$)	11700	11700	9770	0.49	1782
Core Material (for Skin Sandwich)	256	256	22	0.3	200
Core Material (for Shear Web Sandwich)	25	25	12	0.3	45

`Note:` E_l is Young's modulus in longitudinal direction, E_t is Young's modulus in transverse direction and G is the Shear Modulus.

of moduli) $\gamma_m = 1.35 * 1.1 * 1.1 * 1.25$ and for core, the scattering for moduli effect is dropped off, giving $\gamma_{mc} = 1.35 * 1.1 * 1.25$.

- Material partial safety factors for strength analysis have been again derived from GL guidelines (Section 5.5.2.4 and 5.5.3.2.2). For maximum stress criteria (which would be used to evaluate the fiber failure), $\gamma_m = 1.35*1.35*1.1*1.1*1.0$. For inter-fiber failure, $\gamma_m = 1.35 * 1.25$. This is based on consideration of ageing, temperature effects, resin infusion method and post-cured laminate.
- Material partial safety factors for core is not considered during static strength analysis as laminate is the point of interest here and not the sandwich structure, which core is a part of.
- Consequence of failure safety factor has been taken to be 1.0 for all cases based on IEC guidelines.

It has to be noted these safety factors are just mentioned with reference to standards. For getting an exact understanding on each of the numbers within a safety factor, standards should be referred.

Table 2-4 summarizes the factors used during the different structural analysis.

Material and load partial safety factors are applied to their respective characteristic values to get the design values[4] (with the exception for usage of mean strength values for buckling analysis and static analysis; GL 2010 guidelines) :

$$F_d = \gamma_f . F_k \tag{2-1}$$

$$f_d = \frac{1}{\gamma_m} . f_k \tag{2-2}$$

Table 2-3: Mean Strength Properties of UpWind Blade for Static and Fatigue Analysis

Material	$\sigma_{ltensile}$, MPa	σ_{lcomp} , MPa	$\sigma_{ttensile}$, MPa	σ_{tcomp} , MPa	τ, MPa
Unidirectional Laminate (SC and TE Tape)	776.50	-521.82	53.95	-165.00	56.08
Triax Laminate (Skin)	519.81	-443.71	-	-	-
Biaxial Laminate (Shear Web)	112	-112	-	-	-

`Note:` $\sigma_{ltensile}$ is tensile strength in longitudinal direction, σ_{lcomp} is compressive strength in longitudinal direction, $\sigma_{ttensile}$ is tensile strength in transverse direction, σ_{tcomp} is compressive strength in transverse direction and τ represents shear strength (in-plane).

Table 2-4: Partial Safety Factors

Partial Safety Factor	**Critical Deflection Analysis**	**Buckling Analysis**	**Static Strength Analysis**	
			Maximum Stress Criteria	Tsai Wu Criteria
Load (γ_f)	1.10	1.10	1.10	1.00
Material: Fiber Reinforced Laminate (γ_m)	1.10	2.04	2.21	1.69
Material: Core (γ_{mc})	-	1.86	-	-
Component Class (γ_n)	1.00	1.00	1.00	1.00

where,
F_d is the "design value" for the aggregated internal load (based on combination of aerodynamic, gravity, operational and inertia forces) for the considered Design Load Case (DLC);
γ_f is the partial safety factor for load as defined in Table 2-4;
F_k is the "characteristic value" of load obtained from 'FAST'

f_d is the "design value" of the material properties (stiffness or strength);
γ_m is the partial safety factor for materials as defined in Table 2-4;
f_k is the "characteristic value" of material properties.

Consequence of failure factor γ_n is kept to be unity during the analysis mentioned in Table 2-4 as wind turbine blade is considered to be a 'non fail-safe' component meaning, failure of the blade would result in the failure of a major part of the wind turbine. [4].

At this point, it has to be realized that each type of analysis requires a different formulation of the limit state function and deals with different sources of uncertainties through the use of safety factors.

The basic parameters of the wind turbine under consideration has been put in Table 2-5 [16].

It should be noted here, that transport and manufacturing safety factors can also have a significant impact on overall structural behavior of the blade. These, however, have not been considered in present analysis due to the complexity in achieving the exact values.

Table 2-5: Turbine Configuration

Wind Turbine Rating	5 MW
Rotor Orientation, Configuration	Upwind, 3 Blades
Control	Variable Speed, Collective Pitch
Drivetrain	High Speed, Multiple-Stage Gearbox
Rotor, Hub Diameter	126 m, 3 m
Hub Height	90 m
Cut-In, Rated, Cut-Out Wind Speed	3 m/s, 11.4 m/s, 25 m/s
Cut-In, Rated Rotor Speed	6.9 rpm, 12.1 rpm
Rated Tip Speed	80 m/s
Overhang, Shaft Tilt, Pre-cone	5 m, 5°, 2.5°
Blade Mass (One)	21,358 kg
Nacelle Mass	240,000 kg
Tower Mass	347,460 kg

2-3 Limit State Function and Blade FEM

2-3-1 Limit State Function For Preliminary Structural Analysis

The limit state function can be separated into load (or action) and resistance (material properties) functions; S and R respectively, and the condition to prevent any failure, then becomes:

$$\gamma_n.S \leq R \Rightarrow \gamma_f.F_k \leq \frac{1}{\gamma_m.\gamma_n}.f_k \tag{2-3}$$

The formulation above is based on the following definition of S and R:
S for the critical deflection analysis, static strength analysis and buckling analysis is defined as the maximum value of the blade's response in terms of load (stresses resulting from bending moment or forces) while R is defined as the maximum allowable "design value" of the material.

The formulation of Equation 2-3 would be used in all the structural analyses except for Fatigue. Separate formulation would be give for Fatigue analysis that would be discussed in later sections.

2-3-2 Blade Finite Element Model (FEM)

Structural Analysis (inter-fiber strength, buckling and preliminary work of fatigue analysis) is done in ANSYS with high-fidelity FEM of blade hinged at the root section. The FEM is a technique used for analyzing behavior in a variety of situations, including wind turbine blade structures. The technique is based on dividing the structure into a large number of relatively small elements. Each element includes a number of nodes. Some of these nodes may be interior to the element; others are on the boundary. Elements only interact through the nodes at the boundary. Each element is characterized by a number of parameters, such as thickness, density, stiffness, elastic modulus, etc. Also associated with each node are displacements or degrees of freedom. These may include translations, rotation, axial motion, etc. The FE method is most often used to study in detail individual components within a larger system (here, a blade as a part of wind turbine). A finite element model may then be used subsequently, for example, to study variations in stresses within a component [17]

Figure 2-5, 2-6 and 2-7 depict the Finite Element (FE) model of full blade, blade part with Uni-Directional (UD) material and a cross section of it respectively. Most part of this 3-Dimensional FE model is made up of SHELL 181 element in ANSYS. This is a four-node element with six degrees of freedom at each node: three translation and three rotational Degree of Freedom (DOF) in and about x, y and z directions respectively. This type of element is used for analyzing thin to moderately-thick shell structures. It is well suited for linear and/or large strain non-linear applications with change in shell thickness accounted for, in non-linear analysis [18]. In the present model SHELL 181 is used for modeling composite shells and sandwich constructions of wind turbine blade (layered application). The Multipoint Constraint (MPC), MPC184 rigid beam elements (3-D) are used to model rigid constraints between shear center and blade shell to transmit forces and moment from this location. This rigid beam element has two nodes possessing six DOF at each node (three translation and three rotational). This is depicted in figure 2-8. It has to be noted here, that these rigid beams are fabricated at all the sections where the load (forces) are applied. The load, then, applied at the shear center of the cross section is transmitted evenly to the blade shell structure through these rigid beams.

Table 2-6 gives information about the aerodynamic and structural twist at different section of the blade. Aerodynamic twist is important for the profile and aerodynamic performance of the blade while structural twist is important from loads perspective. The two words 'spar caps' and 'trailing edge tape' would be used quite rigorously in this report as they are the main load carrying component in a wind turbine blade and major focus of this project. Hence they have been highlighted in Figure 2-6 and 2-6 for clarity. It should be noted that spar caps extend till 58 m and trailing edge tape till 45 m of blade.

It may be reasoned as to why are reinforcement mostly provided in trailing edge and not leading edge (Figure 2-6). This is because, fatigue and stresses are more critical in trailing edge than leading edge due to the fact that neutral axis is farther from trailing edge than leading edge (From basic mechanics, it is known that longitudinal stress is directly proportional to distance of neutral axis from point of consideration). The blade under consideration, also has just trailing edge tape for this very reason.

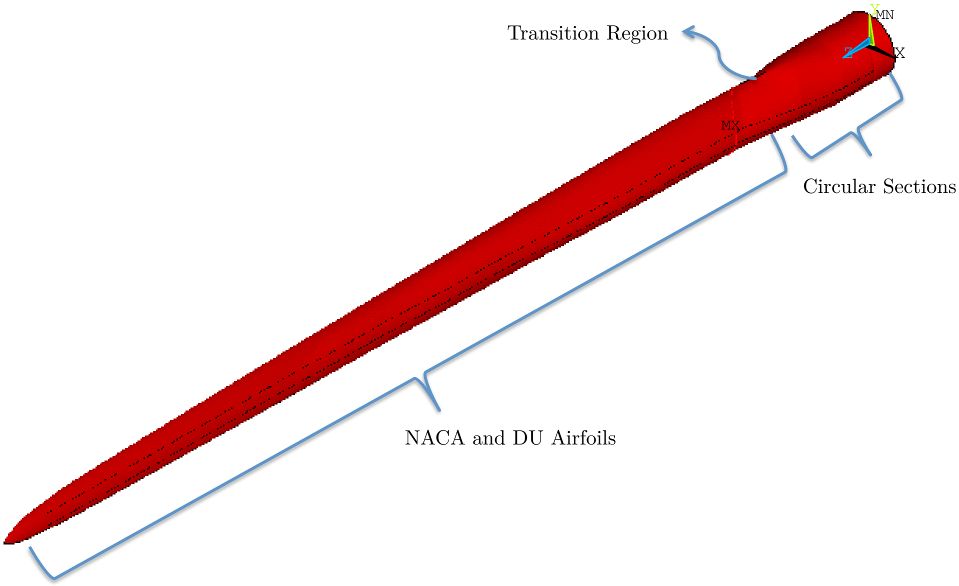

Figure 2-5: Blade Model in ANSYS With a Brief Sectional Description

2-3-3 Critical Deflection Analysis

As rotor blades become larger and slender to reduce cost and increase energy yield in today's wind turbine industry, it is of utmost importance to make sure that no mechanical interference occurs between the blade and tower. IEC-61400-1 Ed.3 stipulates that maximum deflection the most unfavorable direction must be calculated incorprating the partial safety factors for calculation of loads, materials and consequence of failure. In this analysis, DLC 2.3 (Table 2-1) is used for this deflection calculation as this is considered to be the most severe of load cases with an abnormal event of extreme operating gust for a recurrence period of 50 years. In this load cases the timing of the gust and occurrence of grid loss is chosen in a way to achieve the worst possible loading. Following scenarios are analyzed:

- The grid loss occurs at the time of the lowest wind speed.
- The grid loss occurs at the time of the highest gust acceleration.
- The grid loss occurs at the maximum wind speed.

Based on this, nine scenarios are considered as highlighted in Table 2-7.

`Note`: From basic structural mechanics, the lateral deflection at the tip of a cantilever beam under a uniform distributed load is given by,

$$\delta_{max} = \frac{q.L^4}{8.E.I} \tag{2-4}$$

where,
q: Uniformly distributed load along the length of beam
L: Length of the beam

Table 2-6: Blade Span Information With Sectional Properties

Span No.	Radius from Hub Center, m	Airfoil Section	Aerodynamic Twist angle, [°]	Structural Twist angle, [°]
Span1	2.8	Circular	13.308	13.309
Span2	5.6	Circular	13.308	13.309
Span3	8.3	Circular	13.308	13.309
Span4	11.8	DU40_A17	13.308	13.123
Span5	15.9	DU35_A17	11.480	11.356
Span6	28.2	DU25_A17	7.795	7.708
Span7	36.4	DU21_A17	5.361	5.301
Span8	44.5	NACA64_A17	3.125	3.097
Span9	56.2	NACA64_A18	0.863	0.853

E: Young's Modulus of material of beam
I: Bending moment of inertia (Area moment of inertia) of the cross section of the beam.

As it is well known, wind turbine blade is a type of long and slender composite thin shell structure and clamped at the root section by the hub (analogous to cantilever beam). Though a wind turbine blade is not uniformly loaded along the span, Equation 2-4 gives good insight into the structural parameters that effect its tip deflection. Generally, the flapwise and edgewise stiffness are very close at the root section while there is an order of 10 difference at the tip section (edgewise, being 10 times stiffer than flapwise). For the current analysis, the flapwise and edgewise stiffness at the root are 4.18E10 $N-m^2$ and 4.17E10 $N-m^2$ respectively. The same values at the tip are 1.25E3 $N-m^2$ and 3.55E4 $N-m^2$ respectively. Detailed section-wise plots of stiffness and mass densities can be found in Appendix B.

Gust Profile

[h] The wind speed time series for operation during three different wind conditions (described in Table 2-1) during the period of gust is calculated based on IEC 61400-1 ed. 3 [4]. Hence $V_{hub} = 9.4m/s, 13.4m/s \; and \; 25m/s$ would be used.

For the steady extreme wind model, the extreme wind speed, Ve_{50}, with a recurrence period of 50 years, and the extreme wind speed, Ve_1, with a recurrence period of 1 year, shall be computed as a function of height, z, using the following equations (power law):

$$Ve_{50} = 1.4V_{ref}\left(\frac{z}{z_{hub}}\right)^{0.11} \tag{2-5}$$

$$Ve_1 = 0.8Ve_{50} \tag{2-6}$$

Here, $V_{ref} = 46.5m/s$, is the reference velocity for the site chosen (Ijmuiden) and z is equal to z_{hub} (hub height) as the gust velocity of interest is at hub height.

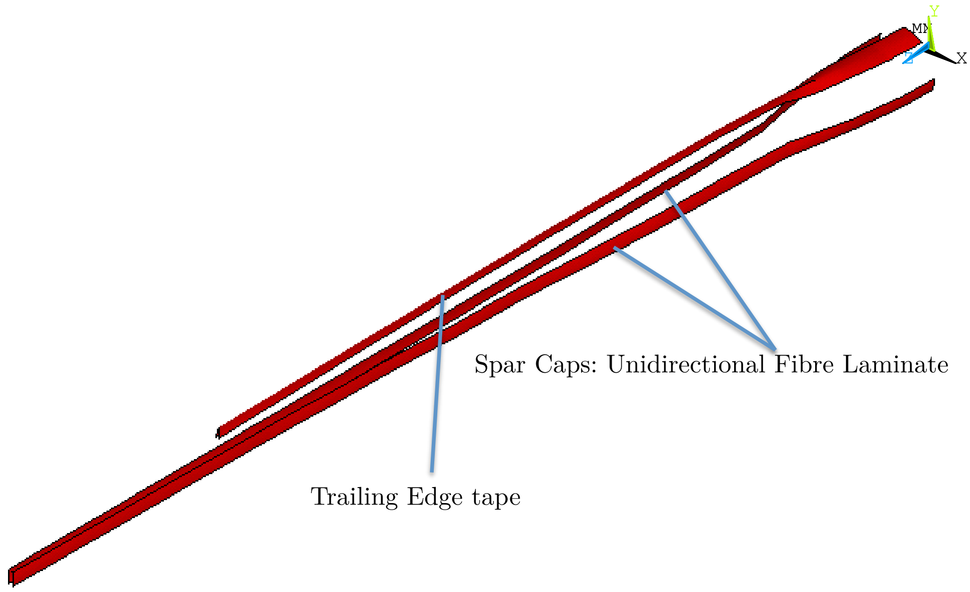

Figure 2-6: Blade Model in ANSYS With Only Spar Caps and Trailing Edge Tape

The hub height gust magnitude V_{gust} is given for the standard wind turbine classes as,

$$min\left[1.35(V_{e1} - V_{hub}), 3.3\frac{\sigma_1}{1 + 0.1(\frac{D}{\Lambda_1})}\right] \tag{2-7}$$

where, $\sigma_1 = 0.12(0.75V_{hub} + 5.6)\ m/s$;
Λ_1 is the turbulence scale parameter,

$$\Lambda_1 = \begin{cases} 0.7z & z \leq 60m \\ 42m & z \geq 60m \end{cases} \tag{2-8}$$

D is the rotor diameter=126 m

Using the values from above equations, the wind speed time series at hub height during the gust can be calculated as,

$$V(t) = \begin{cases} V_{hub} - 0.37.V_{gust}\sin(\frac{3\pi t}{T}).(1 - \cos(\frac{2\pi t}{T}) & 0 \leq t \leq T \\ V_{hub} & otherwise \end{cases} \tag{2-9}$$

Here T=10.5 s Based on the above methodology [4] and for $V_{hub} = 13.4m/s$ of the wind speed and acceleration time series during the gust is given by Figure 2-9 and 2-10 ,

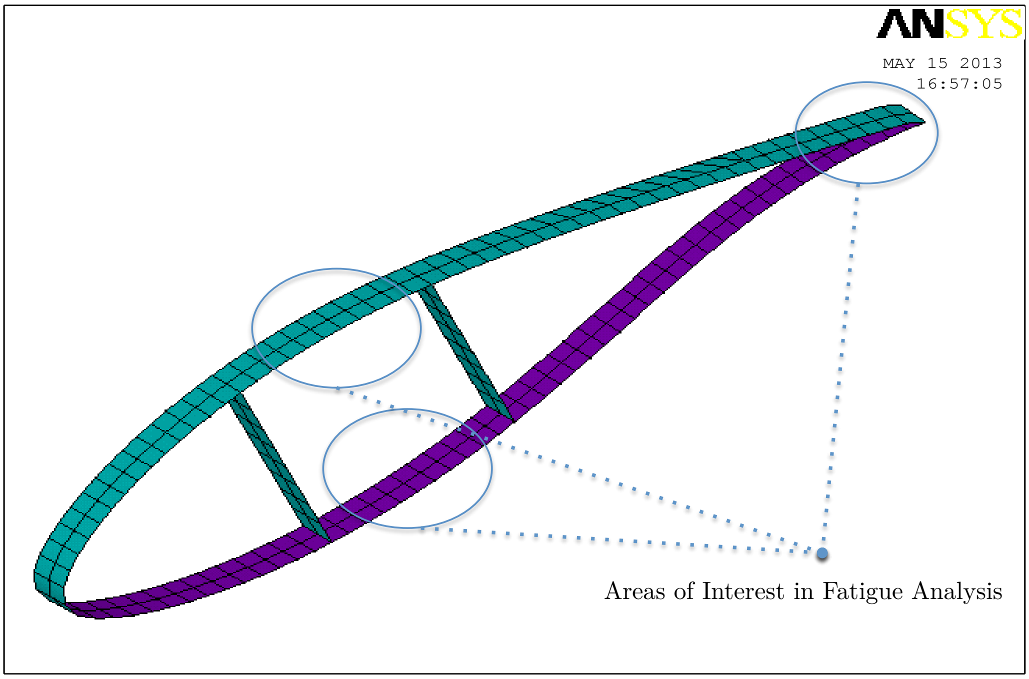

Figure 2-7: Cross-Sectional View of Blade Model in ANSYS at 37 m Length

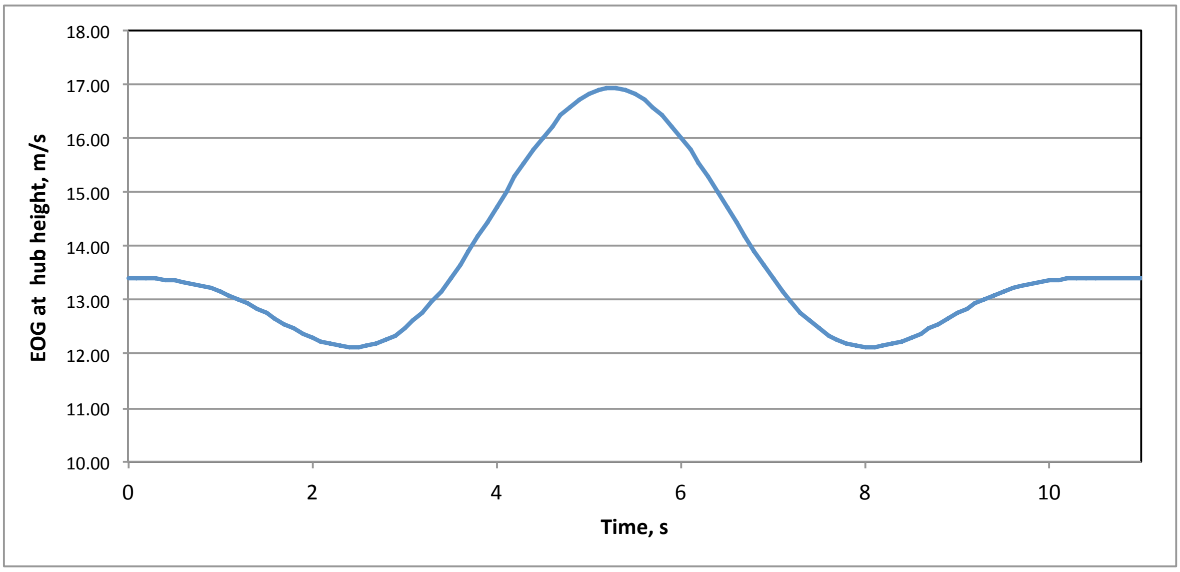

Figure 2-9: Extreme Operating Gust Profile for $V_{hub} = 13.4 m/s$

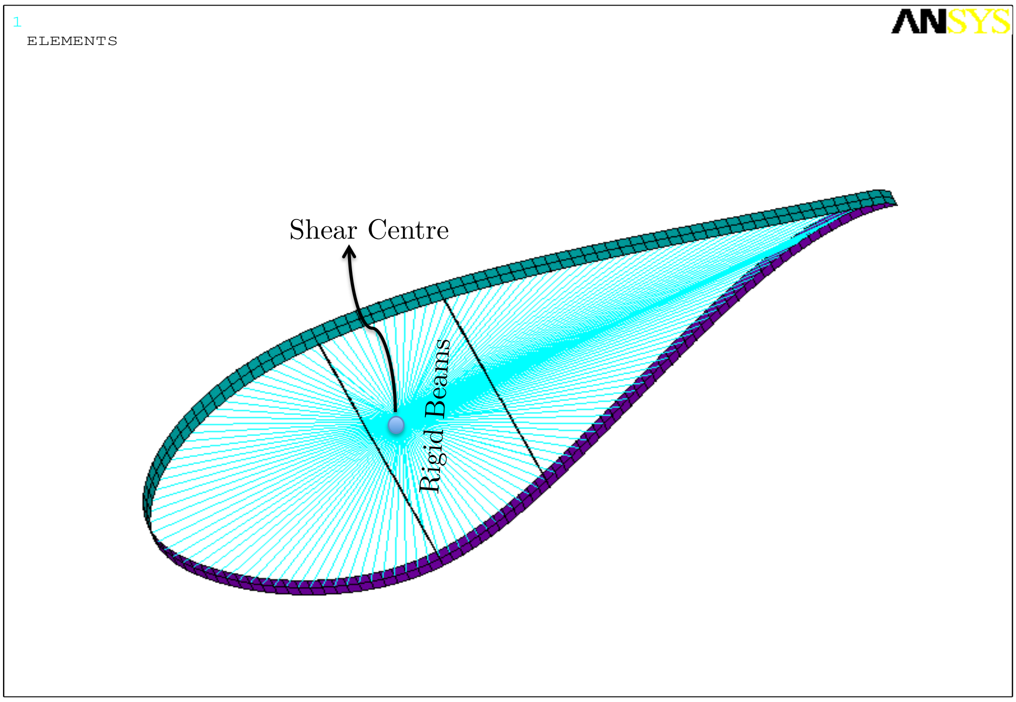

Figure 2-8: Blade Section with Rigid Beams from Shear Center to Outer Shell

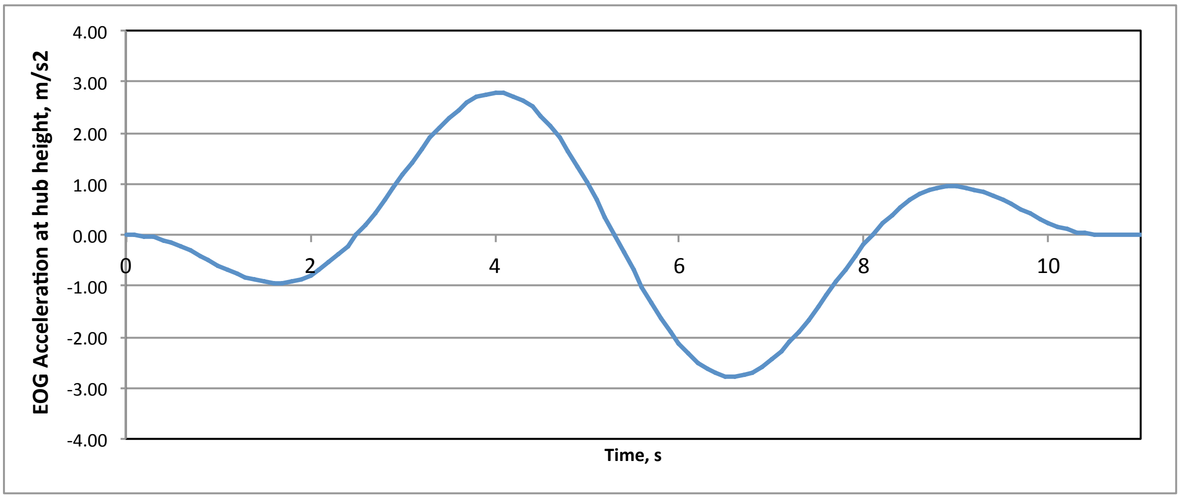

Figure 2-10: Acceleration Profile during Gust for $V_{hub} = 13.4m/s$

Considering the nine scenarios listed in Table 2-7 and the calculations above, wind turbine blade deflections are evaluated using 'FAST'. The worst of all the nine scenarios is then taken for evaluation of critical deflection. This is done after analyzing the blade for maximum out of plane deflections in all the scenarios. The result from the same has been put in Table

Table 2-7: Scenarios for Extreme Operating Gust

Scenario No.	Hub Height Wind Speed, m/s	Remarks
1	9.4	Grid Failure when maximum Gust Speed occurs
2	9.4	Grid Failure when minimum Gust Speed occurs
3	9.4	Grid Failure when maximum Gust acceleration occurs
4	13.4	Grid Failure when maximum Gust Speed occurs
5	13.4	Grid Failure when minimum Gust Speed occurs
6	13.4	Grid Failure when maximum Gust acceleration occurs
7	25	Grid Failure when maximum Gust Speed occurs
8	25	Grid Failure when minimum Gust Speed occurs
9	25	Grid Failure when maximum Gust acceleration occurs

2-8 and Figure 2-11. It can be observed from this table that the maximum deflection occurs for fourth scenario where the grid failure occurs at maximum gust speed. Also, this worst condition entails, the mass imbalance in three blades (3 %, 0 % and -3 % respectively).

Definition: Out-of-Plane Tip Deflection This is the blade tip deflection in out-of-plane direction (perpendicular to the chord at the tip when twist and pitch angle are zero) relative to the pitch axis and considered positive downwind.

Blade Tip Deflection and Tower Clearance

IEC 61400-1 ed. 3 [4] stipulates the maximum elastic deflection in unfavorable deflection be multiplied by a combination of partial safety factors for loads, materials and consequence of failure. Hence, the partial safety factors used for this analysis (critical deflection) have been put in Table 2-4.

Now, the actual clearance available between the tower and blade needs to be calculated. For that, few angles like precone and shaft tilt as well as overhang needs to be understood. The same has been depicted in Figure 2-12 for clarity. All these three parameters (tilt, precone and overhang) aid in maintaining a proper tower clearance with the blade. Table 2-9 summarizes the overall calculations for blade tip deflection and tower clearance.

Here, the horizontal overhang, H_o and horizontal distance between blade axis and un-tilted rotor plane (H_b) are calculated as,

Table 2-8: Maximum Out of Plane Tip Deflections for Nine Different Scenarios of DLC 2.3

Scenario	Out of Plane Blade Tip Deflection, m
1	5.00
2	3.85
3	3.85
4	**5.35**
5	3.57
6	3.95
7	3.00
8	1.36
9	1.85

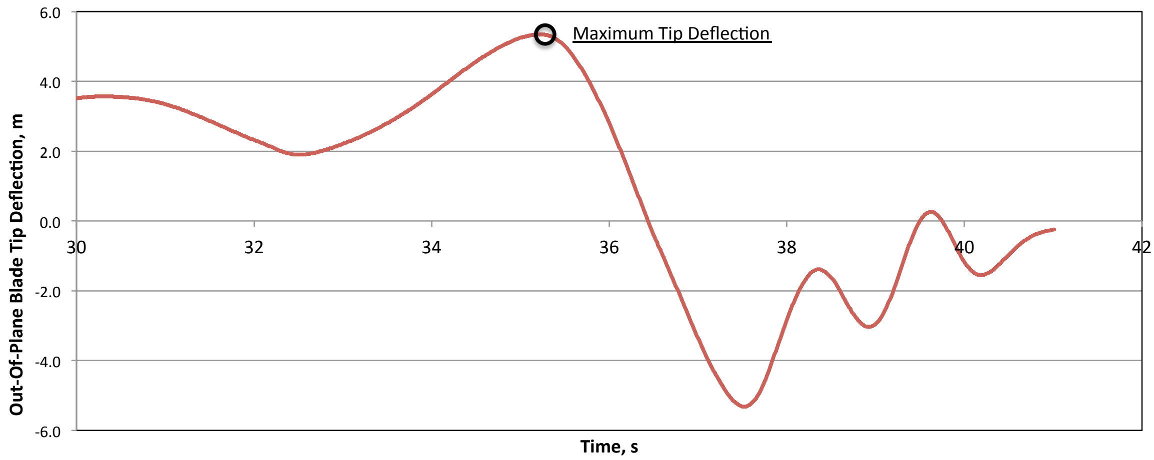

Figure 2-11: Out of Plane Tip Deflection For Worst Case Scenario (4) in DLC 2.3

$$H_o\text{=Shaft Overhang.}\cos(\theta)$$
$$H_b\text{=R.}\sin(\theta+\phi)$$

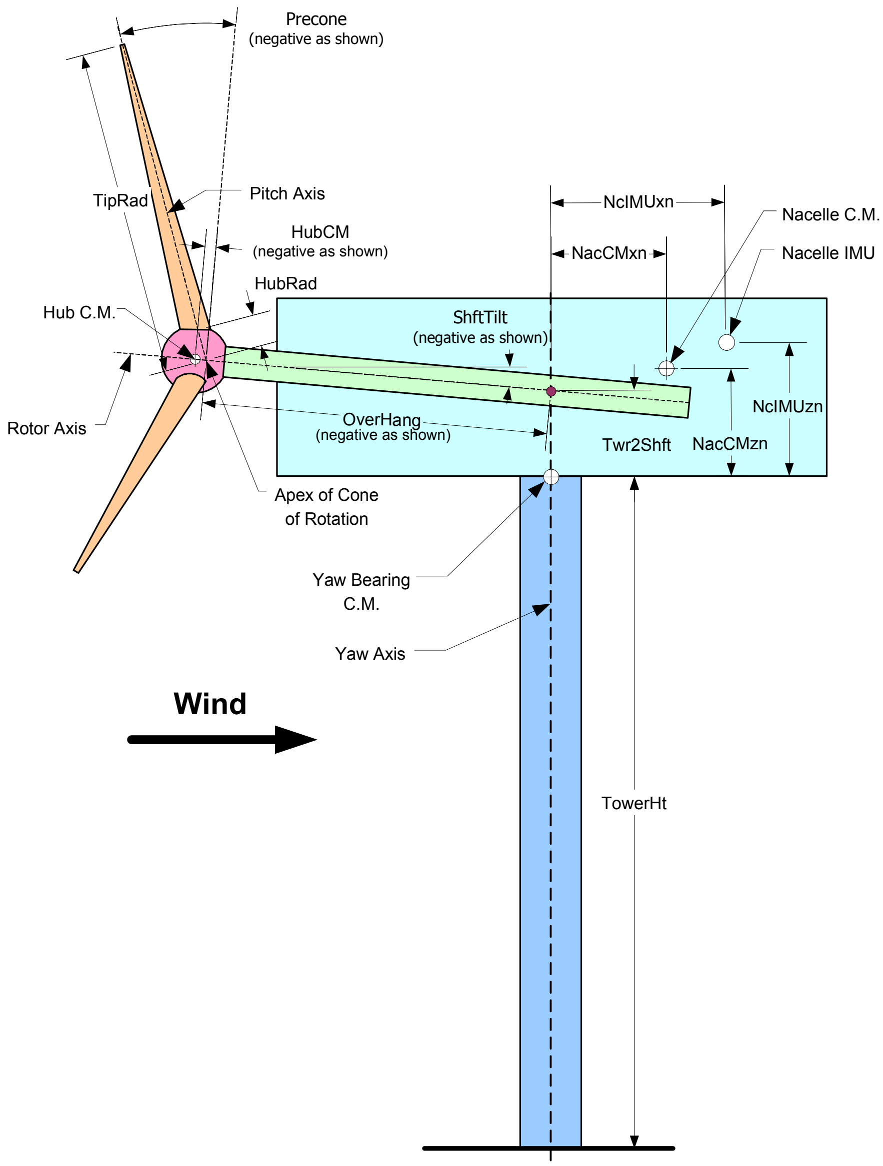

Figure 2-12: Layout of a Conventional 3-Bladed Turbine [8]

2-3-4 Buckling Analysis (Stability)

IEC 61400-1 ed. 3 states that the load carrying parts of the rotor blade should not buckle under the design load. The design load is calculated based on characteristic load derived from DLC 2.3 (ultimate loads from 50 year extreme operating gust) and partial safety factor for loads (table 2-4, γ_f). Also, material partial safety factors are applied on mean values of the stiffness to assess the buckling failure criteria

Table 2-9: Tower-Blade Clearance Calculations

Parameter	Value
Shaft Overhang, m	5.02
Shaft Tilt (θ), degrees	5.00
Precone (Φ), degrees	2.50
Approximate tower width at blade tip region, m	5.30
Rotor Radius, (R), m	63.00
Horizontal Overhang, (H_o), m	5.00
Horizontal distance between blade axis and untilted rotor plane, (H_b), m	8.22
Tower radius at clearance location (at approx. 30 m height of tower), (T_r), m	2.65
Approximate horizontal tower clearance, ($H_c = H_o + H_b - T_r$) *m*	*10.57*
Maximum Out of Plane Deflection, ($OoP_{deflmax}$), m	5.35
Maximum horizontal deflection based on perpendicular distance, (H_{defl}), m	5.30
Maximum horizontal deflection after applying partial safety factors, ($H_{deflmax} = H_{defl} \cdot \gamma_f \cdot \gamma_m \cdot \gamma_m$), *m*	*6.42*

Fundamentals of Buckling in Context of Long Slender Columns

Definition : In general buckling is the phenomena of (rapid) deformation of structures under loading. During this deformation, the elastic strain energy in the structural elements (bars, flat or curved plates, blades, columns) is transferred to local bending energy of the structure. It is characterized by sudden failure of structure when the compression stresses at a point of failure are much below the ultimate strength of the material. [19]

From this definition it becomes clear that buckling is not likely to occur under tension because the tensile stresses are not released with local bending of the structural elements. It also follows that buckling only occurs if the elastic strain energy of the loaded structure exceeds the local deformation energy of the collapsed structure.

Based on Euler buckling theory for long slender columns, the critical load at which the structure buckles is given as,

$$P_{critical} \propto \left(\frac{EI}{L^2}\right) \tag{2-10}$$

where,
E: Young's Modulus of material of the structure
I : Bending Moment of Inertia
EI: Bending Stiffness of the structure
L: Length of the structure

`Note`: The above equation for critical load is derived for an ideal column in which deflections are small, the construction is perfect and material follows Hooke's law (elastic range of load-deflection curve). Such columns are called ideal elastic columns. It is important to recognize that the maximum load that can be supported by an inelastic column may be considerably less than the critical load $P_{critical}$.

Examination of this formula reveals the following interesting facts with regard to the buckling load-bearing ability:
- Stiffness and not compressive strength of the materials of the column determines the critical load.
- The critical load is directly proportional to the second moment of area of the cross section.
- The longer the structure, the more prone is it, to buckling.

Buckling in Wind Turbine Blades

The analogy of slender columns can be applied to long slender wind turbine blades as well. Hence, the strength of a blade may be increased by distributing the material so as to increase the moment of inertia. This can be done without increasing the weight of the blade by distributing the material as far from the principal axis of the cross section as possible, while keeping the material thick enough to prevent local buckling. This bears out the well-known fact that a tubular section is much more efficient than a solid section. It should be understood that as blades become bigger and slender, instead of failing by direct compression, it may bend and deflect laterally to an extent that it can no longer sustain the shape and hence, buckles.

In general, the wind turbine blade works in much the same way as the steel I-beam, except that there are shells around the outside that form the aerodynamic shape and resist buckling and torsional loads. Utility-scale wind turbine blades use extensive sandwich construction, in both the aerodynamic shells and shear webs. To meet stiffness constraints such as deflection limits, the fiber composite materials in the broad unsupported spans of shell and shear web laminates are stiffened through the use of sandwich construction to prevent local deformation and buckling. In blade structures, the largest single role of the sandwich core is to assure adequate stability of the large panel regions against buckling. As such, the most significant attributes of the core materials are the transverse shear modulus and the core thickness [20].

Four scales of buckling mode, in general, can occur in wind turbine blade, namely:

1. Blade Length: Euler Buckling
2. Blade Chord: Section Panel Buckling
3. Laminate Thickness: Local Buckling (wrinkling, dimpling, crimping)
4. Fiber Size: Micro Buckling

These scales of buckling depend upon the thickness of the shell relative to the length of the blade, sectional properties and whether inner stiffeners exist or not. All these scales of buckling will decrease the performance of the wind turbine and even cause failure of the blade, so it is necessary to investigate the structural stability of the blade under extreme conditions.

Generally, Euler buckling and micro buckling are not an issue in wind turbine blade, the major task is to prevent buckling of section or due to inappropriate skin thickness.

Sandwich Structures and Buckling

A sandwich can be described as consisting of three main parts. Two thin, stiff and strong laminates separated by a thick core material of low density. A sandwich structure operates in much the same way as a traditional I-beam where as much material as possible is placed in the flanges situated furthest from the neutral axis.

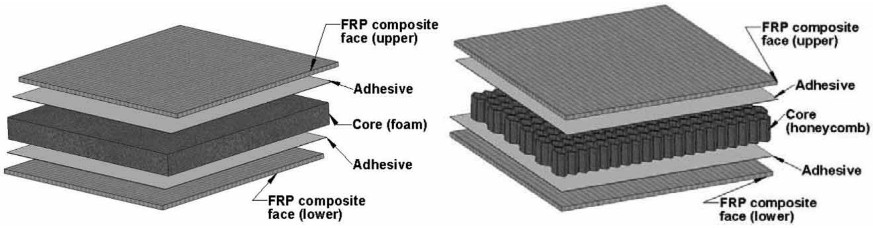

Figure 2-13: Sandwich Principle in Wind Turbine Rotor Blade [21]

The connecting web makes it possible for the flanges to act in concert and resist shear stresses. In a sandwich structure, the laminates can be considered to be the flanges of the I-beam and the core material replaces the web. The two forms differ in the way that in a sandwich, the core and laminates are dissimilar materials and the core provides continuous support for the laminates rather than being concentrated in a narrow web. When subjected to bending, the laminates act in unison, resisting the external bending moment so that one laminate is loaded in compression and the other in tension. The core resists transverse forces while at the same time supports the laminates and stabilizes them against buckling and wrinkling (local buckling). Hence the purpose of the sandwich structure is to increasing local bending stiffness of laminate to control local bending and prevent buckling.

Buckling strength is generally increased by increasing the core thickness in sandwich panels. Increasing the core thickness, increases the bending moment of inertia, which in turn increases the stiffness of the sandwich structure and hence, suppresses buckling. It has to be understood that core optimization is a natural part of blade design optimization as it affects weight, cost and structural performance.

Methodology and Scenarios Considered

The type of buckling analysis considered here is a linear one. Linear buckling (also called as Eigenvalue buckling) analysis predicts the theoretical buckling strength of an ideal elastic structure. This method corresponds to the textbook approach to elastic buckling analysis: for instance, an eigenvalue buckling analysis of a column will match the classical Euler solution. However, imperfections and non-linearities prevent most wind turbine blades from achieving their theoretical elastic buckling strength. Thus, linear buckling analysis often yields quick but non-conservative results.

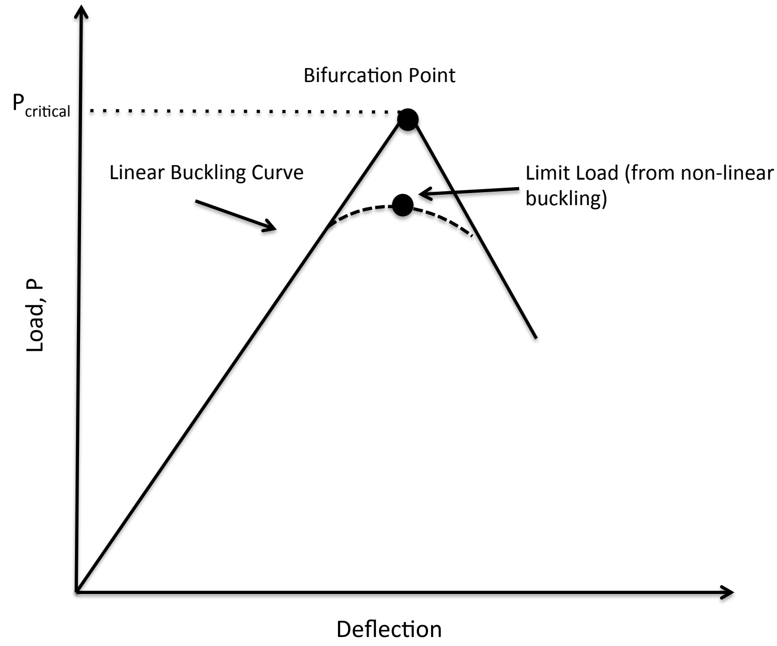

Figure 2-14: Linear Eigenvalue Buckling Curve: Qualitatively

Three main reaction loads have been considered in buckling analysis:
- Flapwise Bending Moment
- Edgewise Bending Moment
- Axial Forces.

Based on these loads, different scenarios are considered for analysis buckling. These scenarios are obtained from the DLC 2.3 (50 year extreme operating gust load case scenario).

- Maximum Flapwise Bending Moment
- Maximum Edgewise Bending Moment
- Maximum Flapwise Bending Moment+ Corresponding Axial Forces
- Maximum Edgewise Bending Moment+ Corresponding Axial Forces
- Maximum Flapwise Bending Moment+ Corresponding Edgewise Moment+ Corresponding Axial Forces.

`Note 1`: 'Corresponding' term above, means at the same time interval. Remember, the gust duration is 10.5 seconds and maximum (worst case) loads are considered during different scenarios.
`Note 2`: Different scenarios have been considered here to analyze the effect of different loading conditions on buckling. However, the last scenario where all three component of loads have been taken into consideration represents the most realistic situation of all cases. The same has been depicted in Figure 2-15.

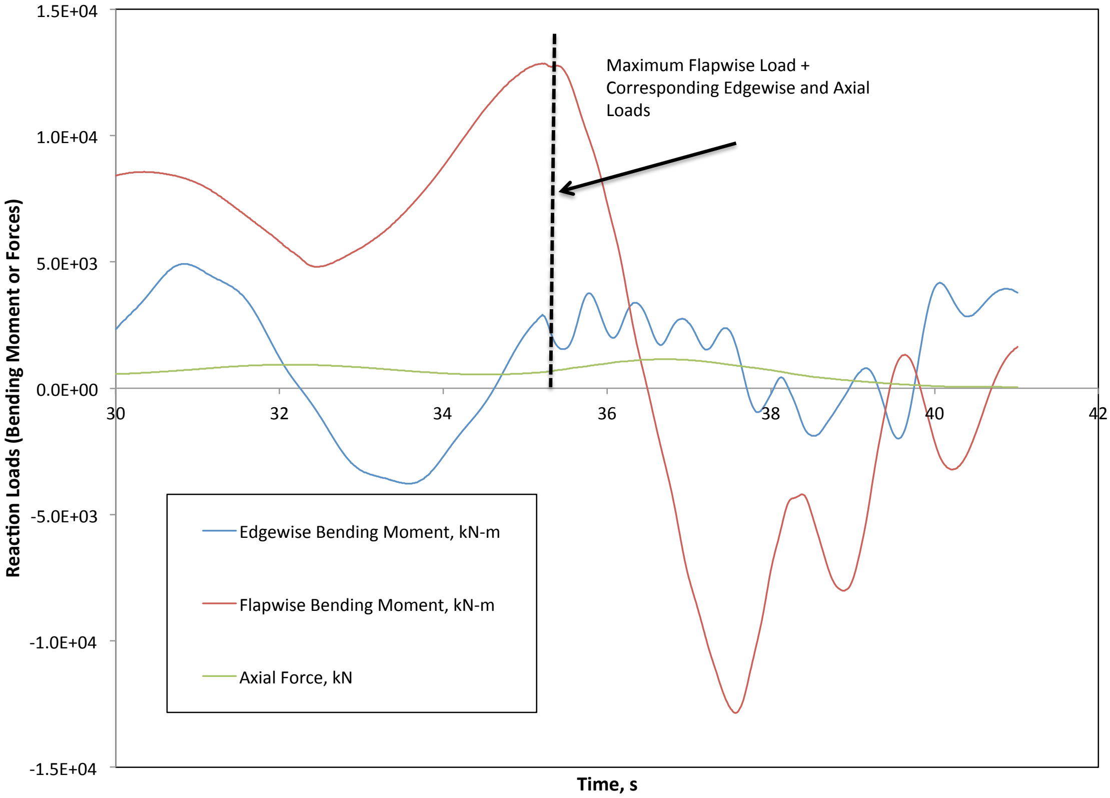

Figure 2-15: Loads Time Series at the Root Section of the Blade for DLC 2.3

Based on such set of loads (from 'FAST') for each section of the blade (total of 9 sections), the buckling load factors are calculated in ANSYS after applying corresponding set of forces.

The results calculated by the linear buckling analysis (i.e. buckling load factors) scale the loads applied in the static structural analysis. Thus, for example, if the applied flapwise, edgewise and axial load is x, y and z N respectively and if the linear buckling analysis calculates a load factor of f, then the predicted buckling load is xf, yf ,zf for the individual components. Lastly, to conclude this analysis part, blade can have infinitely many buckling load factors. Each load factor is associated with a different instability pattern (a different buckling mode). Typically, the lowest load factor is of interest.

2-3-5 Modal Analysis

Modal analysis can be used to identify natural frequencies, damping characteristics and mode shapes of wind turbine blades. The goal of this analysis in structural mechanics is to determine the natural mode shapes and frequencies of a structure during free vibration. The result of the analysis are eigenvalues and eigenvectors which come from solving the system of equations and they represent the frequencies and corresponding mode shapes. Analytically, modal analysis is a method used to solve the equations of motion in multiple degree of freedom vibrating systems. The modal analysis approach allows coupled equations of motion to be transformed into uncoupled 'modal' equations which can each be solved separately. The results from each of the modal equations are then added ('superposition') to give the complete result.

Using Newton's second law of motion, a multi-degree of freedom body can be represented, in general, with the help of following equation,

$$[M]\{\ddot{x}\} + [D]\{\dot{x}\} + [K]\{x\} = \{F(t)\} \tag{2-11}$$

where,
$[M]$ is the mass matrix representing the lumped mass of structure under consideration (in this case, the wind turbine blade).
$\{\ddot{x}\}$, $\{\dot{x}\}$ and $\{x\}$ represent acceleration, velocity and displacement vectors corresponding to degrees of freedom for each individual masses of a lumped mass system,
$[D]$ is the damping matrix,
$[K]$ is the stiffness matrix, and
$\{F(t)\}$ is the external harmonic force

To find the eigen values and eigen vectors $\{F(t)\}$ is equated to zero in 2-11 (damped free vibration).

`Note: Reference Frame Consideration`:: It has to be understood here, that the reference frame (stationary or rotating) can have impact on modal analysis as the different effects act differently on the structure, based on chosen reference frame. For example gyroscopic moment (an inertial effect that is induced in the blade due to its rotation and changes the blade rotor dynamics) should be considered in stationary reference frame while Coriolis and centrifugal forces are also present in rotating reference frame. In rotating reference frame centrifugal stiffening, which arises due to the spanwise stretching of the blade under the action of the radial centrifugal loads, must be taken into account. It should be understood that this centrifugal stiffening is different from spin-softening (another term commonly used in modal analysis which is the 'axial' softening in stiffness of a rotating blade due to non linear deformation).

The primary application for a rotating (rather than a stationary) frame of reference is in the field of flexible body dynamics where, generally, the structure has no stationary parts and the entire structure is rotating. The analysis of a standalone wind turbine blade can be one example. The primary application for a stationary (rather than a rotating) frame of reference is in the field of rotor dynamics where a rotating structure (rotor) is modeled along with a stationary support structure. Analysis of whole wind turbine would fall in this category with blades and tower/support structure as rotating and stationary part respectively.

As, only one wind turbine blade is being studied here, rotating frame of reference has been chosen for analysis.The gyroscopic effect is not included in the dynamics equations expressed in a rotating reference frame. Therefore, the results obtained in the rotating reference frame may not compare well with stationary reference frame results (due to large inertia of wind turbine blade, which would lead to gyroscopic moments).

Damping in a wind turbine blade comes from both structure and aerodynamic side (aerodynamic damping is not included in current analysis) while the stiffness is based on geometry and material property of the blade. There might be other factors like Coriolis effect and centrifugal stiffening that might change the damping and stiffness of the blade, and hence the eigen frequencies.

Again, it should be understood that damping decreases the natural frequency while stiffness increases it. In the present analysis, damping due to structure and Coriolis effect would be considered while stiffness effect due to structure and centrifugal stiffening would be considered. If the right hand side of Eq. 2-11 is equated to zero (free vibration) and if its solved for one degree of freedom system, the following relation would result between damped and undamped natural frequency (standard relation found in any vibration related book),

$$\omega_d = \omega_n . \sqrt{1 - \zeta^2} \tag{2-12}$$

where, $\zeta = \dfrac{c}{2\sqrt{k.m}}$, defined as structural damping ratio of the actual damping over the amount of damping required to reach critical damping.

The damped natural frequency is less than the undamped natural frequency, but for many practical cases the damping ratio is relatively small and hence the difference is negligible. The structural damping ratio of the blade (for all modes) that has been used in the present analysis is 0.477 % [16]. Damping due to Coriolis effect still needs to be observed, though.

This frequency (both damped and undamped) would be calculated using ANSYS and then the centrifugal stiffening effect would be incorporated to get more precise results. The following relation would be used to evaluate the final natural frequency of blade considering all the effects (damping and stiffening) in rotating reference frame, [22]

$$\omega_R = \sqrt{\Omega^2 + C.\omega^2} \tag{2-13}$$

where,
ω_R is the final blade natural frequency in rotating reference frame
Ω is the rotational speed of the blade
ω is the blade natural frequency without any centrifugal stiffening
C is the factor for non-linear effects and damping term in blade (here assumed equal to 1 due to preliminary design consideration).

The modes that are of interest in a wind turbine blade are flapwise, edgewise and torsion mode. Generally, in common practice today, blade's edgewise and torsional stiffness are far more than the flapwise one. But as blade's are becoming larger and slender these two modes are becoming more prominent.

2-3-6 Static Strength Analysis

The design values for the stresses (and strains) are determined by the requirement to prevent laminate failure with regards to short term strength. IEC 61400-1 Ed. 3 just calls for assessment of most critical limit state condition (least margin basis) as highlighted in Equation 2-3. GL guidelines, on the other hand, calls for verification of both fiber and inter fiber failure.

In this study, DLC 2.3 (50 year EOG, [4]) is used to evaluate the static strength failure criteria along with consideration of both, fiber and inter-fiber failure. The material and loads safety factors, thus, have been taken from GL 2010 [15] (for this analysis only). The same have been tabulated in Table 2-4. As inter-fiber failure is not mentioned in IEC standards, GL guidelines are used to evaluate it.

This analysis is performed in ANSYS with emphasis on two major criterias for fiber and inter-fiber failure: Maximum stress failure criteria ($S_{maxcriteria}$) and Tsai Wu Strength Index Failure criteria ($TWSI_{criteria}$) respectively.

Fiber failure occurs when dominant strain parallel to the fiber direction exceed the tensile or compressive strength capacity of the individual fibres. Hence, longitudinal strength has a dominant role during fibre failures. Fibres generally do not yield, they experience brittle fracture.

Inter-fibre failure occurs in the matrix (or adhesive) between adjacent plies/ laminae due to shear stresses (in fibre plane) and/or transverse stresses acting perpendicular to direction of fibre orientation ("out of plane" of fibre lay up). This failure can lead to separation of the individual laminae/ply forming a de-lamination that can grow further once initiated. The inter-fibre failure modes have been depicted in Figure 2-16. Mode 1 is due to the transverse tensile stresses while Mode 2 and 3 are due to in-plane shear stresses.

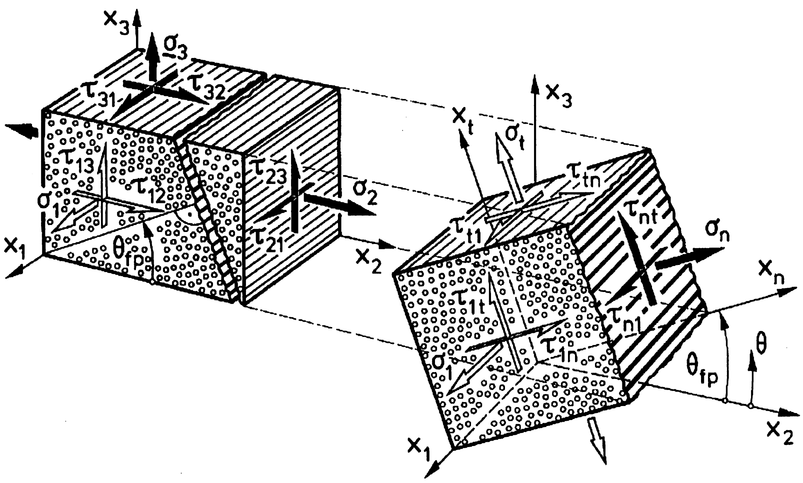

Figure 2-16: Inter Fibre Failure modes According on Puck [23]

`Note:` Three-dimensional stresses on a UD composite element. (x1,x2,x3) coordinate system is fixed to fibre direction (x1), laminate mid-surface (x2) and thickness direction (x3). The (x1,xn,xt) coordinate system is rotated by an angle θ_p from the x2 direction to the xn direction which is normal to the fracture plane. The inter-fibre fracture is influenced by the the three stresses σ_n (Mode 1), τ_{nt} (Mode 2), τ_{n1} (Mode 3) only (according to Mohr's strength theory).

During evaluation of fibre failure using $S_{max.criteria}$, only the longitudinal components of strength in the direction of fibres are used. All the shear and transverse component of the strength values are set to very high value (assuming no failure mode occurs because of those). For evaluation of inter-fibre failure using $TWSI_{criteria}$, all the available strength values have been taken especially the shear and transverse strength. The core material strength has been neglected during both the analysis (set to a very high value, so that it doesn't fail) as sandwich structures are not the topic of interest during this analysis.

The maximum stress failure criterion, is a non-interactive failure criterion applied to an individual composite ply. Non-interactive means that the $S_{max.criteria}$ evaluates failure based on a single stress component and does not take into consideration a multi-axial stress state and how the combination of different stress components affect the failure initiation in a composite ply. The $S_{max.criteria}$ is most useful in composite laminates that utilize 0/90/45 plies exclusively, and are loaded in a predominately uni-axial manner.

$$Failure\ Index\ _{Smax} = maximum\ of \begin{cases} \frac{\sigma_{xt}}{\sigma_{xt}^f}\ or\ \frac{\sigma_{xc}}{\sigma_{xc}^f} & whichever\ is\ applicable \\ \frac{\sigma_{yt}}{\sigma_{yt}^f}\ or\ \frac{\sigma_{yc}}{\sigma_{yc}^f} & whichever\ is\ applicable \\ \frac{\sigma_{zt}}{\sigma_{zt}^f}\ or\ \frac{\sigma_{zc}}{\sigma_{zc}^f} & whichever\ is\ applicable \\ \frac{\sigma_{xy}}{\sigma_{xy}^f} \\ \frac{\sigma_{yz}}{\sigma_{yz}^f} \\ \frac{\sigma_{zx}}{\sigma_{zx}^f} \end{cases} \quad (2\text{-}14)$$

where,
- terms with subscript 'xt', 'yt', 'zt' represent tensile stresses in x, y and z direction respectively.
- terms with subscript 'xc', 'yc', 'zc' represent compression stresses in x, y and z direction respectively.
- terms with subscript 'xt', 'yt', 'zt' and superscript 'f' represent failure tensile stresses in x, y and z direction respectively.
- terms with subscript 'xc', 'yc', 'zc' and superscript 'f' represent failure compression stresses in x, y and z direction respectively.
- terms with subscript 'xy', 'yz', 'zx' represents shear stresses in x-y, y-z and z-x plane respectively.
- terms with subscript 'xy', 'yz', 'zx' and superscript 'f' represents failure shear stresses in x-y, y-z and z-x plane respectively.

`Note:` The compression stresses take negative value and tensile ones positive. If no information is provided, zero is taken as the default value. Also, Failure Index > 1, to prevent failure.

As, only longitudinal failure mode is considered here, $S_{max.criteria}$ would give a good insight into fibre failure.

The $TWSI_{criteria}$ is a quadratic, interactive failure criterion used to evaluate failure in an individual composite ply. Interactive means that the Tsai Wu failure criterion evaluates failure based on a combination of stress components and is designed to take into consideration a multi-axial stress state and how the combination of different stress components affect the failure initiation in a composite ply. Quadratic means that the individual stress components in each term of the failure criterion are either squared or multiplied by another (different) stress component.

$$\begin{aligned} Failure\ Index_{\ TWSI} = &-\frac{(\sigma_x)^2}{\sigma^f_{xt}.\sigma^f_{xc}} - \frac{(\sigma_y)^2}{\sigma^f_{yt}.\sigma^f_{yc}} - \frac{(\sigma_z)^2}{\sigma^f_{zt}.\sigma^f_{zc}} + \frac{(\sigma_{xy})^2}{(\sigma^f_{xy})^2} + \frac{(\sigma_{yz})^2}{(\sigma^f_{yz})^2} + \frac{(\sigma_{zx})^2}{(\sigma^f_{zx})^2} \\ &+ \frac{C_{xy}.\sigma_x.\sigma_y}{\sqrt{\sigma^f_{xt}.\sigma^f_{xc}.\sigma^f_{yt}.\sigma^f_{yc}}} + \frac{C_{yz}.\sigma_y.\sigma_z}{\sqrt{\sigma^f_{yt}.\sigma^f_{yc}.\sigma^f_{zt}.\sigma^f_{zc}}} + \frac{C_{zx}.\sigma_z.\sigma_x}{\sqrt{\sigma^f_{zt}.\sigma^f_{zc}.\sigma^f_{xt}.\sigma^f_{xc}}} \\ &+ (\frac{1}{\sigma^f_{xt}} + \frac{1}{\sigma^f_{xc}}).\sigma_x + (\frac{1}{\sigma^f_{yt}} + \frac{1}{\sigma^f_{yc}}).\sigma_y + (\frac{1}{\sigma^f_{zt}} + \frac{1}{\sigma^f_{zc}}).\sigma_z \end{aligned} \tag{2-15}$$

`Note`: 'C_{ij}' terms represent the coupling coefficients between different stress states.
When compared to the Max Stress failure criterion, the Tsai Wu failure criterion will typically provide more accurate first ply failure predictions for a composite ply that is part of a composite laminate that is loaded by multiple stresses (bi-axial normal stresses or a combination of normal and in-plane shear stress). Engineering judgment would be used to reason that most of the failures predicted by the Tsai Wu failure criterion are matrix or inter-fibre failures. The one exception would be laminae that are predominately loaded in longitudinal tension or compression.

2-4 Fatigue Analysis

The fatigue design of a rotor blade has to be in agreement with the design requirements as described in the IEC 61400-1 ed. 3 [4] or in the widely accepted national recommendations from e.g. the GL (Germanischer Lloyd) [15]. In this report GL guidelines have been used as very elaborate details have been given, explaining fatigue requirement in detail.

Fatigue damage calculation is only done for spar caps ('girder' in blade terminology) and trailing edge tape as they are considered to be major load bearing part in a wind turbine blade (although bond lines, root connection and shear webs are also important from structural ambit). Three types of reaction loads are considered for fatigue analysis: two bending moments (flap-wise and edgewise) and an axial force (due to blade rotation). Finally, torsion and shear forces (flap and edge) have been neglected in fatigue study as all the forces are applied at (or very close to) shear center of the cross section to be analyzed. It should be however, noted, that there is torsion due to out-of-plane and in-plane deflections (coupled response) and this would produce extra load in blade. During large deflections, large torsional peaks could be noted and hence would play a critical role in fatigue analysis as blades become more flexible (and larger). The loads acting on the rotor blade are typical in two ways: first they are subjected to extremely high number of load cycles (typically of the order of 10^8 to 10^9 loading-unloading fatigue cycles during their life of 20 years [24]) and secondly high variability of loads due to stochastic nature of wind (due to the phenomenon of turbulence).

Before jumping onto the actual analysis, lets take a brief overview of some typical terminologies used in fatigue world:

- R- ratio: Wind turbine blades are subjected to highly variable loads as described above, but the fatigue load predictions are based on constant amplitude data. Typically 'rainflow counting' method is used to convert the variable amplitude data to a bunch of constant amplitude cycles. It has to be understood clearly here, that the amplitude of the cyclic loading has a major effect on the fatigue performance and this amplitude is expressed as the R-ratio value, which is the minimum peak stress divided by the maximum peak stress. To determine the type of loading in a particular component of a blade, R-value is often used. For eg. trailing edge of the blade is subjected to a load governed by R=-1 value (tension-compression cycles) while, for spar cap on suction side, R=10 (compression-compression cycles) might be a typical value. It should be noted here that, $R < 0$ represents tension-compression cycles, $0 < R < 1$ represents tension-tension cycles and $R > 1$ represents compression-compression cycles.

- Rainflow Counting: The rain-flow counting method is used in the analysis of fatigue data in order to reduce a spectrum of varying stress into a set of constant amplitude stress reversals. Its importance is that it allows the application of Miner's rule in order to assess the fatigue life of a wind turbine blade subjected to complex loading.

- S-N Curve: A graphical representation of stress, S (or load per unit width or thickness, strain or displacement) occurring in a particular specimen with respect to the number of cycles to failure, N, is depicted with the help of S-N diagram. As, cycle amplitude has a significant effect on fatigue, each S-N diagram is plotted for a particular R-value. The slope of the S-N diagram, generally, determines the fatigue property of a material. A flat curve with small slope is considered to have better fatigue properties than a steep profiled S-N curve [11]. Typically, for glass fibre laminate with epoxy resin, the slope of S-N line is -10 in log-log scale [15] (minus being representative of the fact that stress decreases as number of cycles to failure increase). It has to be noted again that, typically, S-N diagram is plotted on a log-log scale.

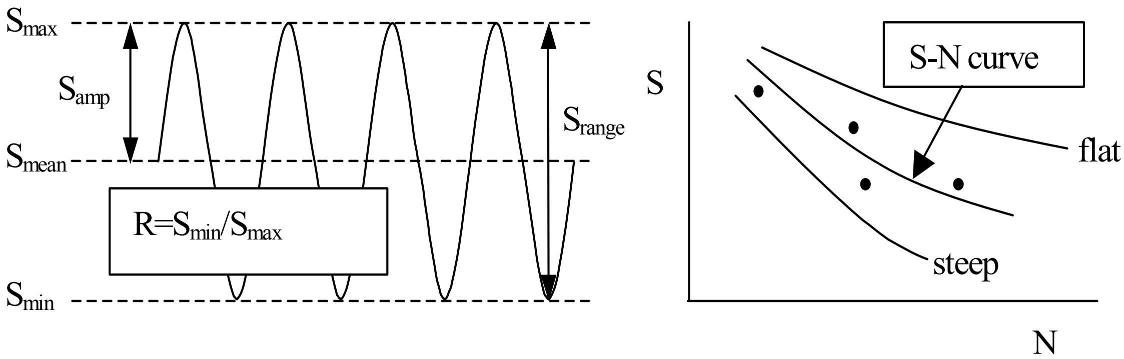

Figure 2-17: Representation of Constant Amplitude Cycle and S-N Diagram in Fatigue Terminology [11]

`Note:` Although, number of cycles to failure, N, is a dependent variable; traditionally, it is plotted on the abscissa instead of the ordinate. But it should be understood that for formulations and curve fitting, N, should always be considered as the 'dependent' variable. Also, there are are several short comings of S-N fatigue data: First, the conditions of the test specimens do not always represent actual service conditions. For example, blades with rough surface conditions from corrosion or bugs which differs from the condition of the test specimens will have significantly different fatigue performance.

Furthermore, there is often a considerable amount of scatter in fatigue data. Since there is considerable scatter in the data, a probabilistic confidence boundary is often applied to the S-N curves to provide conservative values for the design of components.

The general formulation for S-N curve is,

$$\begin{aligned} logN &= a + b.logS \\ or\ N &= C.S^b \end{aligned} \tag{2-16}$$

where,
- $C=10^a$
- S can be either maximum stress, amplitude stress, or equivalent strain. For the same reason, an additional R-value is necessary to complete the definition of constant amplitude fatigue cycle.
- 'b' is the slope of the S-N regression line in log-log scale as formulated in equation 2-16 (generally, of the order of -9 to -10 for glass fibre composites).

- Constant Life Diagrams (CLD): CLD is a projection of a 3D plot in a 2D plane, connecting lines of same predicted fatigue life, as a function of mean stress(abscissa) and stress amplitude (ordinate). The projection is of a constant amplitude (constant R-ratio) data in a plane perpendicular to life axis (N). The same has been depicted via Figure 2-18. The different S-N planes all intersect with a line representing zero stress. This axis is called the life axis. Straight lines from origin are of lines of constant R-value as mean stress and stress amplitude are proportional to each other. The ordinate of CLD, is located at R=-1 line and abscissa at R=1 line. [11].

  In composites, the CLD is not symmetrical about the R=-1 line as static strengths in tension and compression are not equal. For composites, the fatigue damage and the failure mechanism in tension are governed by fibre layup where as in compression, they are governed by the matrix and matrix fibre interaction.

- Shifted Linear Goodman Diagram (sLGD): This is a one of the forms of CLD and is defined as a design standard for fatigue in GL guidelines [15]. Compared to the classical Goodman diagram, the top has moved to the mean of ultimate tensile strength (UTS) and ultimate compression strength (UCS) and for N=1 cycles, the ordinate also takes the same value (See Figure 2-19)

  For any cycle with mean and amplitude stress (S_{mean} and S_{amp}), an equivalent stress (S_{eq}) is derived at R=-1 line. The allowable number of cycles is related to this equivalent S_{eq} via experimental data R=-1 using,

$$N = \left[\frac{R_{k,t} + R_{k,c} - 2.\gamma_{ma}.S_{k,M} - R_{k,t} + R_{k,c}}{2.\gamma_{mb}.S_{k,A}} \right]^m \tag{2-17}$$

  where,
  $S_{k,M}$= mean value of the characteristic actions (mean stresses)
  $S_{k,A}$ = amplitude of the characteristic actions ($\frac{|S_{k,max} - S_{k,min}|}{2}$) (amplitude stresses)
  $R_{k,t}$=characteristic short-term structural member resistance for tension
  $R_{k,c}$=characteristic short-term structural member resistance for compression

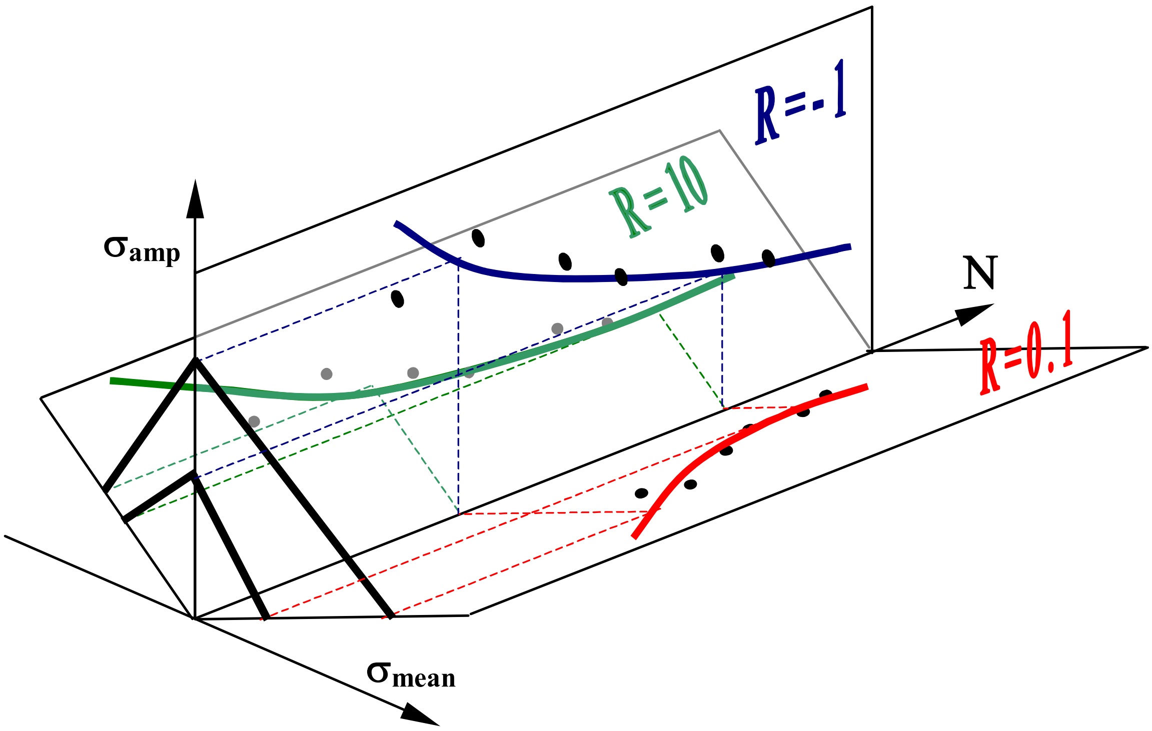

Figure 2-18: Projection of Constant Amplitude S-N curve onto a Constant Life Diagram [11]

m =slope parameter m of the S/N curve (of the order of 10 for glass fibres with epoxy)
N =permissible (allowable) load cycle number
γ_{Ma}=partial safety factor for the material=1.35*1.35*1.1*1.1*1.0 (as per Section 5.5.2.4, short-term strength, GL guidelines [15])
γ_{Mb} partial safety factor for the material=1.35*1.1*1.0*1.0*1.0 (Spar Cap) or 1.35*1.1*1.0*1.0*1.1 (trailing Edge Tape); (as per Section 5.5.2.4, fatigue strength, GL guidelines [15])

The formulation of Equation 2-17 can be derived form Figure 2-20.

- Damage Prediction and Palmgren-Miner Sum Rule: Failure is defined as the instance when the component can no longer bear the intended load. Damage, in general, should refer to strength and stiffness degradation in addition this failure life. It represents all kinds of physical deterioration of material, irrespective of its effect of material performance. This damage can either be based cumulatively, empirically or in terms of micro mechanics. Miner sum rule is a cumulative damage prediction model used widely in fatigue industry owing to its simplicity. The formulation is,

$$D = \sum \frac{n_i}{N_i} \tag{2-18}$$

where,
D is the damage parameter (failure happens when damage=1)
n_i are the actual number of fatigue cycles in a specimen/component for a particular type of

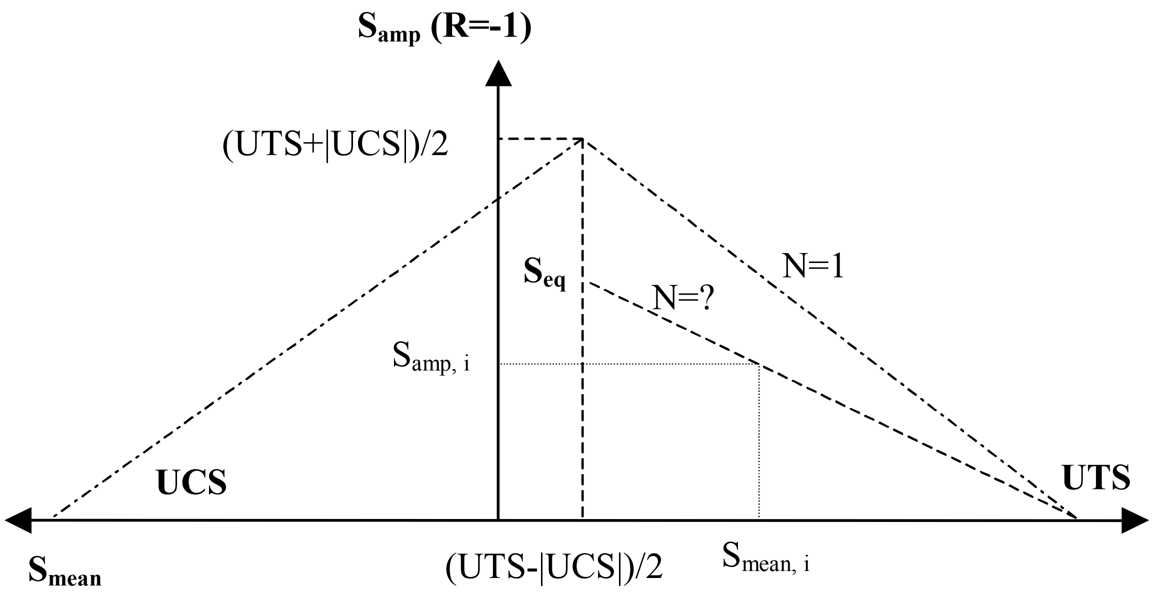

Figure 2-19: Shifted Linear Good Diagram Representation Without Partial Safety Factors

loading (R-value)
N_i is the corresponding number of fatigue cycles to failure (for that particular type of loading).

It has to be, however, understood that Miner sum rule doesn't take into consideration the order of load sequences and hence its effect of fatigue life is neglected. Also, damage doesn't relate to strength or stiffness in this approach of life prediction. It just conveys the information if the material is intact or failed.

Figure 2-21 gives an essence of the terminologies used above along with their interconnections, capturing fatigue calculations.

Some Notes on Stress Factors, Non-Linearity and Load Case Hours Loads (bending moment and forces) achieved from aeroelastic code (FAST) needs to be converted to corresponding stresses to evaluate fatigue life. This is done via finite element blade model in ANSYS as defined in section 2-2. Preliminary approach of deriving the 'linear stress factor' has already been described in Chapter of 'Coordinate System and Importance of Shear Center'. It has to be understood here, that, theoretically speaking conversion of bending moments and axial forces to stresses is done by the following equation (considering linear elastic limit of operation from material perspective: Hooke's law):

$$\sigma_z = \frac{M_{x'}.y'}{I_{x'x'}} + \frac{M_{y'}.x'}{I_{y'y'}} + \frac{F_z}{A} \tag{2-19}$$

where,
$M_{x'}$, $M_{y'}$ and F_z are respectively, the edgewise bending moments, flapwise bending moments

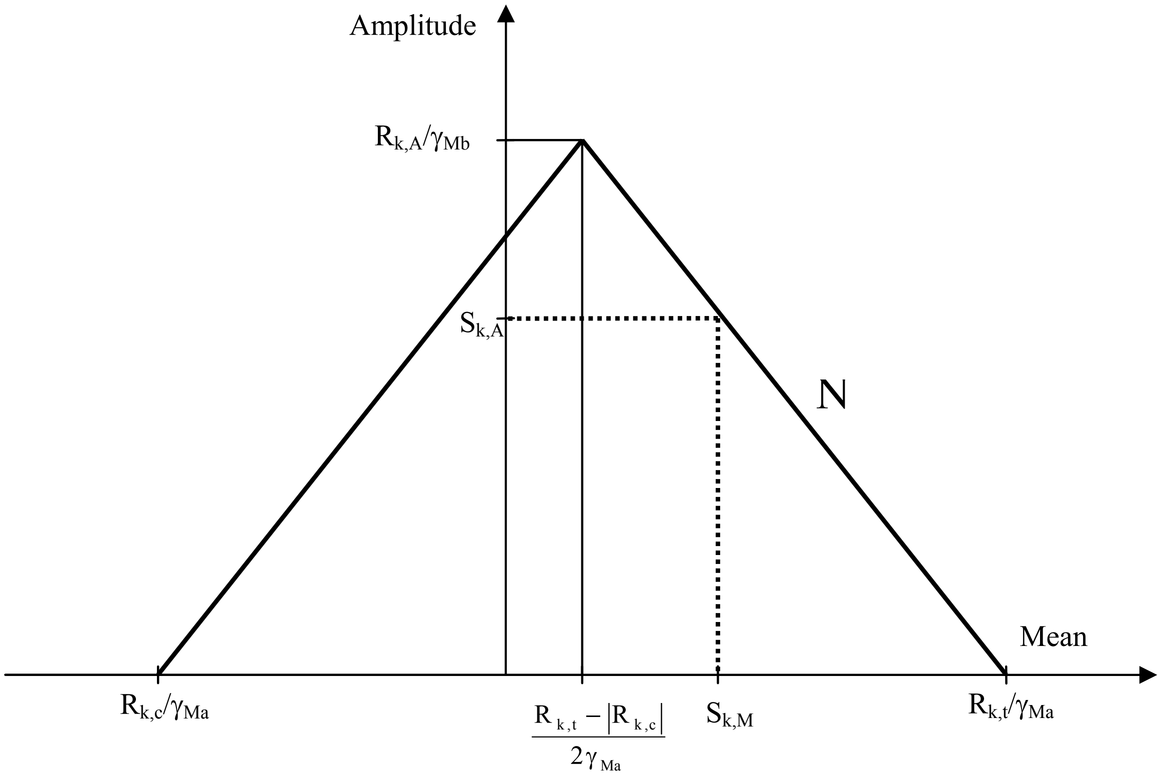

Figure 2-20: Shifted Linear Good Diagram Representation With Partial Safety Factors

and axial forces.
$I_{x'x'}$ and $I_{y'y'}$ are bending moment of inertias about x' and y' axis respectively (refer to appendix A for directions).
x' and y' are the distance along neutral axis (in this case it is structural principal axis as defined in Figure A-1(a)). They should either refer to trailing edge tape or spar cap location for the current analysis.
A is the cross-sectional area of the section under consideration (excluding the hollow part where there is no material).

Note, that this formula should be applied to each section of interest in the blade and should duly consider the tensile and compressive nature stresses based on the location (and bending moment conventions) and change the signs of individual components in Eq. (2-19), accordingly. This equation is mentioned here to give a glimpse to the reader as to what goes behind; for the conversion of load (moments and forces) time series to stress time series.

The Eq. (2-19) has not been used explicitly in the current analysis, but the stress factors $(\frac{y'}{I_{x'x'}}, \frac{x'}{I_{y'y'}}$ and $\frac{1}{A})$ have been calculated based on application of loads in Blade FE model The following approach has been used to device the stress factor matrix :

For Spar Cap

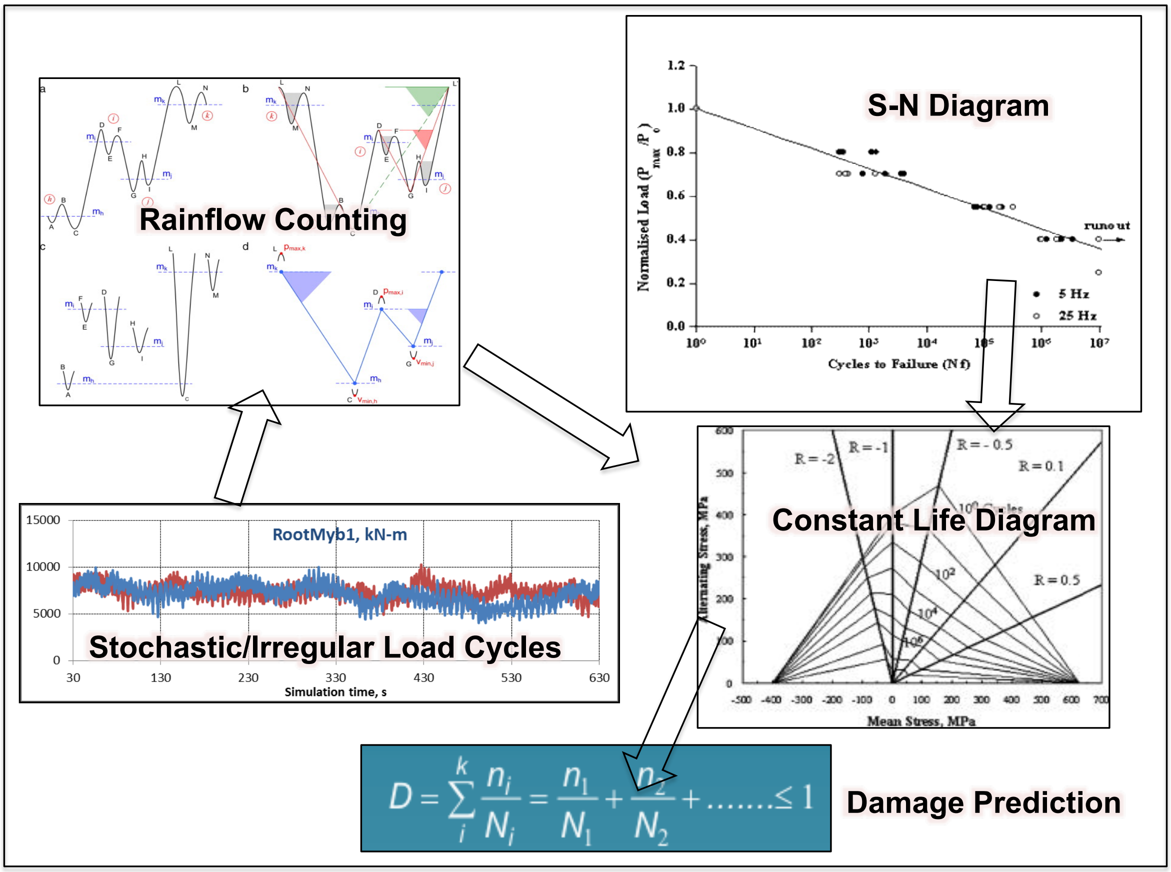

$$D = \sum_{i}^{k} \frac{n_i}{N_i} = \frac{n_1}{N_1} + \frac{n_2}{N_2} + \ldots\ldots \leq 1$$

Figure 2-21: Typical Flow in Fatigue Damage Prediction for a Wind Turbine Composite Blade

1. For a 'flapwise bending moment' of +1kN-m, a node (in sparcap) with maximum value of longitudinal (span-wise) stress is found out in ANSYS. This would be called as a stress factor in spar-cap due to flapwise bending moment ($SFSC_{flap}$).
2. Now, at the same node (as above), longitudinal stress is found out for an 'edgewise bending moment' of +1kN-m. This would be called as a stress factor in spar-cap due to edgewise bending moment ($SFSC_{edge}$).
3. Again, at the same node, longitudinal stress is found out for an 'axial force' of +1kN. This would be called as a stress factor in spar-cap due to axial force ($SFSC_{axial}$).

Now, these three types of stress factors would be evaluated at each of the nine blade spans where load time series would be known from FAST. Hence this would form a [9X3] stress factor matrix with rows representing spans and columns representing type of reaction loads.

For Trailing Edge Tape:

1. For an 'edgewise bending moment' of +1kN-m, a node (in trailind edge tape) with maximum value of longitudinal (span-wise) stress is found out in ANSYS. This would be called as a stress factor in trailing edge tape due to edgewise bending moment ($SFTE_{edge}$).

2. Now, at the same node (as above), longitudinal stress is found out for an 'flapwise bending moment' of +1kN-m. This would be called as a stress factor in trailing edge tape due to edgewise bending moment ($SFTE_{flap}$).

3. Again, at the same node, longitudinal stress is found out for an 'axial force' of +1kN. This would be called as a stress factor in trailing edge tape due to axial force ($SFTE_{axial}$).

A same [9X3] stress factor matrix would be constructed for trailing edge tape. The same have been depicted in Table 2-11 and 2-12. Stress factor in spar cap is for the pressure side (maximum positive stress occurs on this side). It has to be noted, that all the fatigue calculations would represent the damage in these respective nodes at each cross section for a spar cap or trailing edge tape. Also, to be understood here is that +1kN-m flapwise moment produces positive stresses on pressure side of spar cap. If this moment were to be made -1kN-m, the pressure side of spar cap would have negative stresses (with absolute value remaining the same).

A sensitivity analysis is done at all the spans to figure out the best possible distance for application of force from the 'analyzed' location. This is done considering the applied force location should not be too close to the 'analyzed' location so as to avoid any stress concentration due to applied force (concentrated load) and not too far so that the force is not applied to far away from the shear center of the analyzed section. Figure 2-22 and 2-23 shows 3 m as the chosen distance for application of force from the analyzed location. It can be different for different sections. The other spans can have different value and is not shown here as the scales of stress factor are of different order which makes it difficult to put it on one plot.

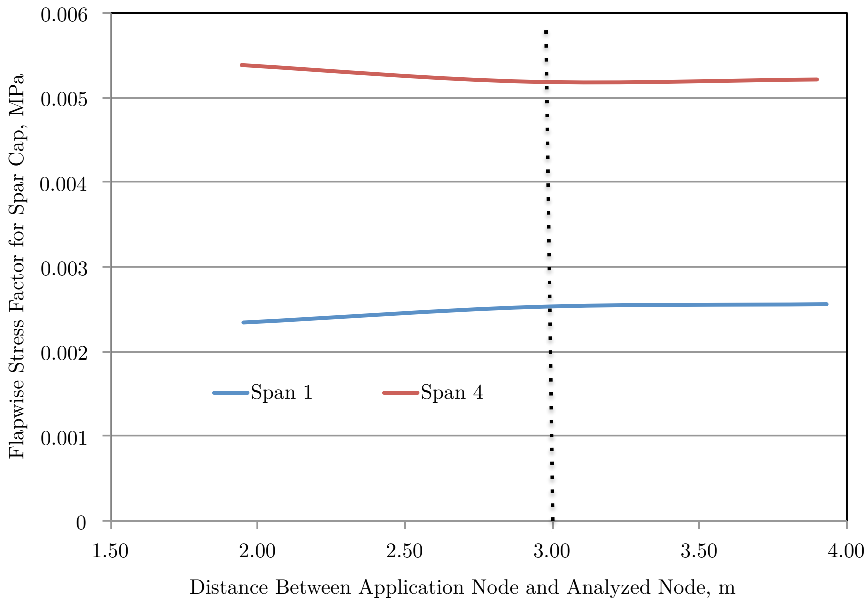

Figure 2-22: Sensitivity Analysis on Location of Force Application in Flap-wise Mode for Spar Cap

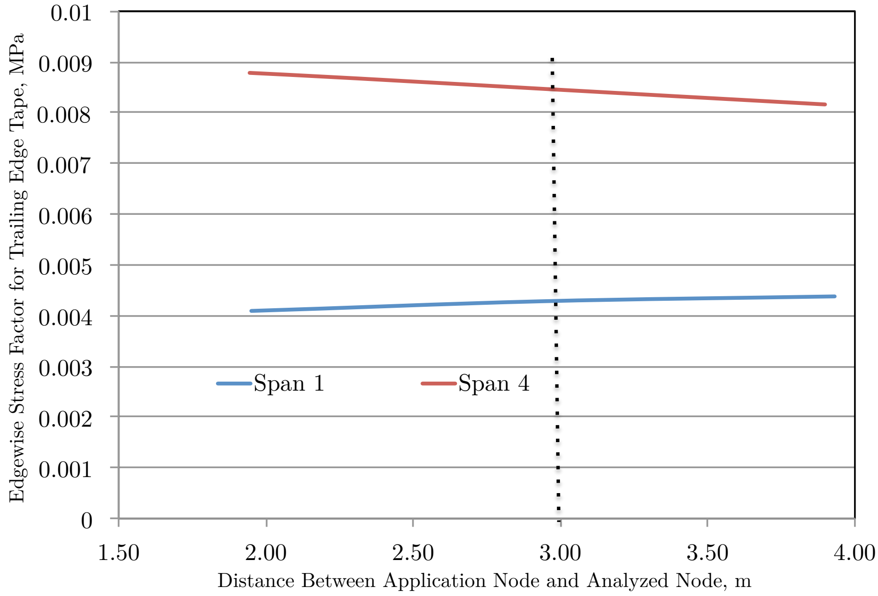

Figure 2-23: Sensitivity Analysis on Location of Force Application in Edge-wise Mode for Trailing Edge Tape

A linear analysis underlies the simplification that loading conditions in a blade are deformation independent, i.e. if a deformation at wind speed of 1 m/s is x then at 100 m/s , the deformation would be $100x$. Hence, the deformation history between the two considered conditions plays no role. Whereas for a non-linear analysis, the deformation history plays a major role. The shape or the stiffness of the blade at 100 m/s may be different to 100 times the value at 1 m/s wind speed. Therefore, to take care of non-linear effects the ultimate load is split in several small sub-loads and deformation is observed at each of these sub-loads. Nonlinear structural behavior in wind turbine blades can arise from a number of causes, which can be grouped into these two principal categories:

1. Geometric Non-Linearity: If a wind turbine blade experiences large deformations, its changing geometric configuration can cause the structure to respond non-linearly. Just to bring an analogy, an example would be the fishing rod shown in Figure2-24 . Similary, large wind turbine loads can cause it to deflect laterally so that the small deformation assumption might become invalid. This is typically the case in longer blades which is the scenario in current project (Blade length of 61.5 m). Hence, geometric nonlinearity can be thought of as, one, that is characterized by 'large' displacements and/or rotations.

2. Material Non-Linearity: Nonlinear stress-strain relationships are a common cause of nonlinear structural behavior in composite blade. Many factors can influence a material's stress-strain properties, including load history (as in elasto-plastic response), environmental conditions (such as temperature), and the amount of time that a load is applied (as in creep response). Typically, in wind turbine composite blade, spar caps (uni-directional material) when loaded in tension produce a linear stress-strain diagram with brittle failure while for shear webs ($\pm$ 45^o fibre orientation), the same behavior is

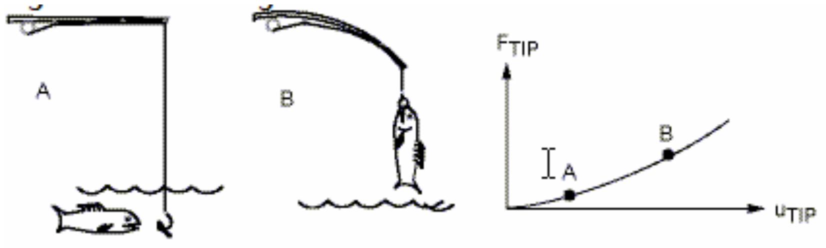

Figure 2-24: Geometric Non-Linearity Demonstrated Via Fishing Rod [18]

non-linear (see Figure 2-25).

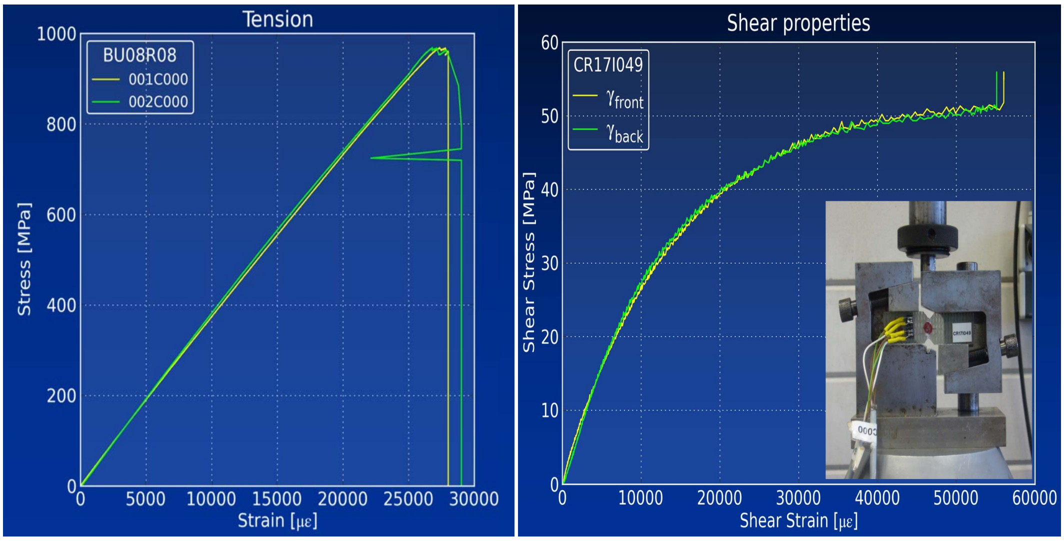

Figure 2-25: Stress-Strain Curve in Composites Representing Tensile and Shear Properties [25]

It can be understood from Figure 2-25 that material non-linearity gives relaxation in stresses for the same amount of strain. It should also be understood that, w.r.t material property, the composites in wind turbine blade application, are operated in linear range to withstand fatigue. As can be imagined, if the material goes to non-linear range even for a little bit, the amount of hysteresis loss and heat generated (mechanical) due to fatigue can be immense leading to breakdown of blade structure. In the end, glass-fiber is supposed to work under its linear limits (whichever part of blade it is used); and hence, any non-linearity due to material is ignored.

Geometric non-linearity is an area in large wind turbine blades, which cannot be avoided to a certain extent (unless a blade is made predominately from carbon fibre material). Hence this non-linearity was considered and its effect was analyzed in axial stresses (along the span of the blade) due to flapwise bending moments in the blade arising from aerodynamic loads. This was done in ANSYS as the ultimate flapwise loads from DLC 2.3 were divided into small loads using several steps. In each load-step the stiffness and mass matrix are recalculated to account for non-linear effects of geometry. The effect of the geometric non-linearity, was then, analyzed on the longitudinal stress. The same has been captured in Table 2-10. It

Table 2-10: Stress Factor for Flapwise Loading Due to Geometric Non-Linearity

Span No.	*Flap-wise Non-linearity, P %*	*Flap-wise Non-linear factor, NLF=(100-P)/100*
Span1	0.29	0.997
Span2	2.50	0.975
Span3	1.87	0.981
Span4	0.87	0.991
Span5	0.80	0.992
Span6	1.40	0.986
Span7	2.87	0.971
Span8	3.65	0.964
Span9	7.16	0.928

can be observed that the maximum non-linear effect is observed near the tip of the blade (span 9), due to the maximum deflection occurring there. These factors (Table 2-10) need to be multiplied with axial stresses (z-direction: along the blade span) obtained from linear analysis of flapwise component ONLY. Hence, the Fatigue Equivalent Damage will, then, be evaluated in 'Octave' [26] with the reduced stresses due to this non-linearity. It should be understood that consideration of geometric non-linearity here, does not lead to any qualitative changes in the distributions of the stresses under investigation. Consequently, it dictates only an appreciable quantitative change in the values of these stresses; arising due to flapwise moments. Consideration of geometric non-linearity gives rise to a reduction in span wise longitudinal stresses. The effect of geometric non-linearity in case of edgewise loading was found to be negligible as the edgewise stiffness prevents the blade from having large deflections.

Based on above linear stress factor description and geometric non-linear effects the final stress factors for spar cap and trailing edge tape are given in Table 2-11 and 2-12. Please note that there is no TE tape for 9^{th} span (TE tape ends at 45 m), hence the factor there is zero.

Load case hours are based on wind speed distribution of a site (in this case IJmuiden, Netherlands) and cut-in, cut-out velocity of the wind turbine. This basically represents the number of hours (in a year), a turbine is going in operate in different modes for fatigue life calculation i.e. for power production, start up and shutdown operation. Figure 2-13 represents the yearly distribution of wind speed at hub height (90 m). Based on this, individual number of hours for different modes of operation can be derived. Following points need to be considered while making load case hours file to be used in damage prediction calculation:

- Load case hours file will contain hours for power production (16 bins), start up (3 bins) and shutdown (3 bins) sequences 'assuming' the whole turbine life (20 years) is captured by these design load cases ONLY.

Table 2-11: Stress Factor to be Used in Fatigue Analysis for Spar Cap

	Final Stress Factors in Spar Cap, MPa/(kN-m)		
Span	$SFSC_{flap}$	$SFSC_{edge}$	$SFSC_{axial}$
1	2.52E-03	2.83E-04	1.61E-03
2	2.95E-03	-5.93E-05	1.81E-03
3	3.70E-03	7.57E-04	1.02E-03
4	5.14E-03	-4.05E-03	2.80E-03
5	5.34E-03	-3.17E-03	1.77E-03
6	1.21E-02	-5.19E-03	2.28E-03
7	2.08E-02	-7.06E-03	2.64E-03
8	4.52E-02	-1.21E-02	4.49E-03
9	2.08E-01	-2.83E-02	1.31E-02

Table 2-12: Stress Factor to be Used in Fatigue Analysis for Trailing Edge Tape

	Final Stress Factors in Trailing Edge Tape, MPa/(kN-m)		
Span	$SFTE_{flap}$	$SFTE_{edge}$	$SFTE_{axial}$
1	-2.16E-05	4.28E-03	2.16E-03
2	-1.54E-03	7.04E-03	8.54E-04
3	9.77E-04	8.46E-03	2.89E-04
4	5.66E-03	8.47E-03	-1.15E-05
5	7.36E-03	1.42E-02	-4.41E-04
6	7.50E-03	2.11E-02	-8.93E-04
7	8.64E-03	2.58E-02	-9.59E-04
8	9.01E-03	2.63E-02	-8.68E-04
9	0	0	0

- For velocity of 3.4 m/s, 11.7 m/s and 24.1 m/s, the subsequent hours from site data have been subtracted to account for the startup and shutdown behavior.

- Power production load cases will incorporate all the three yaws errors and they are divided evenly based on probability of occurrence (assumption). Hence, all the load case hours from Table 2-13 are divided by three (except for Bin no. 1, 7 and 16 for the reason mentioned in the above bullet).

- Start up and shutdown occur at 0 degree yaw error (No mention in standards to incorporate yaw errors for start up and shut down)

- The hours for startup and shutdown sequence are calculated based on FAST simulations as,

$T_{startup/shutdown}$ = Time at which loads become steady - Time at which pitch action starts (to actuate start up or shutdown sequence)

Based on above considerations, Table 2-14 is obtained which would be used to calculate fatigue damage in Octave code.

Table 2-13: Lumped Scatter Representation of Ijmuiden Site [9]

Serial No.	Mean wind speed (at 90 m), m/s	Occurrence (hours/year)
1	3.4	617.1
2	4.8	903.8
3	6.2	1002.8
4	7.6	1089.6
5	9.0	1049.3
6	10.3	899.4
7	11.7	701.3
8	13.1	622.4
9	14.5	424.3
10	15.8	341.9
11	17.2	265.6
12	18.6	165.7
13	20.0	114.8
14	21.4	63.1
15	22.7	35.9
16	24.1	20.2

Fatigue analysis has been done using different softwares starting from 'FAST' for load calculations followed by 'ANSYS' for stress calculations and then finally 'Octave' [26] to formulate and predict damage. The same flow of analysis has been depicted in Figure 2-26.

The final result from this analysis is a [9x3] damage matrix as structured in Figure 2-27. The 'ingredients' in this figure signify the inputs and considerations taken, in order to arrive at those damage values. Across the columns of matrix, the effect of rotor mass imbalance on fatigue damage could be assessed, where as along the rows the blade span-wise effect on damage could be assessed. Note that, there would be two different matrices used to depict damage in spar cap and trailing edge tape respectively.

2-4-1 Edgewise Damage Equivalent Load Calculation

The objective of load-based blade fatigue tests is to verify that the as-built blade structure is capable of sustaining the full spectrum of loads it will experience during its life. A typical wind turbine load spectrum may consist of more than 10^8 million load cycles occurring over a wide range of load ratios (R-ratio) during its life time of 20 years. Because of practical limitations, laboratories cannot test a blade with such a large number of design-load cycles

Table 2-14: Load Case Hours Representation: As Used in Damage Prediction

Load Case Hour Row No.	Description	Hours/year (To be Used in Damage Prediction Code)
1	Power Production 1	171.45
2	Power Production 2	301.26
3	Power Production 3	334.28
4	Power Production 4	363.20
5	Power Production 5	349.76
6	Power Production 6	299.80
7	Power Production 7	233.48
8	Power Production 8	207.46
9	Power Production 9	141.42
10	Power Production 10	113.96
11	Power Production 11	88.54
12	Power Production 12	55.23
13	Power Production 13	38.28
14	Power Production 14	21.04
15	Power Production 15	11.98
16	Power Production 16	6.58
17	Start up at 3 m/s	61.11
18	Start up at 11.4 m/s	0.42
19	Start up at 25 m/s	0.28
20	Shutdown at 3 m/s	41.67
21	Shutdown at 11.4 m/s	0.42
22	Shutdown at 25 m/s	0.14

in a time period that is reasonable. The advantage of laboratory testing is that the load-amplitude may be increased to accelerate the level of damage per load cycle by as much as two orders of magnitude over the design condition in order to achieve the same total damage in a fraction of the time. This analysis is routinely executed by applying linear damage models such as Miner's Rule [27].

Hence, once the damage has been calculated by mathematical models (in this case: Miner's Rule), it is validated through laboratory testing. The way it is done is; for a given number of fatigue cycles (depends on the frequency of test and test lab capabilities), an equivalent load is found for a desired cycle type (R-value), such that this gives an exact same damage as predicted by the analytical model. From a wind turbine blade's perspective, this Damage Equivalent Load (DEL) can either be in the form of flap or edgewise loading (for eg., for spar caps and trailing edge tape respectively). Obviously it can be evaluated in other forms of load components, but should be chosen wisely considering loading in actual scenario.

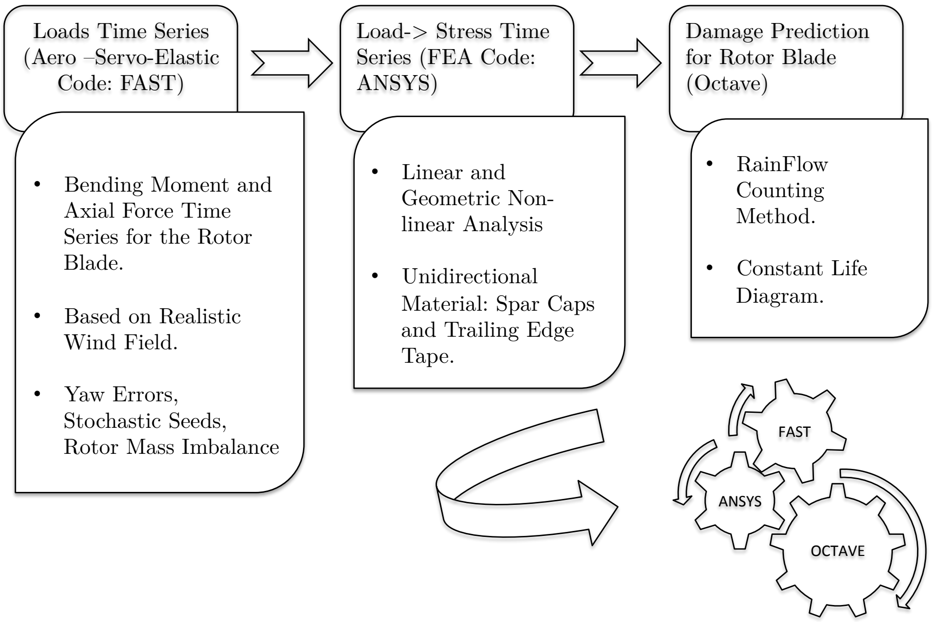

Figure 2-26: Steps and Tools Used During Fatigue Analysis

Based on above definition, formulation of DEL can be understood as follows:

A simple description of how fatigue damage accumulates on a structural component is given by Wohler's equation, which is recognized as the basis for fatigue analysis of wind turbines. The same has been depicted in figure 2-28. Wohler's equation assumes that each cycle of a constant stress range amplitude, S, causes a particular amount of damage, and that damage increases linearly with the number of stress cycles applied, N until it reaches a prescribed failure level. The damage induced *in any single cycle* is proportional to the stress range amplitude raised to the m^{th} power, where m is a material parameter (sometimes called the inverse slope of log-log S-N diagram) which is generally close to 9 or 10 for the turbine blades (fiberglass composite). A second material parameter, C, is proportional to the number of cycles a material can withstand before failure [28]. Considering N_i to be the number of cycles to failure at stress amplitude of S_i, Wohler's equation may be expressed as:

$$\begin{gathered} N_i.{S_i}^m = C \\ or\ log(S_i) = \frac{(\log C - \log N_i)}{m} \end{gathered} \tag{2-20}$$

Note, to avoid confusion, this is same equation as 2-16, where m=-b.

Based on this equation and Miner's formulation (equation 2-18), for a series of n_i number of cycles (calculated via rainflow counting), fatigue damage can be written as,

$$D = \Sigma\left(\frac{n_i}{N_i}\right) = \Sigma\left(\frac{n_i.{S_i}^m}{C}\right) \tag{2-21}$$

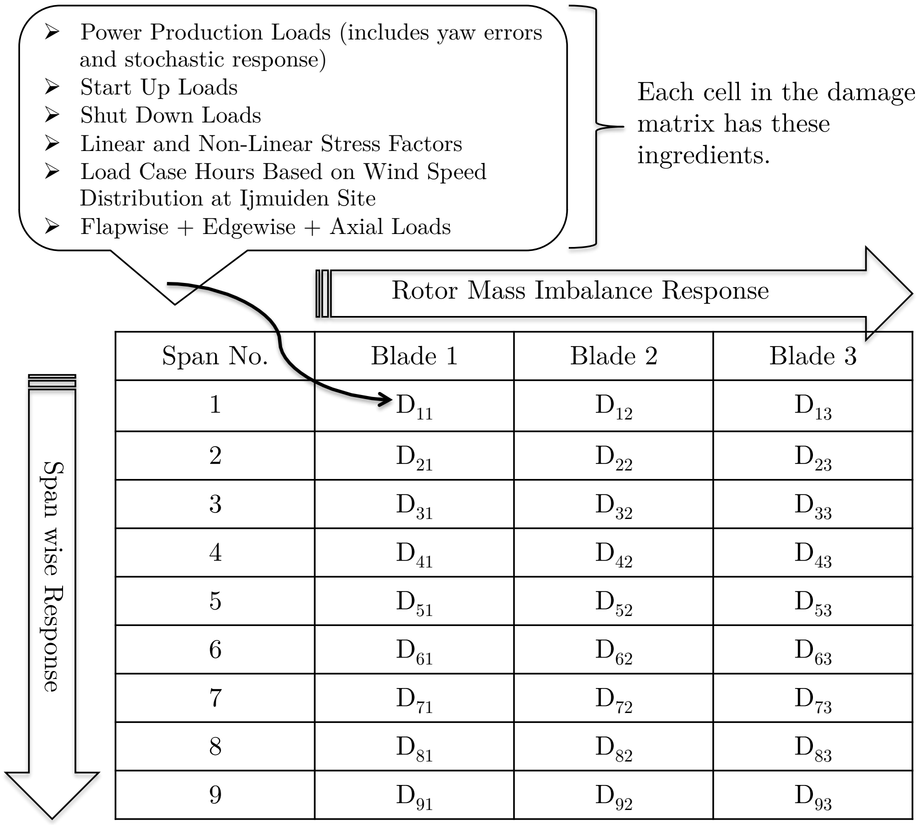

Span No.	Blade 1	Blade 2	Blade 3
1	D_{11}	D_{12}	D_{13}
2	D_{21}	D_{22}	D_{23}
3	D_{31}	D_{32}	D_{33}
4	D_{41}	D_{42}	D_{43}
5	D_{51}	D_{52}	D_{53}
6	D_{61}	D_{62}	D_{63}
7	D_{71}	D_{72}	D_{73}
8	D_{81}	D_{82}	D_{83}
9	D_{91}	D_{92}	D_{93}

Figure 2-27: Damage Matrix Representation and its Essential Ingredients

where,
N_i is number of cycles to failure for an i^{th} load cycle.

Based on definition of DEL, to obtain the same damage, D, as above, an equivalent fatigue load, S_{eq}, can be defined for N_{eq}, equivalent number of cycles in test, as,

$$D = \frac{N_{eq}}{N_{eqf}} = \frac{N_{eq}.{S_{eq}}^m}{C} \tag{2-22}$$

where,
N_{eqf} is number of cycles to failure at equivalent load.

Equating equations 2-21 and 2-22, one can obtain,

$$S_{eq} = \left(\frac{\Sigma n_i.{S_i}^m}{N_{eq}} \right)^{\frac{1}{m}} \tag{2-23}$$

Hence, analytically speaking, equation 2-23 is enough to evaluate damage equivalent stress (as numerator is known from equation 2-21, m and C from material properties and N_{eq} from the number of applied test cycles as given below).

Number of cycles to failure at equivalent load (N_{eqf}), based on 'equivalent' number of test cycles applied (say $N_{eq} = 10^6$) to achieve a give damage (D: known from Miner's rule) can be calculated as,

$$N_{eqf} = \frac{N_{eq}}{D} \tag{2-24}$$

Based on this equivalent number of cycles to failure and R=-1, for trailing edge tape (tension-compression), mean and amplitude stress can be found out from shifted linear Goodman diagram (for the given material of trailing edge tape). As mean stress is zero for R=-1, amplitude stress gives the net longitudinal stress that should be produced due to loading ($S_{net} = S_{mean} + S_{eq}$). This approach is exactly same as evaluating S_{eq} from equation 2-23.

This stress can now be transformed to edgewise moment value based on the stress factor for edgewise loading in trailing edge tape (Table 2-12),

$$M_{edgewise(DEL)} = \frac{S_{net}}{SFTE_{edge}} \tag{2-25}$$

Now, this exercise should be done at all the 8 spans where damage is calculated. Based on this, an edgewise bending moment distribution would be obtained along the span of the blade, which can then be converted into concentrated loads (so as to obtain the best fit for the obtained moment distribution). These concentrated loads would then be called damage equivalent loads (DEL) in edgewise direction for trailing edge tape.

Importance of Damage Equivalent Load: Apart from its use in full-scale blade testing, the importance of DEL is that, it can be seen as a summary of all types of loads occurring in one number (at a particular frequency and under constant amplitude condition). This form of representation of loads is very convenient in doing quick preliminary assessment of wind turbine model. Also, it is a useful parameter while evaluating load differences for various scenarios, say, for example, flapwise bending moment in blades for their entire life in collective pitch control mode vs. individual pitch control mode. Lower the damage equivalent value, better the performance of the pitch controller.

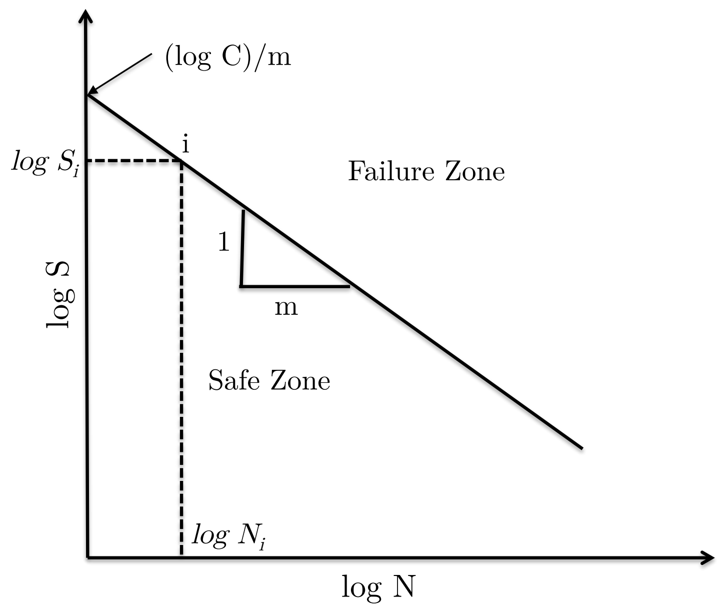

Figure 2-28: Representation of S-N Fatigue Curve for Damage Equivalent Load Calculation

Chapter 3
Results and Discussions

3-1 Critical Deflection

From the table 2-9, it can be seen that, since $H_{clearance}$ (10.6 m)>$H_{deflmax}$ (6.4 m), there would be no interference of tower and blade.

3-2 Buckling (Stability)

Table 3-1 represent results after applying loads from 50 year gust DLC. As can be seen, the flapwise mode governs the buckling failure criteria to a very large extent. Based on the results, blade would buckle under all the scenarios, except for the case where maximum edgewise and corresponding axial load act together. Even when all the three component of loads act on the blade, flapwise mode dominates with slight increase in load factor when compared to the case of 'Only Flapwise' (due to a small induced stiffness because of axial loading).

Table 3-1: Buckling Analysis Results

	Load Factor				
Buckling Mode	All three Components Together	Only Flapwise	Only Edgewise	Flapwise + Axial	Edgewise+ Axial
1	0.239	0.235	0.702	0.239	1.153
2	0.247	0.243	0.755	0.247	1.249
3	0.355	0.350	0.774	0.356	1.289
4	0.360	0.356	0.799	0.362	1.333
5	0.406	0.394	0.805	0.406	1.346
6	0.411	0.405	0.819	0.413	1.360
7	0.418	0.412	0.823	0.420	1.381
8	0.424	0.412	0.828	0.424	1.391
9	0.465	0.458	0.838	0.467	1.399
10	0.475	0.467	0.845	0.477	1.403

`Note`: Load Factor > 1.0 would imply that blade is safe under buckling.
Hence, clearly, there is a problem of buckling under flapwise loading for the blade under consideration.
Figure 3-1 and 3-2 depict a plot from 1st and 4th buckling mode when all the three component of loads (maximum flapwise+corresponding edgewise+ corresponding axial loads) are considered. Hence, these modes correspond to column 2 of Table 3-1. It can be observed from these figures that buckling is a severe problem in flapwise mode and that it is critical near the trailing edge (1st Mode: Figure 3-1) near the tip . This region is is very close to the

span where trailing edge tape ends (at ≈ 45 m). Hence, insufficient reinforcement on trailing edge after 45 m span is the reason for this buckling mode.

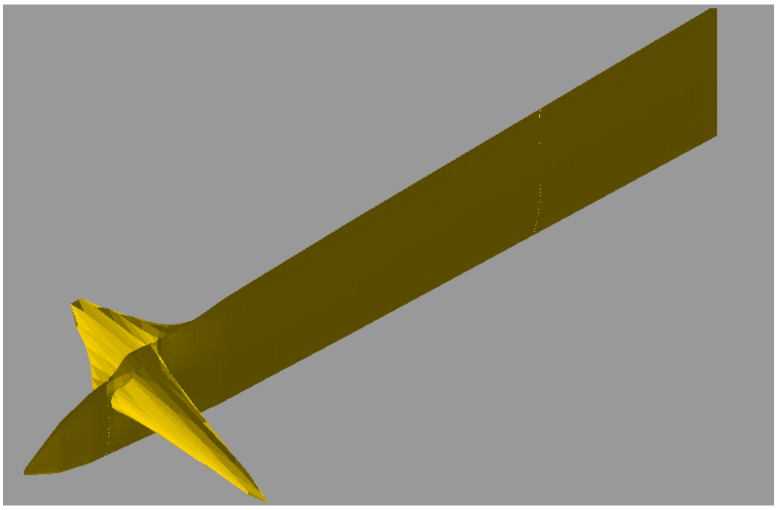

Figure 3-1: Cut-Section of Rotor Blade for 1st Buckling Mode Shape: All three components of load considered

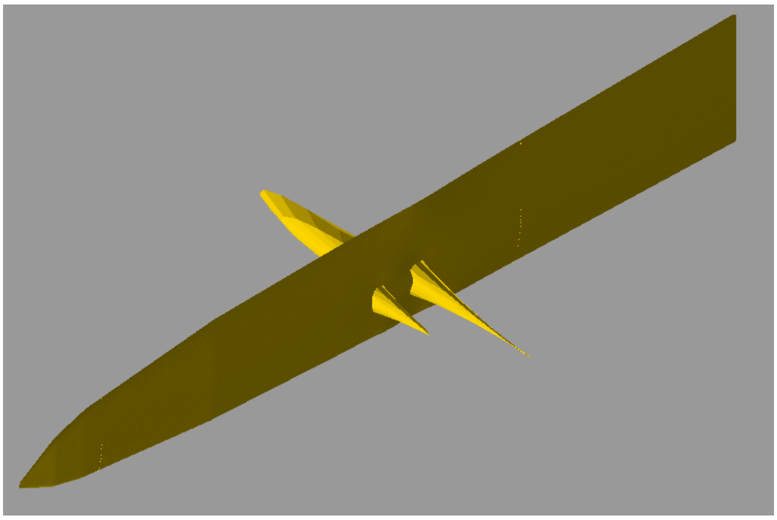

Figure 3-2: Cut-Section of Rotor Blade for 4th Buckling Mode Shape: All three components of load considered

3-3 Static Strength

The inter-fibre failure occurs due to inadequate strength of shear webs. If the mean value of tensile and compressive strength of shear web are increased by 20 % in the longitudinal direction, the failure index was observed to drop below 1 (0.93). Figure 3-3 and 3-4 depict the

Table 3-2: Static Strength Analysis Results

Failure Criteria	Strength Failure Index (FI)	Remarks
Maximum Stress	0.0016	FI $<$ 1; hence the blade material is far off from 'fibre failure'
Tsai Wu Strength Index	1.34	FI $>$1; hence inter-fibre failure takes place. It happens in the shear web.

`Note`: Failure Index $<$ 1.0, for blade to be safe under static strength.

failure index plot for the two criterias described already. From the plot, it is observed that, critical region from this analysis perspective is 9.5 m from root section (in the shear web: Figure 3-5). It is well probable, that this failure is because of insufficient matrix strength in shear webs.

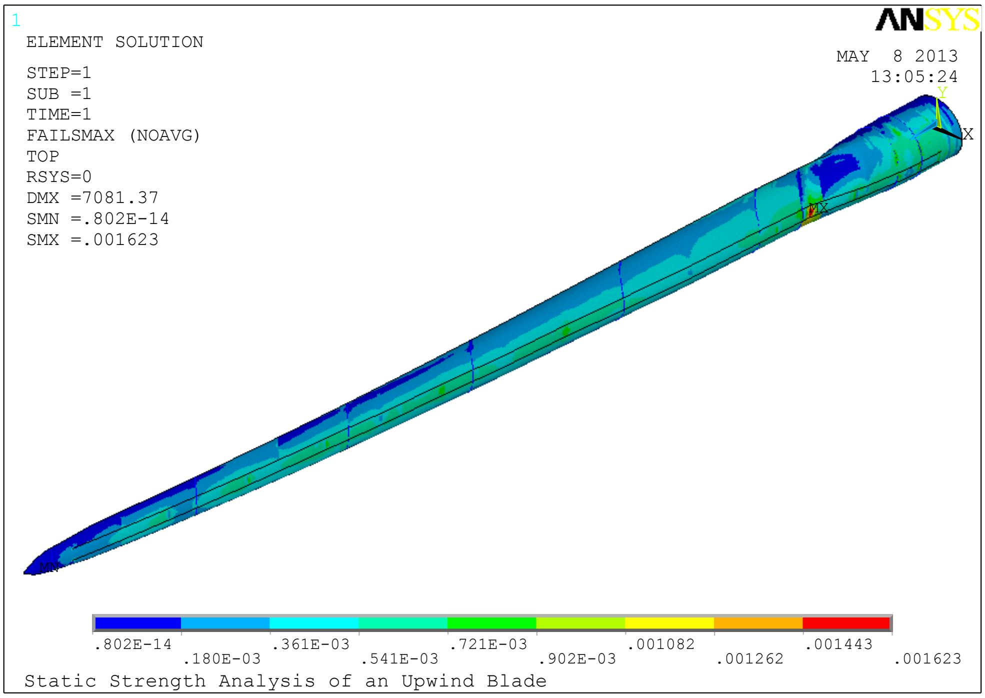

Figure 3-3: Failure Index Plot for Blade Based on Maximum Stress Failure Criteria

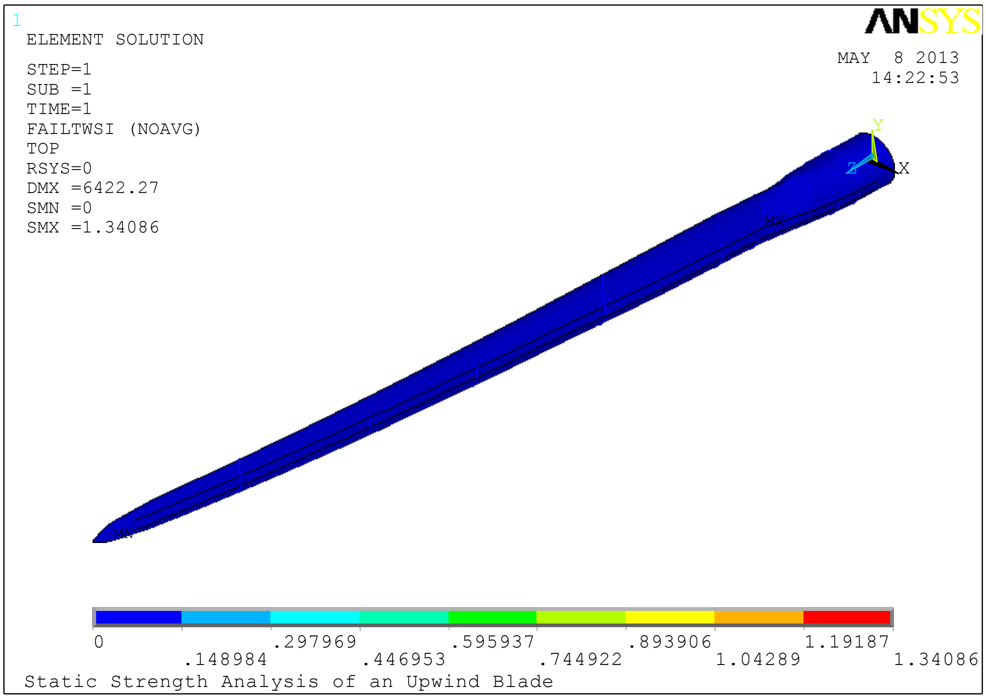

Figure 3-4: Failure Index Plot for Blade Based on 'Tsai Wu' Failure Criteria

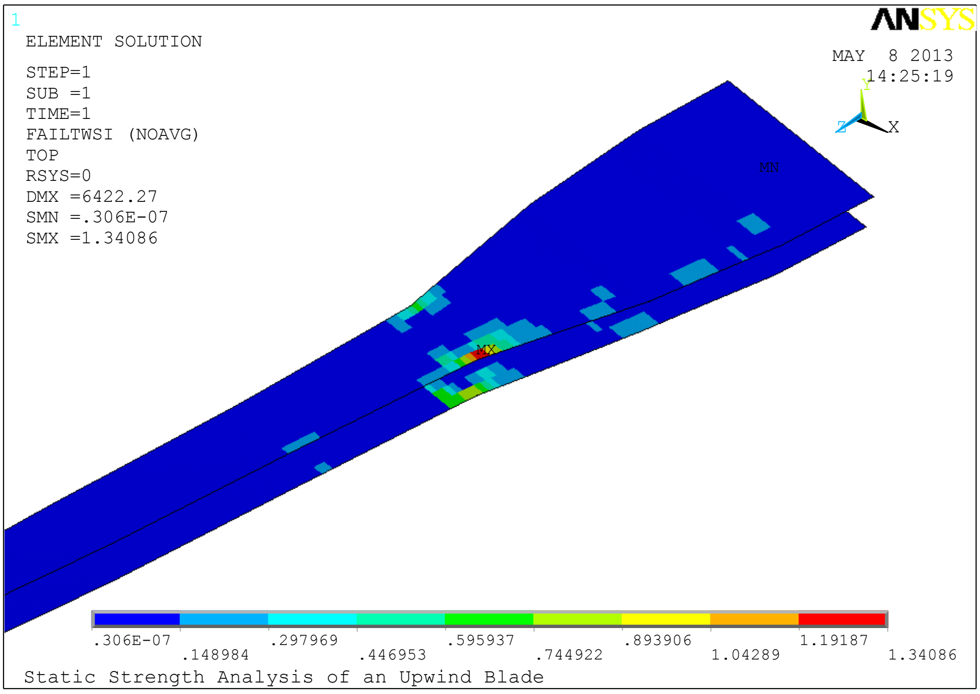

Figure 3-5: Cut Section of Shear Web: Failure Index Plot for Blade Based on 'Tsai Wu' Failure Criteria

3-4 Modal Analysis

Table 3-3 and figure 3-6 represent the eigen values from the first five modes of the blade. The shape of the first four modes have been depicted in figure 3-7. It has to be noted here that all the eigen frequencies listed in table 3-3 and depicted in figure 3-6 include structural damping and centrifugal stiffening effect. The effect of centrifugal stiffening is to increase the eigen frequencies with rotor speed (see Campbell diagram) while damping has a marginal decreasing effect (as depicted in table 3-4). Note that damping effect does not change with the rotor speed as only structural damping is considered.

Table 3-3: Modal Analysis Results

	Damped Eigen Frequencies, Hz				
Rotational Blade Velocity, rpm	Mode 1	Mode 2	Mode 3	Mode 4	Mode 5
0	0.701	1.019	1.942	3.753	4.070
3	0.703	1.021	1.943	3.754	4.070
5	0.706	1.023	1.944	3.754	4.070
7	0.711	1.026	1.946	3.755	4.071
9	0.717	1.030	1.948	3.756	4.072
11	0.725	1.036	1.951	3.758	4.074
13	0.734	1.042	1.954	3.760	4.075
15	0.744	1.050	1.958	3.762	4.077

`Note`: Mode 1, 3 and 5 represent first, second and third flapwise blade modes while mode 2 and 4 represent first and second edgewise modes respectively.

It can be observed from table 3-3, that 1st flapwise frequency increases by approximately 6 % as rotor speed increases from 0 rpm to 15 rpm. Also it can be seen from Campbell diagram that there is no danger of resonance (eigen frequency=1P or 3P frequencies), occurring in the operating range of rotor speed (6.9 rpm to 12.1 rpm). It has to be further understood that this analysis is based on a standalone blade and not the complete system of wind turbine (and hence no coupling effects of other blades and tower has been considered).

Table 3-4: Effect of Damping on Eigen Values

Mode	Eigen Frequency without any damping, Hz	Eigen Frequency with damping, Hz
1	0.7012	0.7012
2	1.0194	1.0194
3	1.9425	1.9423
4	3.7546	3.7534
5	4.0712	4.0696

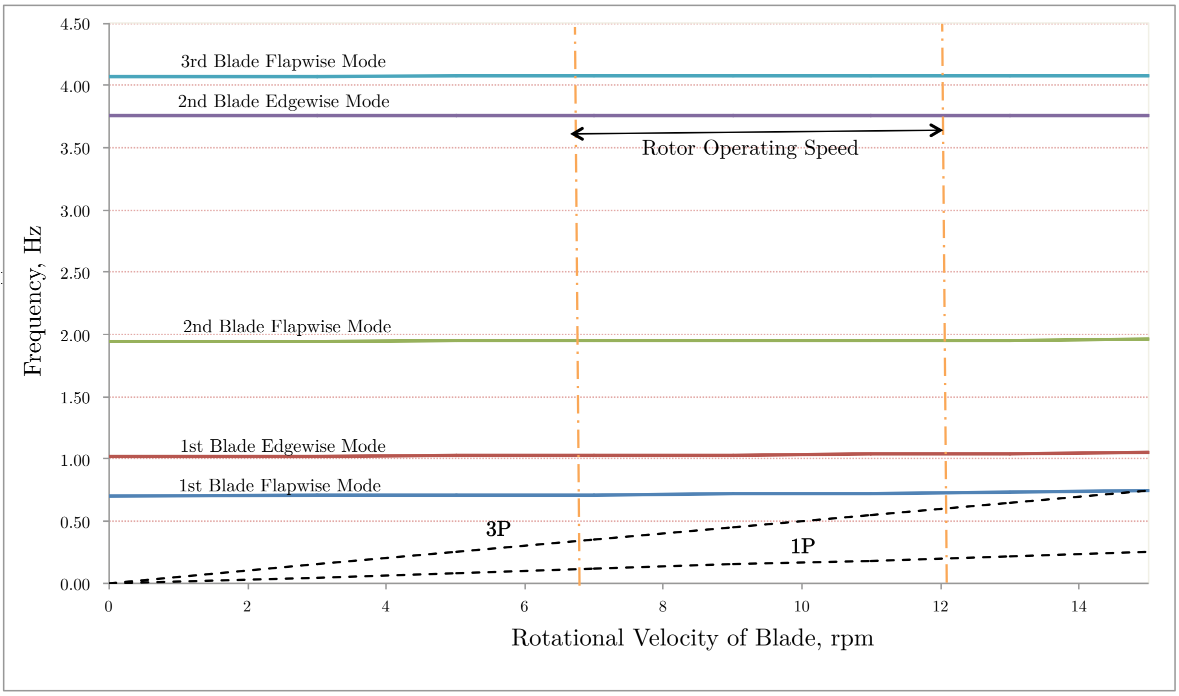

Figure 3-6: Campbell Plot Showing Different Blade Mode Frequencies

`Note:` 1P represents 1 excitation per revolution of the blade while 3P represents 3 excitations in one revolution for a 3-bladed turbine. An operational wind turbine is subjected to harmonic excitation from the rotor. The blade's rotational frequency is the first excitation frequency and is commonly referred to as 1P. The second excitation frequency to consider is the blade passing frequency, often called 3P (for a three-bladed wind turbine) at three times the 1P frequency. These are the critical excitation sources, although multiples of 3P must also be analyzed in a detailed modal design of blades.

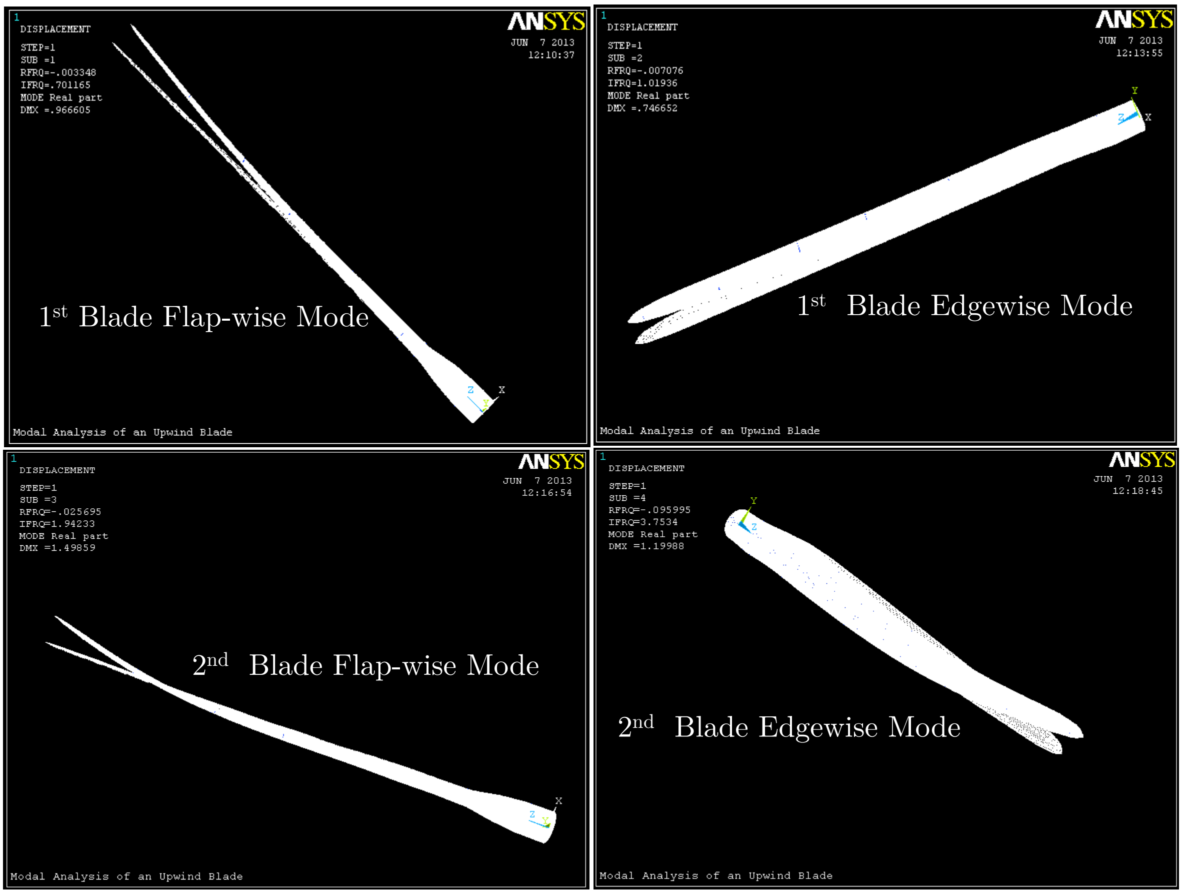

Figure 3-7: Blade mode shapes

3-5 Fatigue

Table 3-5 represents the fatigue damage value predicted for spar cap and trailing edge tape across three blades and nine different spans. It can be clearly seen from here that fatigue life of trailing edge tape is more critical than that of spar cap, even though, both the parts of blade are far off from their fatigue life (as D $\ll$ 1). It can also be observed that blade 1 seems to have the worst performance as it is the heaviest (contributing to worse effect on trailing edge tape damage).

The reader should keep in mind that geometric non-linear effects in the blade due to the flap wise bending moment have been incorporated in the fatigue damage calculations. But, there are no (negligible amount) non-linearity effects in blade stresses due to edgewise bending and axial forces.

Table 3-6 and 3-7 represent the break up of damage based of the load sequences. It can be very clearly observed that start-up and shut-down load cases have negligible share, when compared to power production operation of turbine.

Table 3-8 and 3-9 depict the contribution of yaw errors to fatigue damage for power production load sequences. It can be clearly seen that the effect of yaw error is felt more by spar caps than trailing edge (TE) tape as yaw errors directly influence the aerodynamic forces which in turn impact fatigue damage on spar caps. Gravity loading, which majorly influences damage in TE tape, is not effected yaw error.

For spar caps, the effect of positive yaw error ($+8^o$) is most prominent, due to considerable increase in loading as a result of a much severe cross wind component when compared to negative yaw error case (-8^o). This can be understood as follows: Refer to fig. 1-3 (which depicts the positive orientation of yaw error) and imagine a counter-clockwise rotating turbine (as is the case for this project). The component of cross wind (in rotor plane) for positive yaw error would be against the direction of rotation when blade is above hub height while it would be in the direction of rotation below hub height. This would mean, the relative velocity of the wind w.r.t rotating blade would be much higher on the top (above hub height) than at the bottom (below hub height). Now it is known that wind velocity increases with height (due to wind shear), hence the relative velocity at which wind is hitting the blades at the top is much higher (velocity of wind + velocity of rotation of blade) than the relative velocity at the bottom (velocity of wind - velocity of rotation of blade). This would mean much higher aerodynamic forces and ultimately higher loads. The scenario would reverse for the negative yaw error case where the wind velocity would be added to rotor velocity below the hub height where as rotor velocity would be subtracted from wind velocity above hub height. Going by the same reasoning of wind shear, this would reduce the severity of loads. Note this is only true for an anticlockwise rotating turbine. The nature of loads would reverse for a clockwise rotating turbine (same is observed in fig. 2-2, where loads are represented for a clockwise rotating turbine in FAST).

TE tape is typically loaded due to gravity and hence the same effect of yaw errors (as for spar caps) is not observed here. Having said that, the contribution of three yaw errors is not exactly same for trailing edge tapes of corresponding blades (table 3-9). This variation is due to the cross wind component which contributes to loads on trailing edge tape and is not same for different yaw error scenarios.

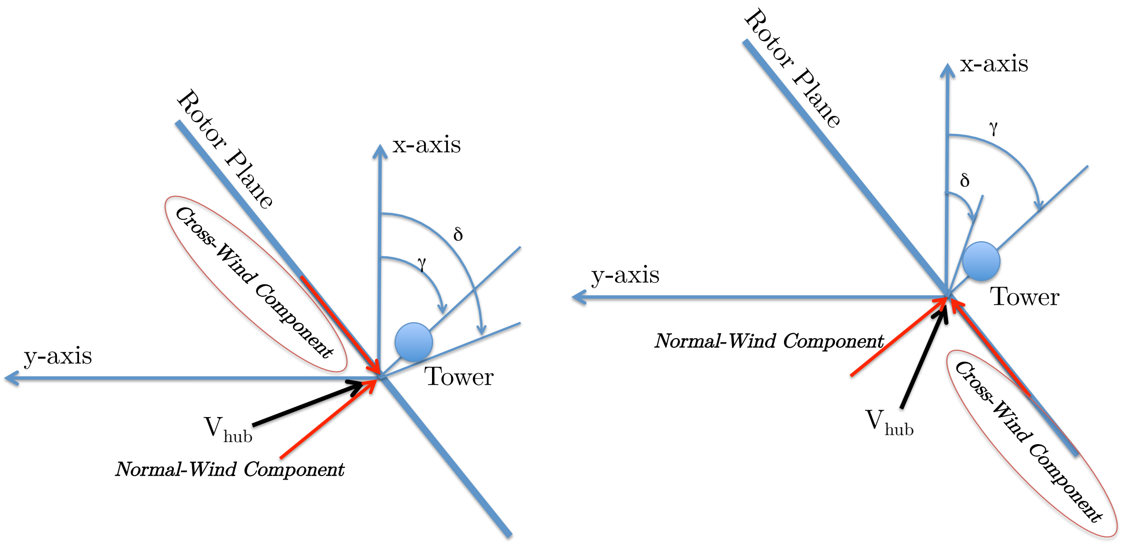

(a) Positive Yaw Error (b) Negative Yaw Error

Figure 3-8: Depiction of Yaw Error Along With Cross Wind Component

Figure 3-9 gives reader a feeling of the location of different spans in a 61.5 m blade. This is a scaled representation of the original blade, courtesy ANSYS.

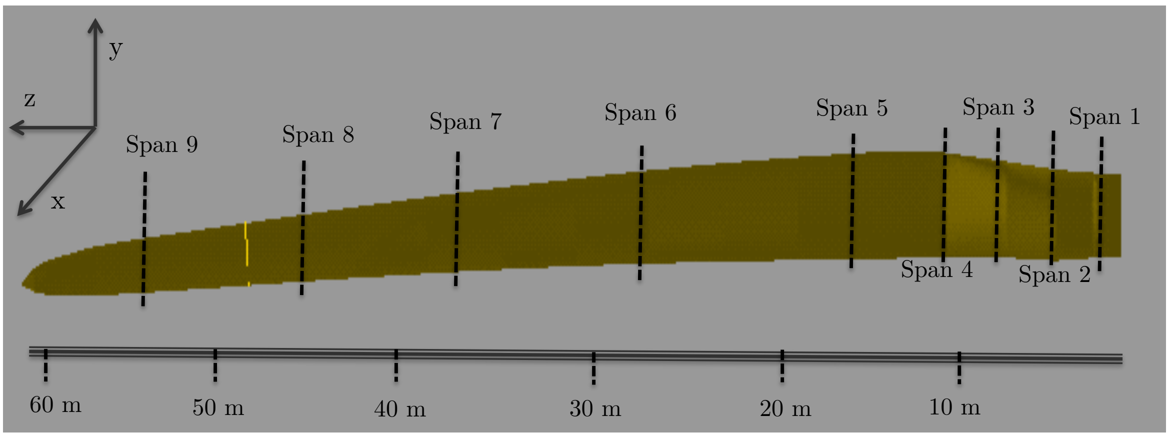

Figure 3-9: Visualization of a Scaled Blade Along With Original Spans where Fatigue Damage are Calculated

Figure 3-11 and 3-12 show a plot of radial span of blade vs. fatigue damage. They show the absolute values of fatigue damage along the span of the three blades for spar caps and trailing edge tape respectively.

The first observation that can be made here is for spar caps is fatigue damage is highest for blade 1 followed by blade 2 and blade 3. This is due to the difference in masses of three blades (blade 1 being the heaviest and blade 3, lightest). The blade starts pitching after rated

Table 3-5: Fatigue Damage Value of Wind Turbine Composite Blade Predicted Based on Miner's Rule: Benchmark Case

		Spar Cap			Trailing Edge Tape		
Span	Radial Span, m	Blade 1	Blade 2	Blade 3	Blade 1	Blade 2	Blade 3
1	2.80	1.1E-09	1.2E-09	7.9E-10	1.7E-06	1.6E-06	1.5E-06
2	5.60	2.8E-09	3.7E-09	1.7E-09	9.6E-05	9.4E-05	6.7E-05
3	8.40	5.3E-09	7.4E-09	4.5E-09	4.0E-05	3.0E-05	3.0E-05
4	11.8	9.1E-07	7.0E-07	6.2E-07	6.2E-06	4.7E-06	4.7E-06
5	15.9	1.2E-07	7.4E-08	9.4E-08	6.0E-05	5.0E-05	5.4E-05
6	28.2	1.4E-07	1.2E-07	1.8E-07	2.3E-06	1.7E-06	1.6E-06
7	36.4	1.2E-07	1.0E-07	2.2E-07	3.0E-08	2.6E-08	3.3E-08
8	44.5	3.0E-07	1.3E-07	1.3E-07	1.8E-11	1.2E-11	2.7E-11
9	56.2	3.9E-09	2.3E-09	1.9E-09	-N.A.-	-N.A.-	-N.A.-

`Note 1:` Damage <1 for part to be safe from fatigue life perspective.
`Note 2:` 'Benchmark Case' represents yaw error of 0^o, $+8^o$ and -8^o and rotor mass imbalance of $\pm$ 3 % (blade 1 heaviest and blade 3 lightest).
`Note 3:` In case of rotor mass imbalance, the mass is uniformly added or reduced throughout the span of the blades. It is not added or reduced in a concentrated manner at a particular location.

wind speed of 11.4 m/s after which, the effect of gravity loads is felt more and more by spar caps (also due to the twist in blade). And gravity loads are affected by mass of the blade, hence the difference in fatigue damage across 3 blades in spar caps.

The maximum fatigue damage in spar caps occur at around 11 m radial span, close to the root where the airfoil section has changes to DU profile from a circular section. The circular root of the blade (till 10 m) has flapwise moment of inertia almost equal to inertia in edgewise direction. Hence flapwise loads are well taken care of till this point of the blade. After this point, flapwise inertia tends to reduce more than edgewise moment of inertia (refer appendix B), due to which stress increases which consequently leads to maximum damage at this location in spar cap. It has also to be understood that bending moment decrease from root to tip, hence the effect on fatigue damage is due to combined influence of inertia and bending moments.

There are two peaks (maxima) for fatigue damage in trailing edge tape (figure 3-12); one at $\approx$ 5m and other one at $\approx$ 15 m, the second peak being higher than the first one. Higher fatigue damage at these two spans can be explained as from figure 3-10 which shows the side view of the blade till these spans.

The first peak is due to stress concentration effect as a result of change in geometry of the trailing edge tape (sharp changes in geometry of a structure leads to a local increase in the intensity of a stress field). The second peak (more prominent) can be understood from eq. (2-19). At this section the distance of trailing edge tape from neutral axis is maximum (due to longest chord) and stress is directly proportional to this distance. Hence it can be said that the section with longest chord sees maximum fatigue damage in trailing edge tape.

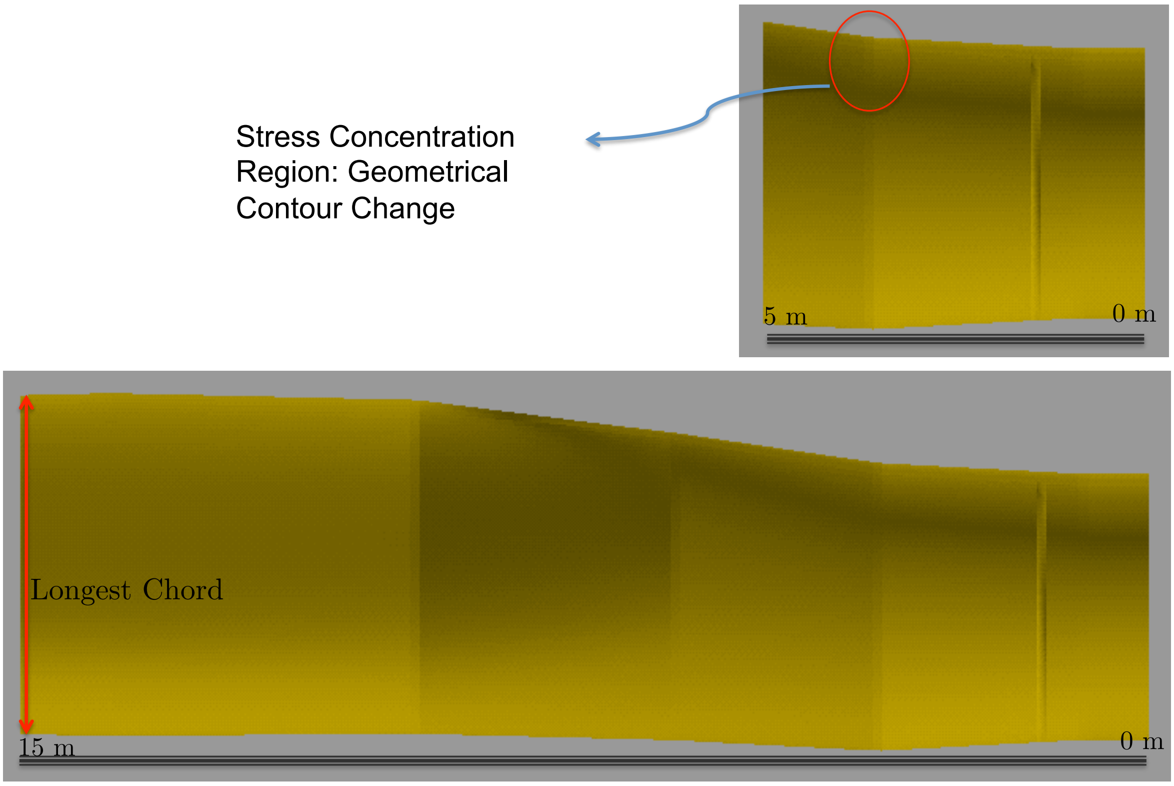

Figure 3-10: Blade Side View at 5m and 15 m Respectively

Figure 3-13 and 3-14 represent a plot which depicts how fatigue damage changes with wind speed in TE tape of blade 1 (benchmark case) at two spans (span 4: 11.8 m, span8: 44.5 m). Similarly, figure 3-15 and 3-16 represent plot for SC of blade 1. Before drawing any conclusions out of these figures, it should be understood that SC is also loaded in gravity due to aerodynamic twist and pitching action of blade. Similarly, TE tape sees wind loads based on same reasoning. Twist angle decreases from inboard part to outboard part of the blade (table 2-6). To aid this understanding, two views of the blade from root and tip section are shown in figure 3-17 along with positive pitching direction.

There are two peaks observed in figure 3-13. The first one at 7.6 m/s has to do with the weibull distribution of site where the probability of occurrence of this velocity is maximum and hence TE remains under the influence of gravity loading for significant amount of time which results in maximum fatigue damage (note that the pitch angle is zero here). Similar nature is not observed in figure 3-14 as the moment near tip section (span 8) is far less than inboard section (span 4) and gravity loading don't depend on wind speed. Looking at span 4 and span 8 plots, there is a shift in the peak of fatigue damage from 15.8 m/s to 17.2 m/s for TE tape and from 13.1 m/s to 18.6 m/s in SC (Figure 3-15 and 3-16). This has to do with pitch, twist and the combined effect of aerodynamic and gravity loads. Inboard portion of the blade (span 4) reach the worst case combination of loading much quicker than outboard part (span 8) during pitching action due to twist in the blade and hence, the fatigue damage peaks.

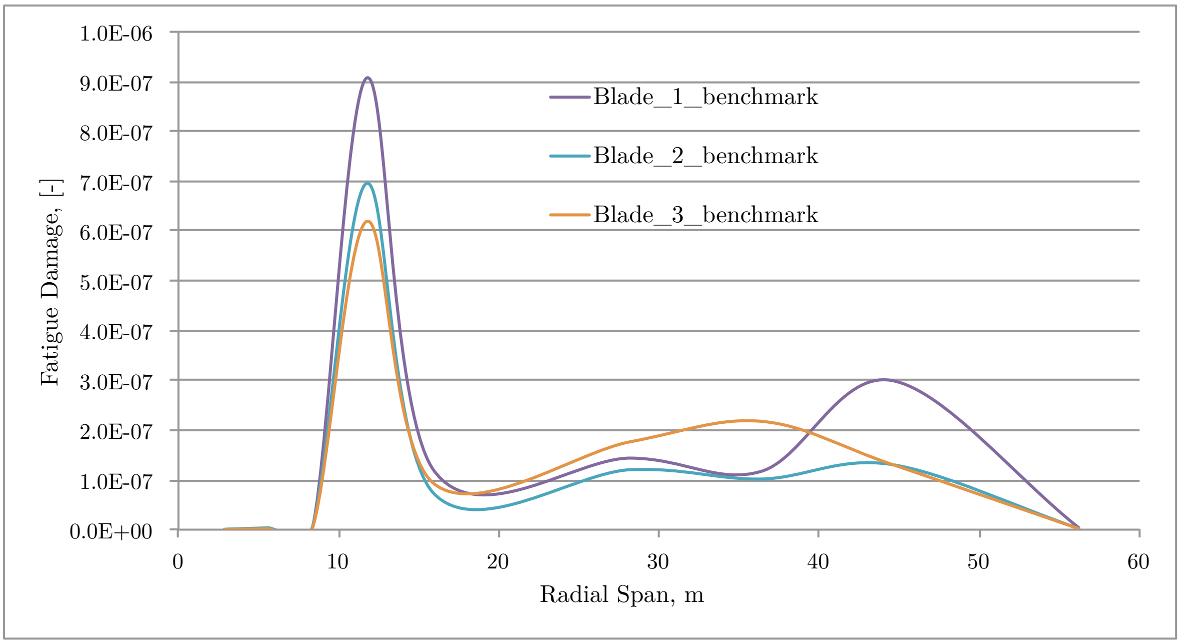

Figure 3-11: Spar Cap Fatigue Damage: Benchmark Case

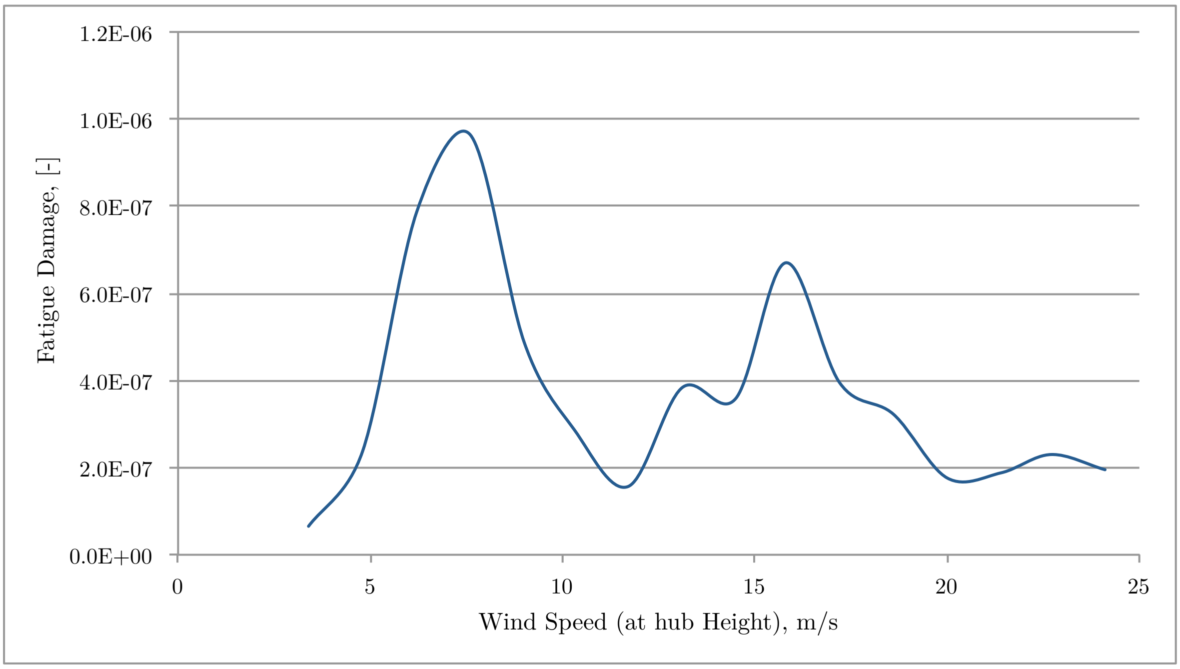

Figure 3-13: Hub Height Wind Speed vs. Fatigue Damage in Trailing Edge Tape at 11.8 m

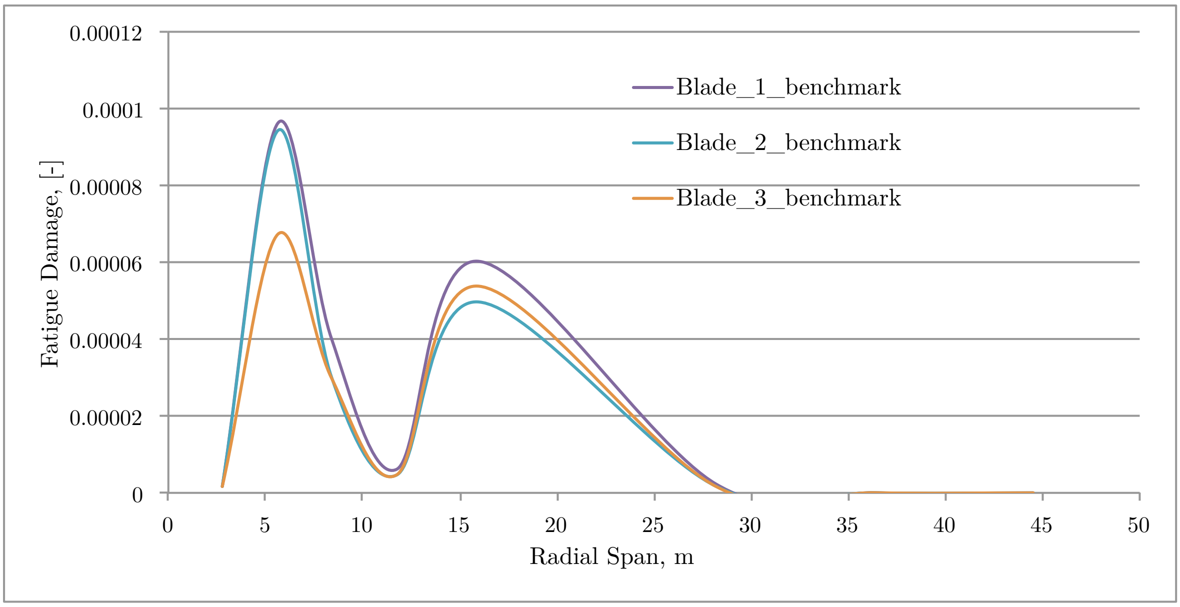

Figure 3-12: Trailing Edge Tape Fatigue Damage: Benchmark Case

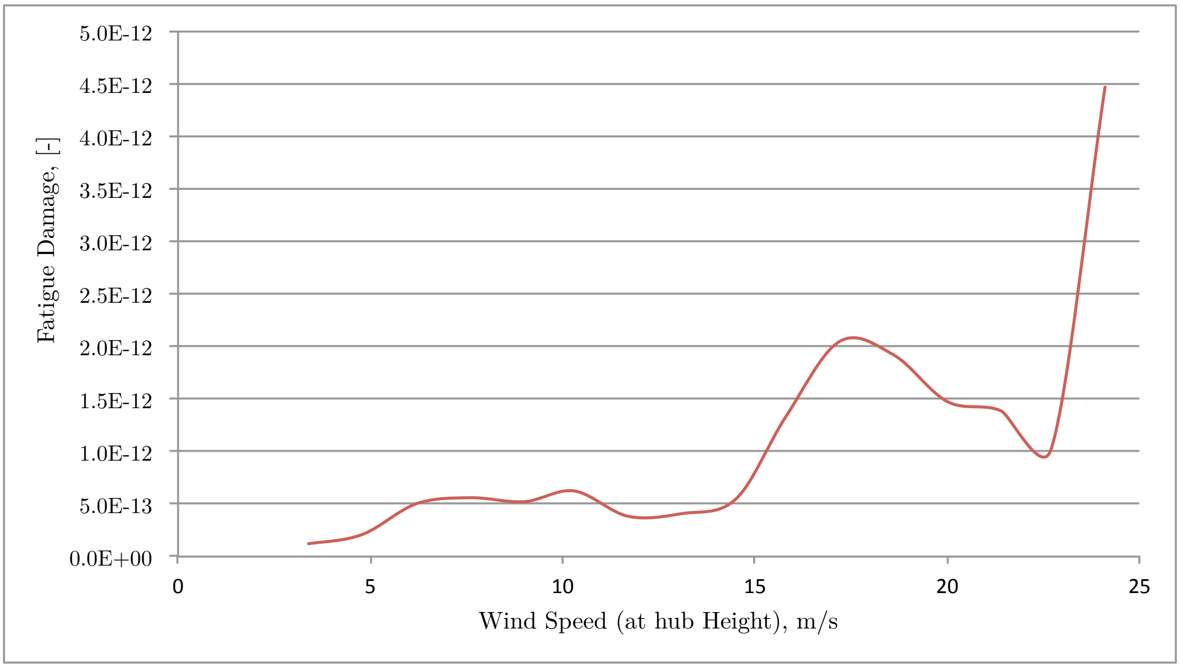

Figure 3-14: Hub Height Wind Speed vs. Fatigue Damage in Trailing Edge Tape at 44.5 m

Figure 3-18 and 3-19 represent the shifted linear Goodman diagram with green lines representing constant life (the bottom-most being equivalent to 10^8 cycles and the top most being equivalent to 1 cycles) and red dots representing the equivalent position of stresses for actual loads (and hence representing damage). It can be clearly observed that, trailing edge tape

Table 3-6: Contribution of Power Production, Startup and Shutdown Sequence Towards Fatigue Damage: Spar Cap

	Power Production Load Case Contribution (%)			**Start up Load Case Contribution (%)**			**Shutdown Load Case Contribution (%)**		
Radial Span, m	Blade 1	Blade 2	Blade 3	Blade 1	Blade 2	Blade 3	Blade 1	Blade 2	Blade 3
2.80	100.00	99.98	99.96	0.001	0.001	0.010	0.001	0.015	0.027
5.60	99.99	99.77	99.71	0.001	0.000	0.284	0.010	0.226	0.002
8.40	99.82	99.85	99.54	0.004	0.002	0.323	0.176	0.153	0.135
11.8	99.99	99.35	99.96	0.001	0.142	0.036	0.014	0.513	0.002
15.9	99.94	98.49	99.98	0.012	0.045	0.014	0.048	1.463	0.003
28.2	99.99	99.71	99.99	0.001	0.075	0.000	0.008	0.214	0.009
36.39	99.95	99.64	98.26	0.026	0.231	1.736	0.028	0.129	0.005
44.5	99.92	92.23	99.97	0.019	0.181	0.000	0.057	7.593	0.030
56.2	99.95	99.95	99.67	0.004	0.005	0.220	0.050	0.050	0.114

has greater damage due to more red dots crossing the 10^8 cycle constant life line. Also, the stress amplitude which are critical for fatigue life, is around 10-30 MPa with mean stress fluctuating from -25 MPa to 25 MPa. It should be realized that this is a two dimensional plot and actual number of cycles (position of red dots) cannot be visualized from these plots. Hence if red dots fall inside the 10^8 cycles ($\approx$ 20 years) to failure line, it can be concluded that the component is safe from fatigue's perspective. If they cross any of the constant life lines, damage value or a 3-D plot can give more in insight into the actual damage. As we know from Table 3-5, D $\ll$ 1 for both trailing edge tape and spar caps, the figures here just give an insight into the magnitude and order of stress levels occurring in an actual load case scenario for the considered wind turbine blade.

Effect of Yaw Error and Rotor Mass Imbalance on Fatigue: Spar caps are majorly effected by yaw errors while rotor mass imbalance has an effect on trailing edge tape. This is due to the fact that yaw errors make the plane of rotor out of phase to wind direction (not perpendicular anymore) while rotor mass has a direct impact on inertial forces acting majorly on trailing edge tape due to gravity. Obviously, there is an effect of yaw error on trailing edge tape due to aerodynamic forces acting on it because of an additional cross wind component. But this effect can be observed to be secondary in comparison to rotor mass imbalance.

Table 3-10 shows the split in different blades for different yaw error scenarios w.r.t benchmark case (table 3-5) for spar caps. It can be observed that, overall, increasing the yaw error increases the fatigue damage. But, it should be noted here that all three values of yaw error (positive, zero and negative) have been distributed evenly over the lifetime of wind turbine. While, large positive yaw error increases the damage, large negative ones tend to stabalize it to some extent and hence there are spans where damage has increased in 5°, 0° and -5° case, while it has decreased in 10°, 0° and -10° case (w.r.t benchmark).

Table 3-7: Contribution of Power Production, Startup and Shutdown Sequence Towards Fatigue Damage: Trailing Edge Tape

	Power Production Load Case Contribution (%)			**Start up Load Case Contribution (%)**			**Shutdown Load Case Contribution (%)**		
Radial Span, m	Blade 1	Blade 2	Blade 3	Blade 1	Blade 2	Blade 3	Blade 1	Blade 2	Blade 3
2.80	99.99	99.91	99.98	0.005	0.094	0.007	0.003	0.000	0.012
5.60	99.40	99.82	99.99	0.596	0.174	0.002	0.001	0.007	0.006
8.40	99.99	99.98	99.96	0.004	0.015	0.001	0.003	0.000	0.037
11.8	99.54	99.56	99.39	0.427	0.412	0.204	0.028	0.029	0.402
15.9	95.86	99.87	97.55	0.793	0.090	2.135	3.345	0.044	0.319
28.2	98.56	98.36	98.32	1.420	0.344	0.002	0.019	1.297	1.675
36.40	99.70	99.85	90.72	0.251	0.006	0.835	0.047	0.148	8.441
44.5	97.12	99.99	99.58	2.837	0.014	0.064	0.045	0.000	0.361
56.2	-N.A.-	-N.A.-	-N.A.-	-N.A.-	-N.A.-	-N.A.-	-N.A.-	-N.A.-	-N.A.-

Table 3-11 shows the split in different blades for different mass imbalance scenarios, again, w.r.t benchmark case, for trailing edge tape. It can be observed, that increasing the mass imbalance increases the fatigue damage. The mass imbalances represented here is in sequence of blade number (for eg. 5% for blade 1, 0 % for blade 2 and -5% for blade 3). However, blade 2 also shows an increase in damage without any imbalance (0, 0 and 0 % case) while there is a decrease in damage for 5, 0 and -5 % case. This could be explained based on dynamics of whole wind turbine and not looking into a standalone blade. Mass imbalance often causes gearbox damages as well as yaw bearing damages. In case of turbines with gliding yaw bearing/break there is no active mechanism to prevent the nacelle from yawing. In this case a yaw moment during operation, much higher than initially designed will cause the nacelle to yaw left-right during each rotation. This will cause fatigue damages on the yaw drives but will also induce variable loading on the other blades. Hence the coupling between the different components in the system need to be well understood to understand this behavior with more clarity.

Table 3-13 shows that during unbalanced case the damping frequency of blades increases (due to coupling effects of blades, tower, nacelle and drive train). Due to this dynamics of the wind turbine, the fatigue damage over the entire life time might be more for blade 2 in balanced rotor (when compared to unbalanced rotor). More in-depth analysis into aero elastic instability would give better insight to the problem. But definitely, rotor mass imbalance has a system effect which cannot be explained just from component level results.

Figure 3-20 and 3-21 show the comparison of benchmark case and different yaw error scenarios w.r.t absolute value of fatigue damage while figure 3-22 and 3-23 show the comparison of benchmark case and different blade mass imbalance scenarios w.r.t absolute fatigue damage.

Table 3-8: Contribution of Yaw Errors Towards Fatigue Damage: Spar Cap

	0^o **Yaw Error Contribution (%)**			$+8^o$ **Yaw Error Contribution (%)**			-8^o **Yaw Error Contribution (%)**		
Radial Span, m	Blade 1	Blade 2	Blade 3	Blade 1	Blade 2	Blade 3	Blade 1	Blade 2	Blade 3
2.80	26.7	22.3	38.0	57.0	52.1	28.6	16.4	25.5	33.5
5.60	23.9	26.5	43.3	58.3	50.3	33.3	17.8	23.2	23.5
8.38	26.0	28.8	39.8	51.8	50.4	45.2	22.2	20.8	15.1
11.8	32.1	15.9	27.1	59.0	70.6	61.7	8.9	13.4	11.3
15.9	19.4	48.8	20.4	60.5	44.0	68.9	20.1	7.2	10.6
28.2	42.1	25.8	21.5	45.8	58.1	69.5	12.1	16.1	9.1
36.4	17.7	28.9	33.2	62.2	53.4	54.9	20.2	17.8	11.8
44.52	24.6	25.0	52.8	68.7	58.9	38.8	6.7	16.1	8.4
56.2	16.7	20.1	31.7	71.7	50.3	48.4	11.6	29.6	19.9

Damage Equivalent Load: Figure 3-24 show the damage equivalent loads to be applied in edgewise direction in the blade to achieve the trailing edge damage as calculated though Miner's rule (Table 3-5). In the figure, red lines represent damage equivalent loads where as white dotted lies represent the span section where damage was calculated. The value of DEL along with their application point have been put in table 3-12.

It should be noted, however, that in actual blade testing in a test hall, so many loading points are not a feasible option due to lack of pneumatic cylinders and complexity of orientation of different loads. Generally, the test is performed for 70% of the blade (from root) and loads are applied at 2-3 locations only. Hence the representation of loads in figure 3-24 should be simplified for fewer locations based on capability of testing facility for performing the actual Damage Equivalent Load (DEL) test. The representation in figure 3-24 is just to give an overview of the damage equivalent loads from a theoretical perspective.

Table 3-13: Full-System Damped Natural Frequencies in Hertz (calculated in FAST)

Mode	Description	Balanced Case	Unbalanced Case
1	1st Tower Fore-Aft	0.37312	0.37314
2	1st Tower Side-to-side	0.37670	0.37674
3	1st Blade Asymmetric Flapwise Pitch	0.6234	0.6239
4	1st Blade Asymmetric Flapwise Yaw	0.7646	0.7652
5	1st Blade Collective Flap	0.8516	0.8522
6	1st Blade Asymmetric Edgewise Pitch	1.0510	1.0520
7	1st Blade Asymmetric Edgewise Yaw	1.1921	1.1930
8	1st Blade Collective Edge	1.2930	1.2940

`Note:` Asymmetric and Collective (symmetric) blade modes are depicted in appendix B (fig. B-3). Also, the values depicted here are for rotor speed of 7 rpm.

Table 3-9: Contribution of Yaw Errors Towards Fatigue Damage: Trailing Edge Tape

	0^o **Yaw Error Contribution (%)**			$+8^o$ **Yaw Error Contribution (%)**			-8^o **Yaw Error Contribution (%)**		
Radial Span, m	Blade 1	Blade 2	Blade 3	Blade 1	Blade 2	Blade 3	Blade 1	Blade 2	Blade 3
2.80	29.7	28.9	34.2	38.8	37.1	38.4	31.4	34.0	27.4
5.60	38.1	34.8	39.9	32.5	35.3	37.9	29.4	29.8	22.2
8.40	29.7	30.3	31.9	38.9	38.4	38.4	31.4	31.4	29.7
11.8	34.0	28.6	35.3	37.9	32.8	32.3	28.1	38.6	32.4
15.9	30.4	32.4	25.0	37.2	33.0	37.8	32.4	34.5	37.2
28.2	35.2	35.1	30.1	28.1	21.7	25.6	36.6	43.2	44.2
36.40	26.0	34.7	33.2	22.0	22.7	28.9	52.0	42.6	37.9
44.52	31.0	28.0	37.5	31.6	40.2	25.1	37.4	31.8	37.4
56.2	-N.A.-	-N.A.-	-N.A.-	-N.A.-	-N.A.-	-N.A.-	-N.A.-	-N.A.-	-N.A.-

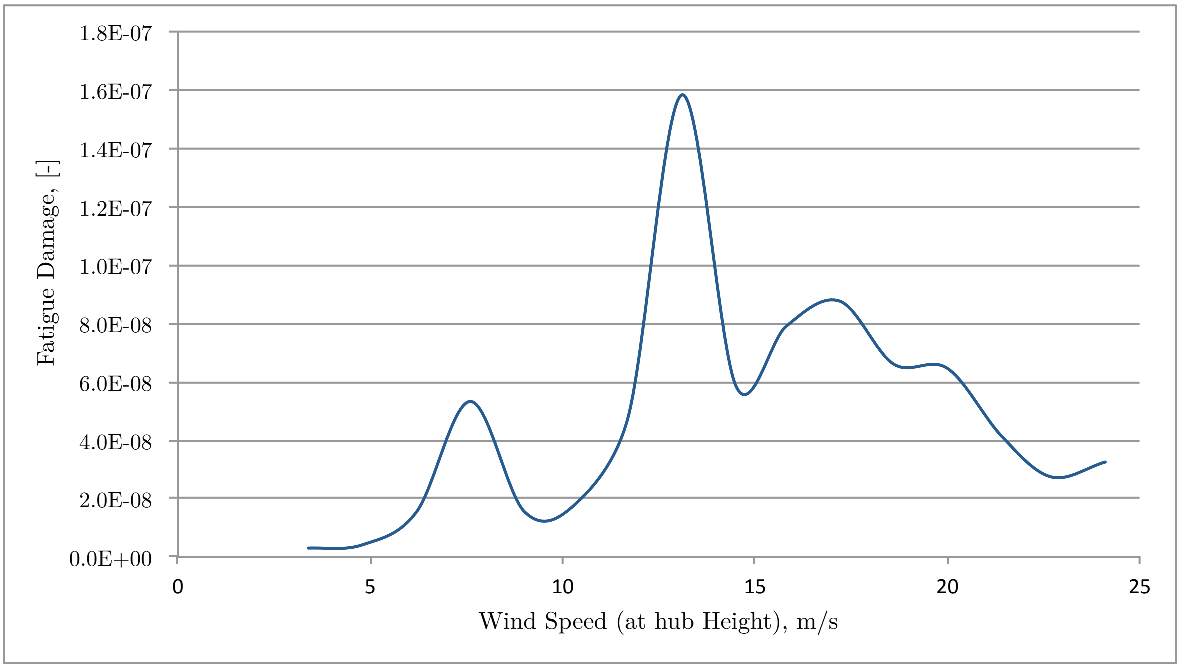

Figure 3-15: Hub Height Wind Speed vs. Fatigue Damage in Spar Cap at 11.8 m

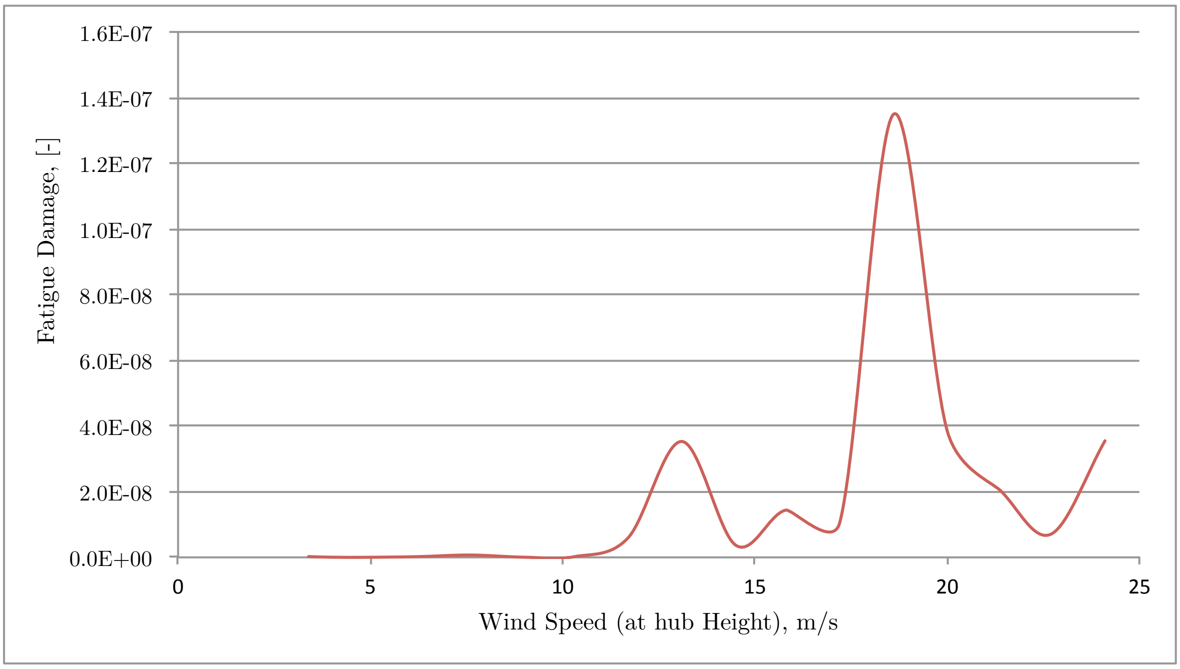

Figure 3-16: Hub Height Wind Speed vs. Fatigue Damage in Spar Cap at 44.5 m

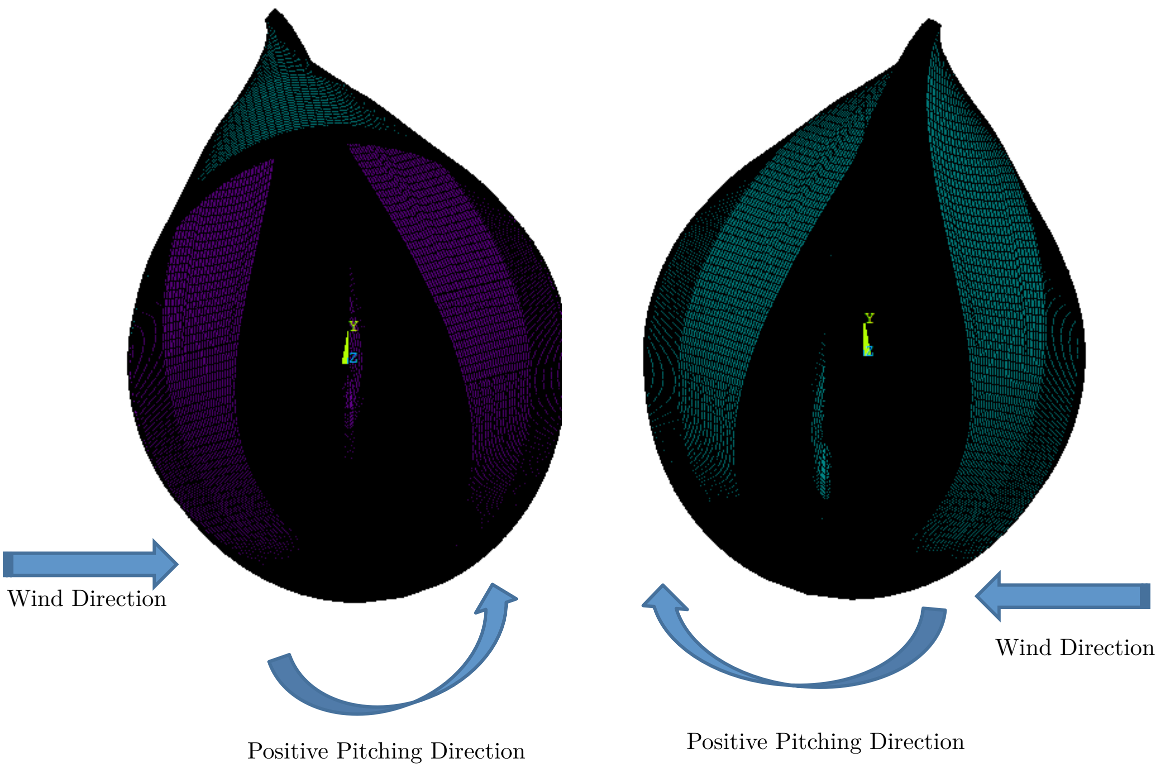

Figure 3-17: Blade View from Root (left) and Tip (Right)

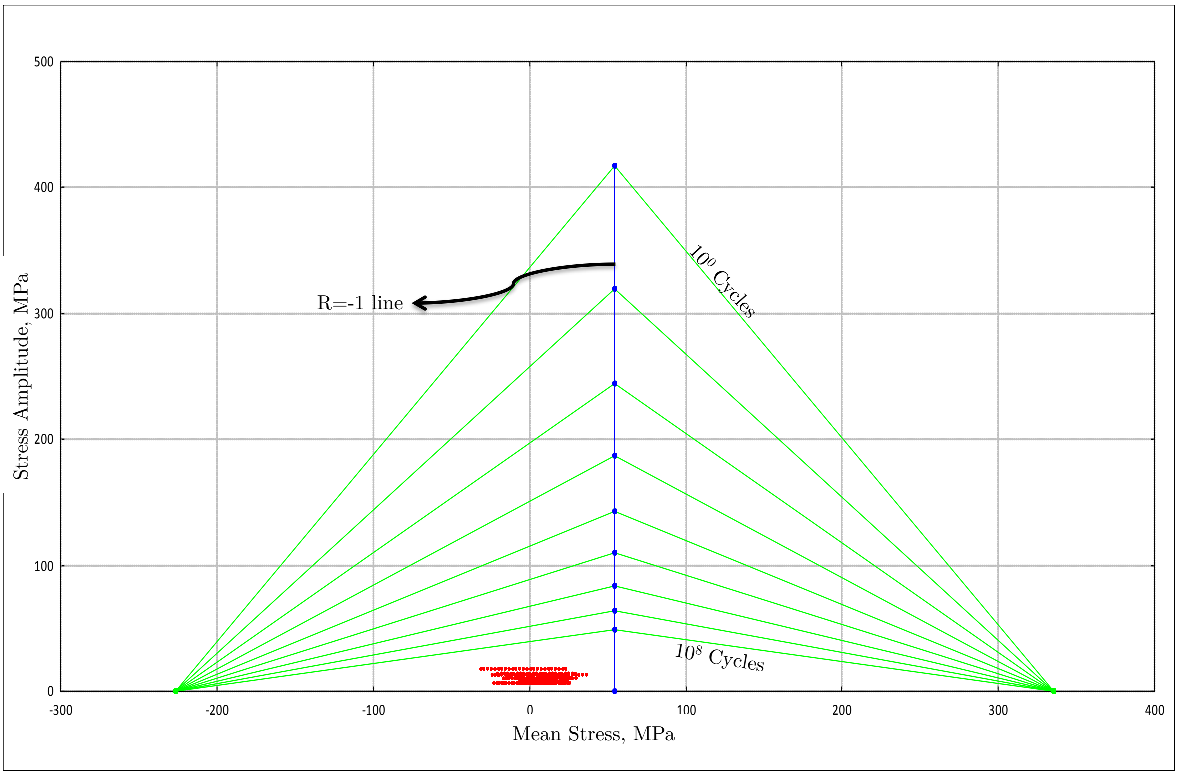

Figure 3-18: Shifted Linear Goodman Diagram Plot for Blade 1: Spar Cap

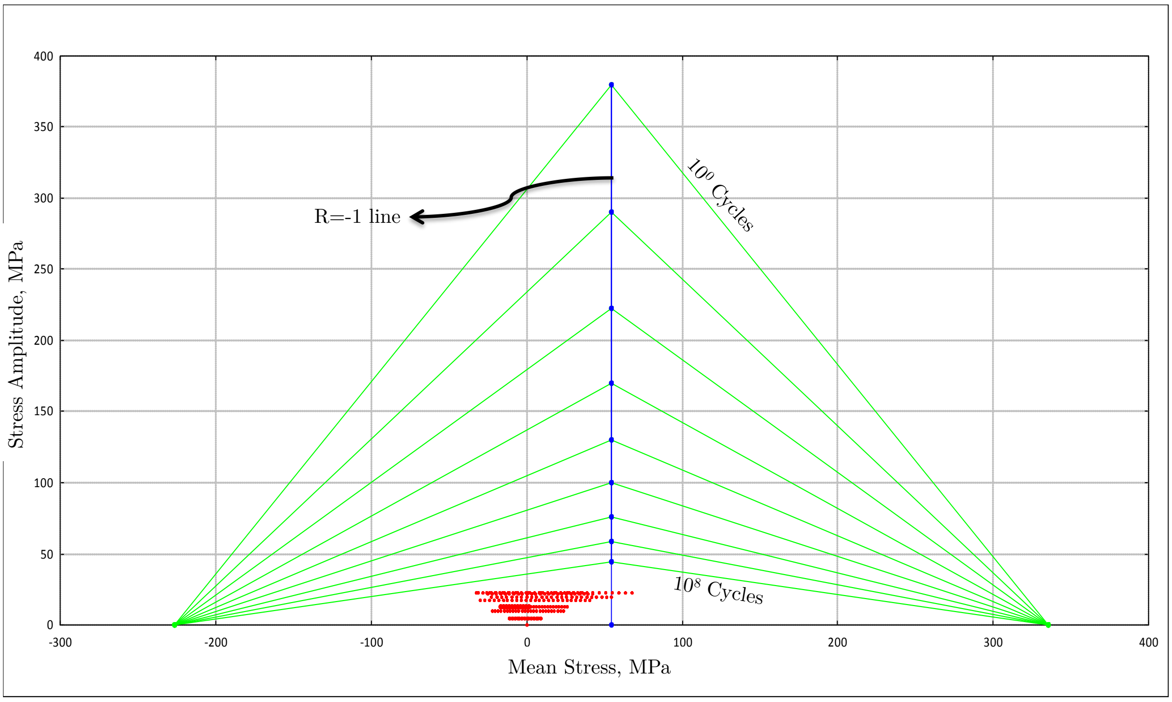

Figure 3-19: Shifted Linear Goodman Diagram Plot for Blade 1: Trailing Edge Tape

Table 3-10: Yaw Error Effect on Spar Caps: Comparison to Benchmark Case (% change)

		5°, 0° and -5° Yaw Error			10°, 0° and -10° Yaw Error		
Span	Radial Span, m	Blade 1	Blade 2	Blade 3	Blade 1	Blade 2	Blade 3
1	2.80	-0.10	2.50	-40.1	27.6	-11.1	-3.60
2	5.60	-14.4	-35.2	27.30	6.100	-32.0	13.90
3	8.40	-25.0	-21.3	-18.3	14.60	-31.1	35.7
4	11.8	-4.70	-0.90	-6.70	-14.8	-4.30	8.30
5	15.9	-11.3	12.30	-16.9	-6.80	33.50	-17.9
6	28.2	-2.90	1.20	-37.8	10.20	-7.10	-34.9
7	36.4	6.00	-5.50	-56.0	29.70	104.0	-24.6
8	44.5	14.30	-11.2	-25.4	2.500	21.60	30.5
9	56.2	-42.3	-25.3	50.50	-53.20	4.60	12.70

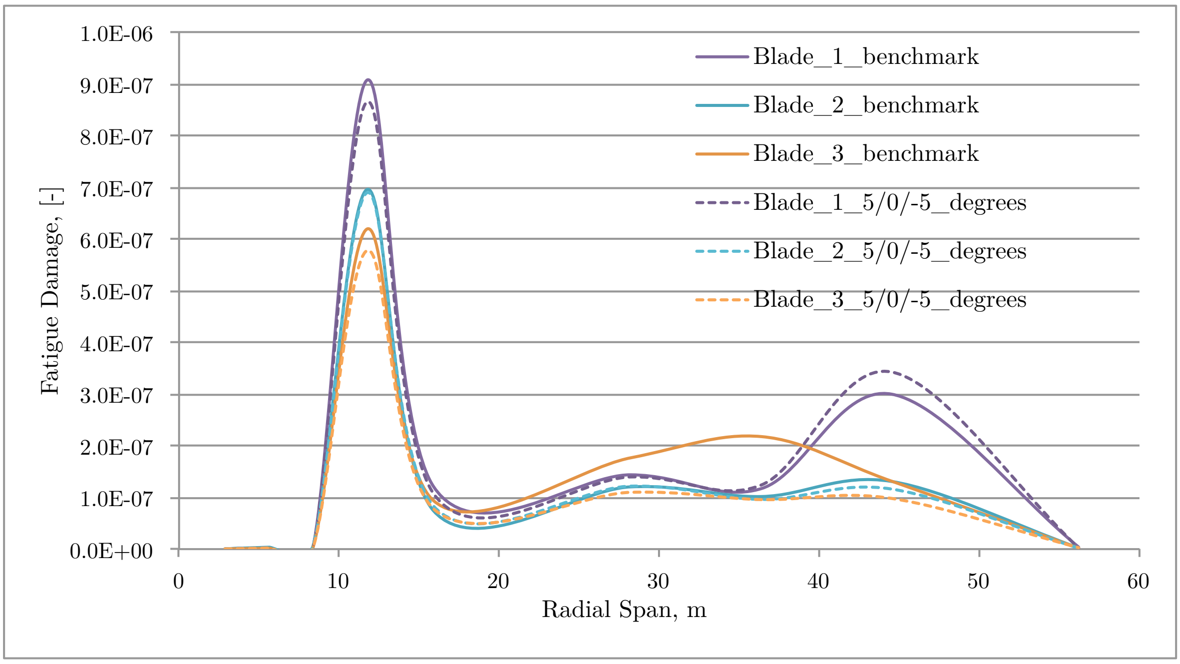

Figure 3-20: Spar Cap Fatigue Damage: Comparison of 5, 0 and -5 Degrees Yaw Error with Benchmark Case

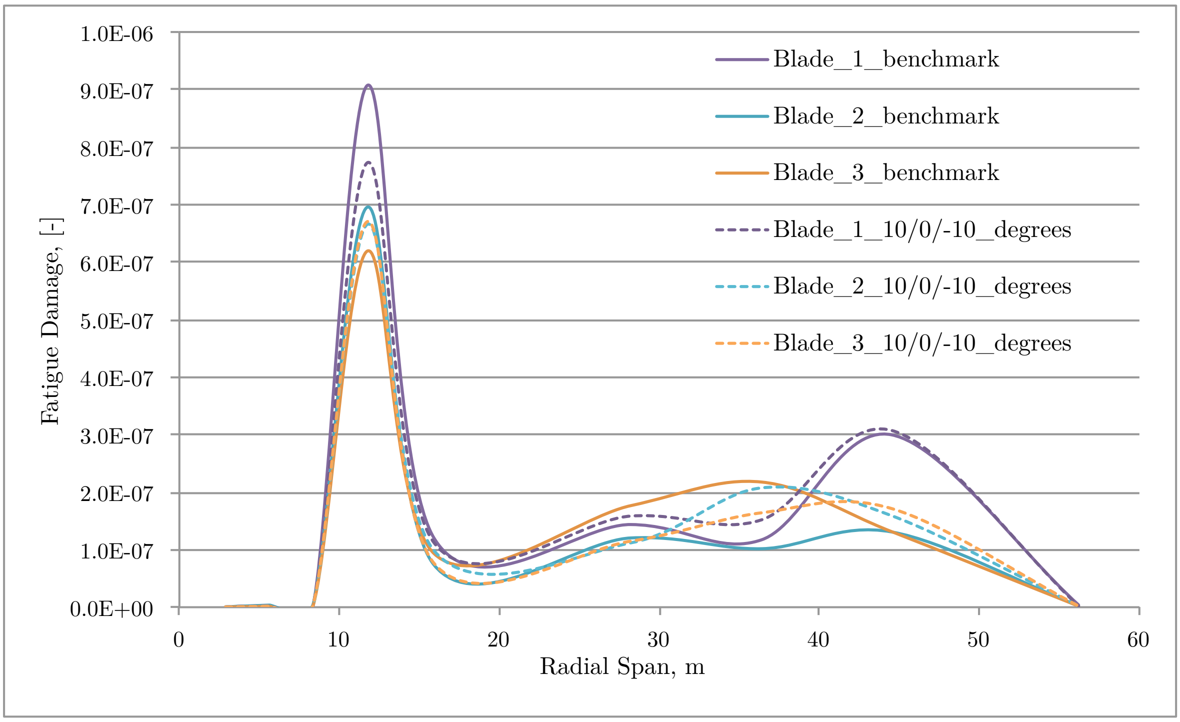

Figure 3-21: Spar Cap Fatigue Damage: Comparison of 10, 0 and -10 Degrees Yaw Error with Benchmark Case

Table 3-11: Rotor Mass Imbalance Effect on Trailing Edge Tape:: Comparison to Benchmark Case (% change)

		0, 0, 0 % Mass Imbalance			**5, 0, -5 % Mass Imbalance**		
Span	Radial Span, m	Blade 1	Blade 2	Blade 3	Blade 1	Blade 2	Blade 3
1	2.80	-17.5	-10.5	6.50	13.60	-9.70	-14.3
2	5.60	-18.5	-5.80	37.90	9.80	-14.3	14.40
3	8.40	-5.40	19.40	34.70	14.60	12.70	-2.80
4	11.8	-29.9	16.40	22.80	-6.60	-6.30	8.40
5	15.9	1.70	14.70	7.70	-7.60	-13.20	-4.30
6	28.2	-27.60	10.60	-0.80	5.50	-13.2	8.20
7	36.4	-3.60	27.10	84.70	2.30	-1.20	23.20
8	44.5	-29.8	23.70	-61.7	25.60	-19.2	-43.9
9	56.2	-N.A.-	-N.A.-	-N.A.-	-N.A.-	-N.A.-	-N.A.-

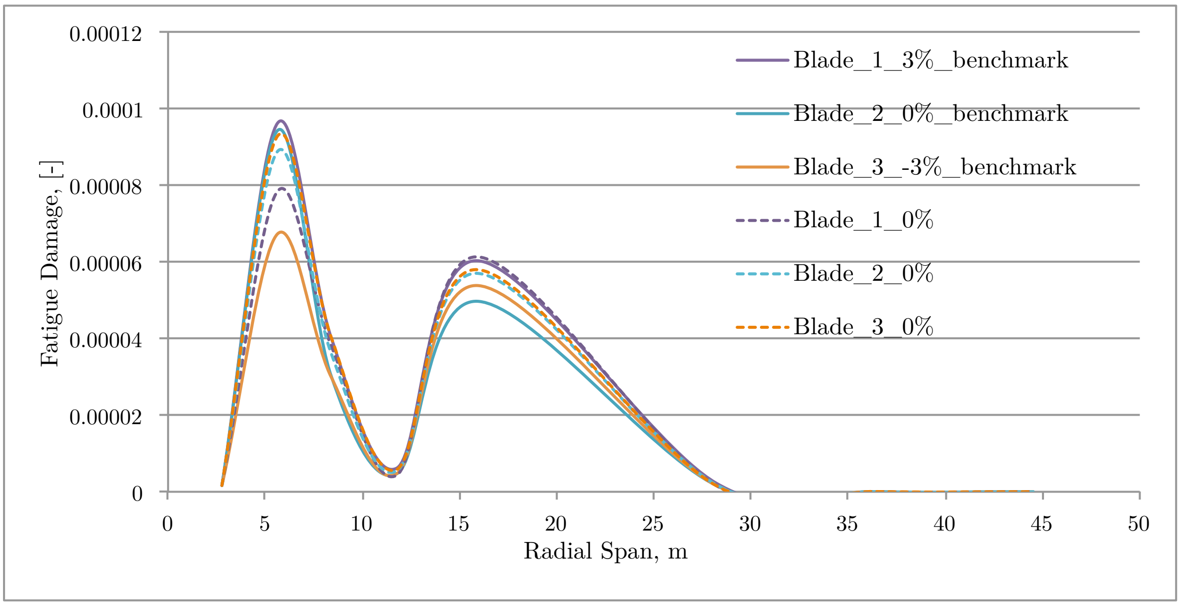

Figure 3-22: Trailing Edge Tape Fatigue Damage: Comparison of 0, 0 and 0 % Blade Mass Imbalance with Benchmark Case

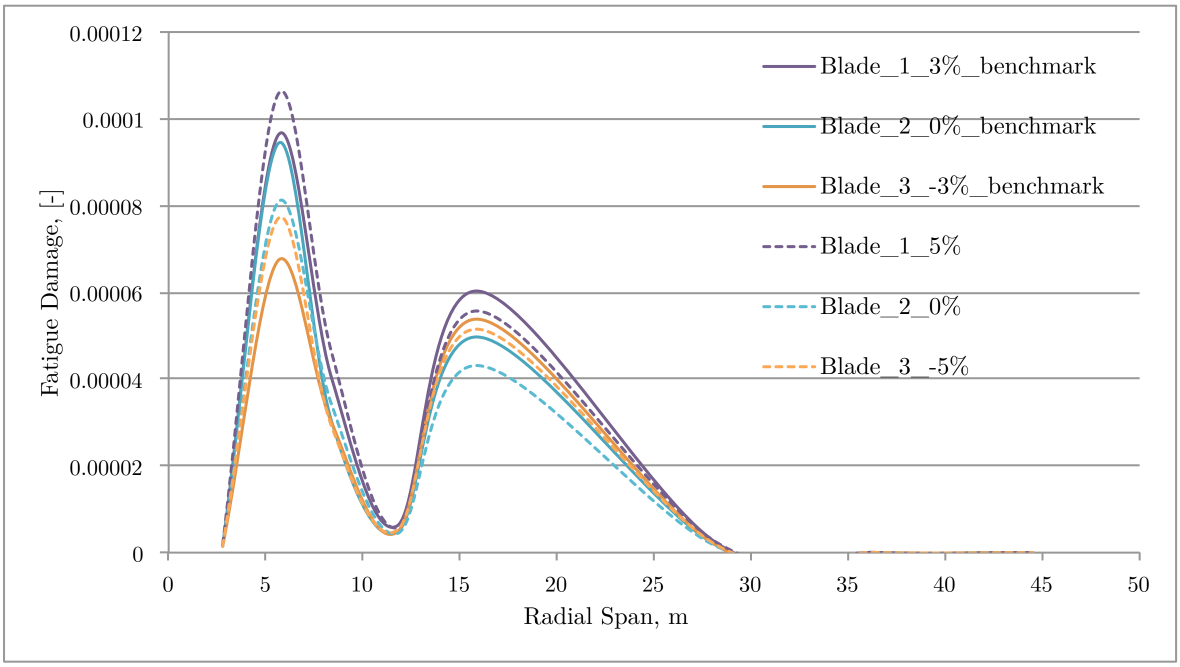

Figure 3-23: Trailing Edge Tape Fatigue Damage: Comparison of 5, 0 and -5 % Blade Mass Imbalances with Benchmark Case

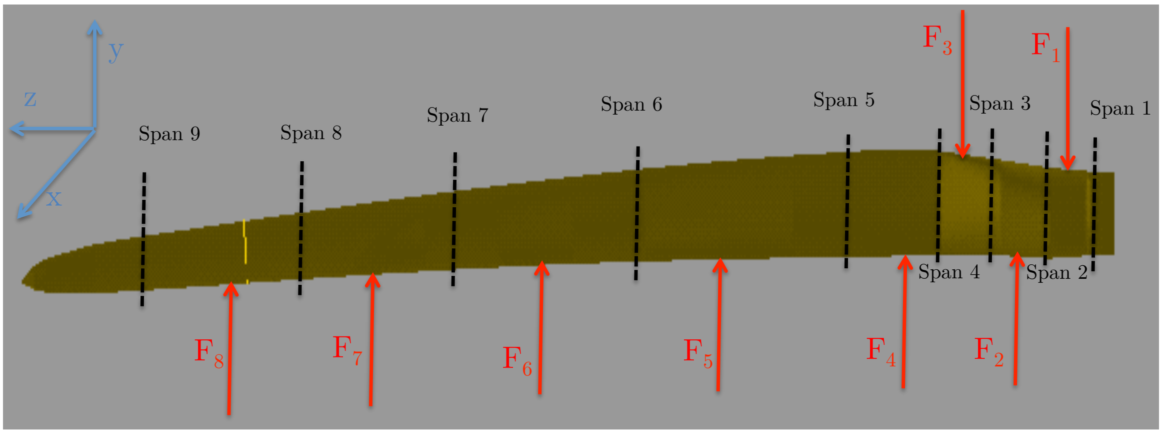

Figure 3-24: Portrayal of Edgewise Damage Equivalent Load for Trailing Edge Tape

Table 3-12: Damage Equivalent Load: Edgewise Loading in Trailing Edge Tape

Span	Radial Span, m	Load Application: Distance Along the Blade, m	Edgewise Damage Equivalent Load, kN
1	2.82	4.23	-798.6
2	5.63	7.01	459.6
3	8.38	10.07	-135.0
4	11.76	13.83	78.57
5	15.90	22.05	12.59
6	28.20	32.30	47.20
7	36.39	40.46	2.72
8	44.52	22.26	32.55

Chapter 4

Conclusions and Recommendations

4-1 Critical Deflection

Due to the presence of considerable amount of cone angle, shaft tilt, overhang and flap-wise stiffness, it can be concluded that the design is safe from blade-tower interference.

4-2 Buckling

Structural modifications to avoid buckling are the use of sandwich material, and/or more shear webs. These modifications lead to an increased complexity of the manufacturing process and of the buckling strength predictions. The buckling of wind turbine rotor blades is characterized by a strongly varying load direction (sectional bending moments) and by the strong variation/difference in material layup within a cross section.

A rotor blade is a slender construction and is typically designed to be able to absorb very large deflections. This means that the shell on the compression side will be subjected to very high in-plane compression stress and thus the local buckling failure mode and the general buckling failure mode will govern the design of the shell components. It follows that the most efficient way to design a sandwich construction against local and general buckling is to increase core thickness and core density. With rotor blades becoming longer but not necessarily wider, the level of in-plane loading will increase and as a result the proportion of core material used is likely to be much greater.

Based on loading criticality for buckling following conclusions are observed:

- Flapwise loads are, by far, the most dominant load as far as buckling is concerned.
- First mode of buckling occurs in trailing edge tape, and hence, is most critical in this design.
- Axial loads have a marginal effect in stabilizing buckling loads in flapwise direction.
- If the blade was just loaded in extreme edgewise and axial condition, it would be safe from buckling failure.
- Buckling load factors in case of edgewise loading are three times more; w.r.t buckling load factors of flapwise loading.
- Finally, it should be considered to increase the length of trailing edge tape close to the tip (beyond 45 m) , thus, stiffening the suction side of trailing edge.

4-3 Static Strength

Ultimate strength of 112 MPa is not enough for shear webs to sustain the static loads. Hence they need to be strengthened atleast near the transition region (change from circular to DU airfoils). Further in-depth analysis must be performed with even more accurate material properties for bi-axial, triaxial and core materials.

Moreover, foam core was neglected in the static strength analysis, but in reality there can be failures in blades caused by reduced strength and stiffness of foam materials and hence their accurate material properties are of much importance.

4-4 Modal Analysis

From the modal analysis, it can be concluded that blade would not undergo resonance under the operating range considering 1P and 3P excitations. More in-depth analysis should be conducted with full wind turbine model (and not just the blade) to obtain precise values of different eigen frequencies including coupling effects between blades and tower.

4-5 Fatigue

From the results obtained on fatigue, it can be concluded that trailing edge tape is more critical in terms of fatigue than spar caps. While trailing edge tape is more effected by mass imbalance in rotor, yaw errors have a major influence on damage value of spar caps.

Also, positive yaw errors have a considerable (majority) share in damage values calculated via Miner sum rule. In terms of load case operations, start up and shutdown cases were found to have negligible amount of contribution to overall damage of blade.

Moreover, it is observed that the maximum fatigue damage in spar caps occur at 20 % of blade span ($\approx$ 10 m) where as for trailing edge tape this occurs at 25 % of blade span ($\approx$ 15 m).

The fatigue analysis was done more in the purview of qualitative understanding of different parameters than to specifically certify or design a blade. Following considerations must be understood before concluding anything about the actual quantitative damage values:

- The damage values represented in this study are representative only of a particular wind site. As the wind conditions change (from onshore to offshore, from plains to mountainous, from low turbulence to high turbulence regions etc.), the fatigue analysis has to be performed again to evaluate its criticality.

- Operations such as icing and heavy leading edge erosion could impact blade fatigue in a significant way and hence should be considered in future, along with the general selection of load cases considered in this project.

- Fatigue damage in bondlines and root joints can be more critical than what is considered here. Hence, this should be taken as a future work to have a better clarity.

- Manufacturing considerations (infusion, curing, layup, fibre-alignments etc.) play a crucial role in determining the final product and hence its structural fatigue properties (although to a certain extent, have been incorporated with the help of safety factors).

- Material properties of 'coupons' and laminate specimen are used for the entire full-scale blade. This blade has different thickness, different temperature effects and different composition at different parts (like adhesives, for example have a different failure mechanism than, say, core material or fibres) due to which the fatigue might be critical at certain other areas as well. The present analysis just looks into spar caps and trailing edge tape.

- Fatigue damage might be significantly impacted by torsional loads which have been out of scope of this study.

- Uniformity in mass imbalance is hard to get in reality (as considered for this project). This may be due to higher resin content during manufacturing. The actual mass imbalance that happens is mostly from blocked water drainage holes. In this scenario, something like 10 - 50 litres of water are trapped at the blade tip. The effect of that could be much more dramatic than a uniform mass difference.

Finally, it can be concluded that, as blades are becoming larger and slender, stiffness is driving the design of a wind turbine rotor and not the strength.

Appendix A
Blade Coordinate System

Important Notes on Coordinate System and its Impications

- x'-y' is the axes system in which *sectional blade* loads have been calculated in *'FAST'*. This is directed along the local principal axes of the blade section. z' axis is along the pitch axis and is out of plane of paper as depicted in Figure A-1. This is for *anticlockwise orientation* of rotor blade.

- x'-y'-z' system of axes for anticlockwise orientation of blade (loads would would be calculated about these axes in 'FAST', IF it were to model an anticlockwise orientated blade: See bullet point 6) pitches and orients itself along the deflected blade.

- Terminology Used:
  - Local Bending Moment about y' axis: **Flapwise Bending Moment** (local out-of-plane bending moment); x' is the flapwise direction.
  - Local Bending Moment about x' axis: **Edgewise Bending Moment** (local in-plane bending moment); y' is the edgewise direction.

- x-y-z is the *Blade Root Coordinate System* (depicted in Figure A-1) such that:
  - Origin is the intersection of the blade pitch axis and the blade root.
  - It rotates and pitches with the blade.
  - x-axis points in the downwind direction and orthogonal to y and z axis forming right hand coordinate system.
  - y-axis points towards the trailing edge of blade and parallel with the chord line at the zero-twist blade station (i.e. tip)
  - z-axis points towards along the pitch axis towards the tip of blade.

- ANSYS x and y axis are just OPPOSITE to the one depicted here for Blade coordinate system. z axis still points along the pitch axis.

- The Blade used in ANSYS for analysis is of *Anticlockwise Orientation* and FAST calculates loads only for clockwise orientation of blade. Hence, to model anticlockwise spinning rotor in FAST, it is required to change the signs of some of the output after modeling it as a clockwise spinning rotor. The relationship between the loads output by FAST and the loads in the x'-y'-z' coordinate system for the local blade loads at station i of blade 1 are:

  - Force directed along x' for a counterclockwise rotor = Spn(i)FLxb1 from FAST for a clockwise rotor.
  - Force directed along y' for a counterclockwise rotor = -Spn(i)FLyb1 from FAST for a clockwise rotor.
  - Force directed along z' for a counterclockwise rotor = Spn(i)Flzb1 from FAST for a clockwise rotor.
  - Moment about x' for a counterclockwise rotor = -Spn(i)MLxb1 from FAST for a clockwise rotor.

- Moment about y' for a counterclockwise rotor = Spn(i)MLyb1 from FAST for a clockwise rotor.
- Moment about z' for a counterclockwise rotor = Spn(i)MLzb1 from FAST for a clockwise rotor.

It is to be noted here that Spn(i)FLxb1, Spn(i)FLyb1, Spn(i)FLzb1, Spn(i)MLxb1, Spn(i)MLyb1 and Spn(i)MLzb1 are span i^{th} flapwise shear force, edgewise shear force, axial force, edgewise bending moment, flapwise bending moment and torsional moment respectively.

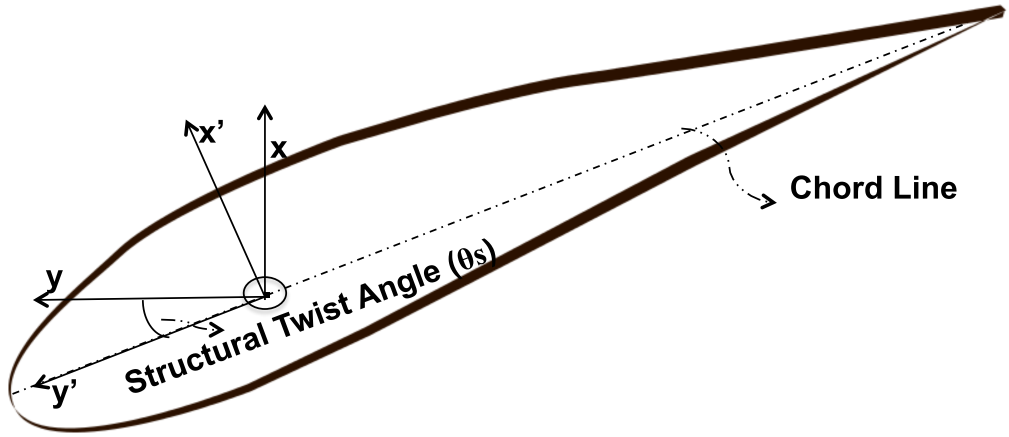

(a) Local Blade Section Principal Axes Orientation

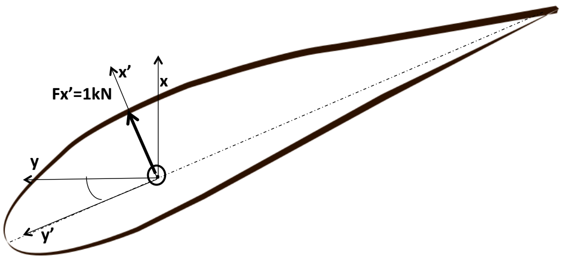

(b) Orientation of Force for Flapwise Bending Moment

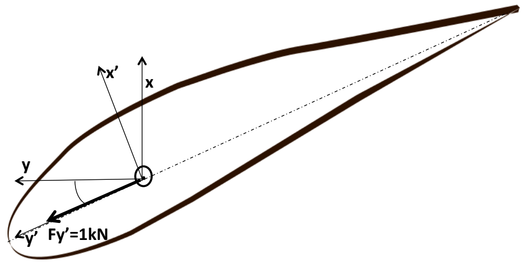

(c) Orientation of Force for Edgewise Bending Moment

Figure A-1: Blade Root Coordinate System (x-y-z) vs. Blade Section Coordinate System (x'-y'-z') Used in Measurement of Loads (Bending Moments and Forces)

Important Note: Force of 1 kN as depicted in Figure A-1(b) and A-1(c), when acting a distance of 1 m from the cross section of the blade to be 'analyzed', produces a flapwise and edgewise bending moment of +1 kN-m respectively in x'-y'-z' axis system. Now, as the composite material are operated under linear limit of force (moment)-stress relationship and considering geometric linearity of blade (to be discussed later); if +1kN-m produce 'a' MPa stress in blade span direction, x kN-m would produce '$a.x$' MPa stress. Hence, keeping in mind this linear scaling and the above consideration of clockwise vs. anticlockwise spinning rotor, time series of blade moments from FAST can be transformed, to arrive at the correct time series of stress (to be used for fatigue calculations). Hence, all the 'linear stress factors'

(a) due to flapwise and edgewise bending moment would be calculated in this way. Non-linear effects would be discussed in later sections of fatigue analysis. Also to be kept in mind is, the structural twist value in Figure A-1 is of the 'analyzed' section and not for the section where the force acts.

Shear Center and its Importance in Wind Turbine Blades The force in the finite element (FE) model of blade, acts at the shear center of the chosen section. Let us briefly look into why this is actually done and what are its implications. Before that, lets look into some important definitions:

- Shear Center: Location in the blade cross section where if one applies a shear load, there will be no torsion.
- Tension Center: Location in the blade cross section where the bending axes cross; a normal force applied at the tension center will not cause any bending.
- Mass Center: Center of mass location of the cross section.
- Aerodynamic Center: Location in the cross section where the specified airfoil lift, drag, and pitching moment coefficients are defined. Lift and drag forces of the whole cross-section is supposed to act through this point.
- Elastic Axis: Loci of shear centers.

Centrifugal and all other inertial forces (gravitational, gyroscopic, coriolis) are calculated at the center of mass and when there is an offset between mass center and tension center, there is a bending moment associated with it (otherwise not). Similarly all the aerodynamic forces are calculated at aerodynamic center and when there is an offset between aerodynamic and shear center there is a torsion (and a bending moment, which changes every time with angle of attack and is present due to offset between aerodynamic center and tension center) associated with it.

The present version of FAST [8] assumes an initially straight blade made up of an isotropic material with no offsets of mass, shear, or tension center from the pitch axis. The local blade loads output from FAST are reaction loads at nodes on this axis. Aerodynamic center is offset from pitch axis by aerodynamic center - 0.25 (fractional offset along the chord line, positive towards trailing edge). This is due to the fact that pitch axis passes through 25 % chord at each airfoil cross-section.

Typically, the shear center is of greater importance to large utility-scale wind turbines than the tension center due to the low rotational speed. With low rotational speed, the centrifugal forces will be small. When the centrifugal forces are small and the aerodynamic forces are the large, the bending moment caused by centrifugal forces and the lateral offset between the tension center and mass center will be less important than the bending and torsion moments caused by the aerodynamic forces and the lateral offset between the aerodynamic center and shear center.

Hence it makes more sense to apply loads output from FAST at the shear center of the FE model. However, if blade has large deviations of the mass, shear, or tension center from the pitch axis, than the present version of FAST may not be accurate for computing the system's response.

To sum up following effects are 'neglected' in this process:

- The bending moment associated with centrifugal forces, due to no offset between mass center and tension in FAST.
- Torsion (twisting moment about shear centers) associated with aerodynamic forces, (acting at aerodynamic center) due to application of force at shear center.
- Delta bending moment (about tension center) associated with aerodynamic forces, due to application of force at shear center.

All these neglected items are in purview of a particular cross-section of blade.

Appendix B

B-1 Blade Distributed Properties

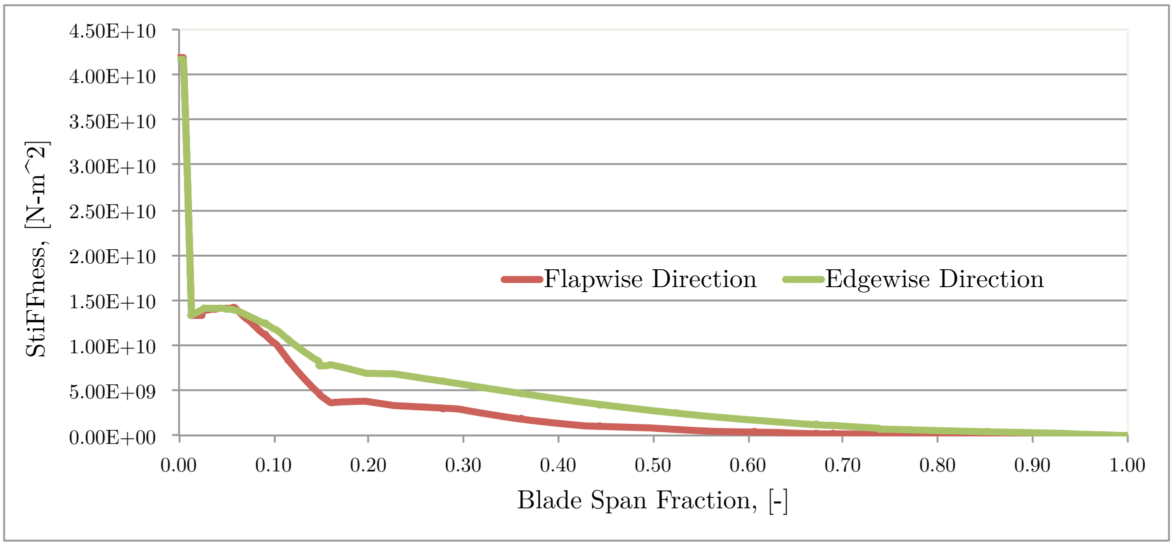

Figure B-1: Blade Flapwise and Edgewise Stiffness Along Different Section

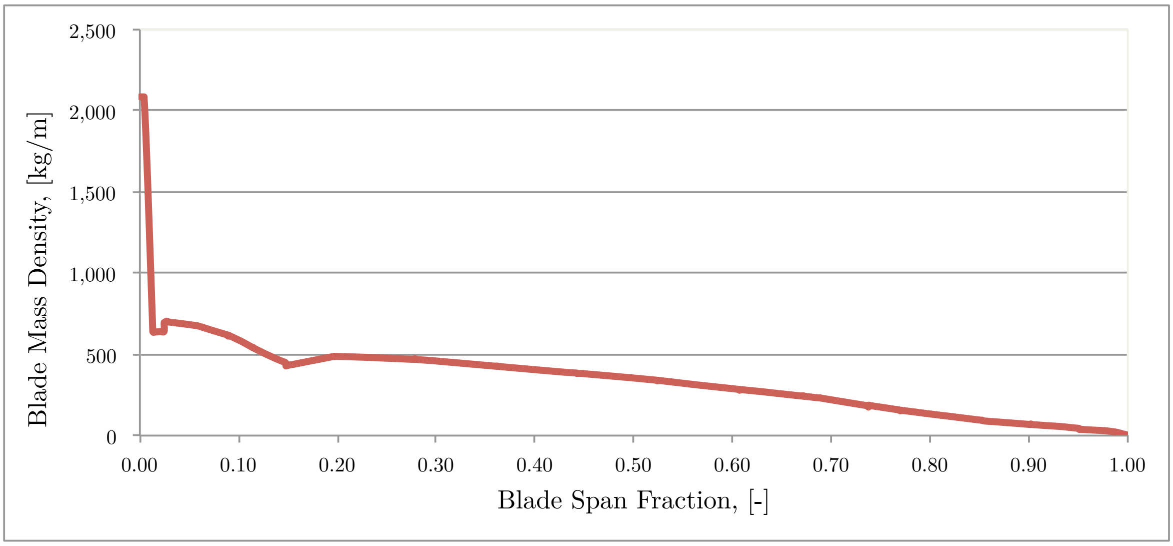

Figure B-2: Blade Mass Density Along Different Section

B-2 Multiblades Modes in a Wind Turbine System

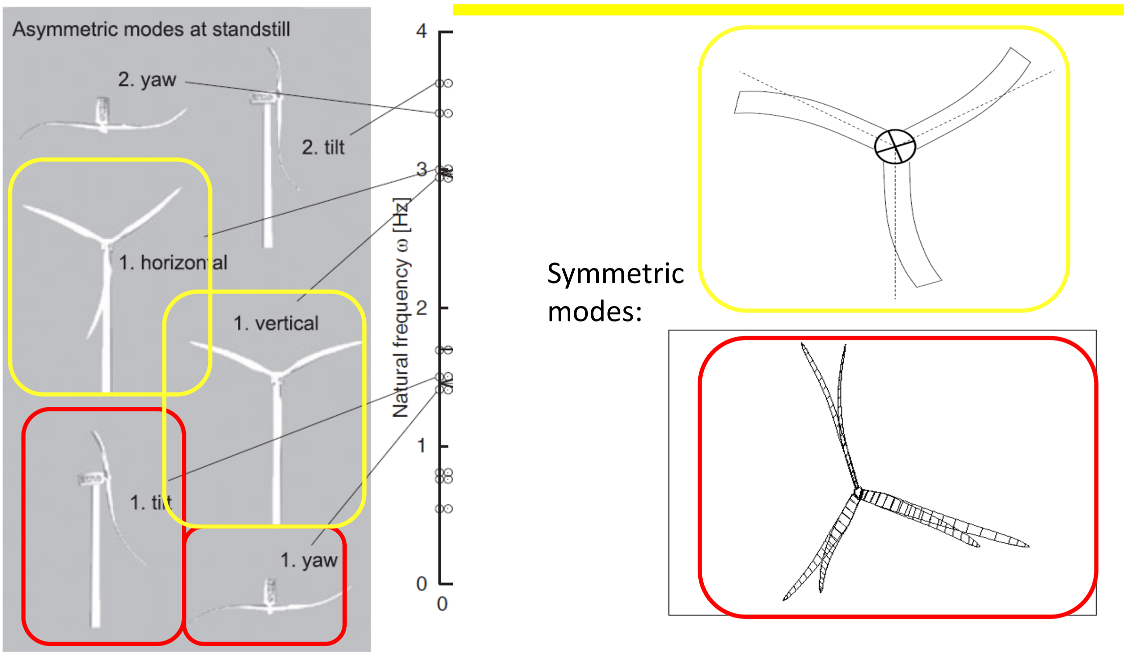

Figure B-3: Multiblades Modes [2]

B-3 Octave Code

Fatigue Damage Calculation

```
% This script predicts the damage parameter according to
% the methods described in report
% "Benchmark of Lifetime Prediction Methodologies OB_TG1_R012 rev. 001 doc.
% no. 10218" (Optimat Blades) by Nijssen, Krause, Philippidis (2004) based
% on measured load data. It basically calculates fatigue damage for different load cases
% in wind turbine operation considering yaw errors and a specific part of blade.
% Program written by Neelabh Gupta, 2013-04-01 (courtesy Roman Braun and Oliver Kranke)

clear all;
close all;
clc;
```

```
% -------------------------------------------------------------------------
% There are different Diagram types available for calculation
% which should be chosen for your calculation:
    % enter "LGD" for Linear Goodman Diagram
    % enter "sLGD" for shifted Linear Goodman Diagram
    % enter "CLD" for Constant Life Diagram with R=-1, 10, 0.1;
      method = 'sLGD'; %enter your input

 % Which part of Blade is to be analysed?
            % Enter 'SC' for Spar Cap
            % Enter 'TE' for Trailing Edge Tape
      part='SC';      % Default

 % In what form Fatigue Damage results are required?
            % Enter 1 for Complete 9*3 Damage matrix which incorporates
               all yaw erros, all the loading (flap, edge, axial),3
               loadcase opearions (power production, startup and shutdown
               ) across all the 9 spans in 3 blades.
            % Enter 2 for observing the effect of power production, start
               up and shutdown opetation separately.
            % Enter 3 for observ6ing the effec of yaw errors in power
               prodcution load case operation

      option=1;
% -------------------------------------------------------------------------
% Material properties
% -------------------------------------------------------------------------
% Measured S-N-curves: S_a = K * N ^ b    (b = -0.xxx...)
% 95/95 confidence fatigue properties
% b is the slope parameter from linear regression
% K is the intercept parameter from linear regression
obj.R_ct = -1;
obj.r_ct = (1 + obj.R_ct) / (1 - obj.R_ct);
obj.b_ct = -0.1161;
obj.K_ct = 797.99 * (1-obj.R_ct)/2; % given value and transfer factor
   from maximum
                                % stress to stress amplitude dependent
                                % S-N-curve [N/mm^2]
obj.R_tt = 0.1;
obj.r_tt = (1 + obj.R_tt) / (1 - obj.R_tt);
obj.b_tt = -0.1023;
obj.K_tt = 1086.37 * (1-obj.R_tt)/2; % given value and transfer factor
   from maximum
                               % stress to stress amplitude dependent
                               % S-N-curve [N/mm^2]
obj.R_cc = 10;
obj.r_cc = (1 + obj.R_cc) / (1 - obj.R_cc);
```

```
obj.b_cc = -0.0108;
obj.K_cc = 439.94 * -(1-obj.R_cc)/(2*obj.R_cc); % given value and transfer factor from
                                                % minimum stress to stress amplitude
                                                % dependent S-N-curve [N/mm^2]
% 95% confidence static properties of mean value
obj.UCS = 499.62;  % ultimate compressive strength, MPa
obj.UTS = 739.77;  % ultimate tensile strength, MPa
obj.dim = 'stress';       % Dimmension of Ordniate in SN-Diagram  ('stress' or 'strain')

%Partial Safety factors for material (for Shifted Linear Diagram Calculations ONLY)
%obj.ma=1.0;
obj.ma=1.35*1.35*1.1*1.1*1.0; %Partial safety factor for short term strength verification (GL-2010, Page 5-20)
if (part=='SC')
%obj.mb=1.0;
obj.mb=1.35*1.1*1.0*1.0*1.0; %Partial safety factor for fatigue verification: Spar cap (GL-2010, Page 5-20)
else
%obj.mb=1.0;
obj.mb=1.35*1.1*1.0*1.0*1.1; %Partial safety factor for fatigue verification: Trailing Edge (GL-2010, Page 5-20)
end

% Represent the constant life lines in Diagram
%obj.cycles = [1; 10^1; 10^2; 10^3; 10^4; 10^5; 10^6; 10^7; 10^8];
obj.cycles = [10^0; 10^1; 10^2; 10^3; 10^4; 10^5; 10^6; 10^7; 10^8];
%--------------------------------------------------------------------------------
if (part=='TE')
    Stress_Factor=load('Stress_Factor_t_e_tape.txt');
else
    Stress_Factor=load('Stress_Factor_s_cap.txt');
end

loadcase_hours = load('loadcase_hours.txt');

% All major functions are called from here
addpath('E:\The Stuffs\Thesis\Fatigue_Runs\Octave_function_2D')

if (option==1)

    option
    part
    method
[N1, D1]=Powerproduction_Damage(obj,method,Stress_Factor,loadcase_hours);
[N2, D2]=Startup_Damage(obj,method,Stress_Factor,loadcase_hours);
[N3, D3]=Shutdown_Damage(obj,method,Stress_Factor,loadcase_hours);

```

```
% IMP!!!! Calculate D1(power production), D2 (startup) and D3 (shutdown)
    and sum them up for D_final to be put below: D_final is 9x3 matrix
D_final=D1+D2+D3;

elseif (option==2)
     option
     part
     method
[N1, D1]=Powerproduction_Damage(obj,method,Stress_Factor,loadcase_hours);
[N2, D2]=Startup_Damage(obj,method,Stress_Factor,loadcase_hours);
[N3, D3]=Shutdown_Damage(obj,method,Stress_Factor,loadcase_hours);

% IMP!!!! Calculate D1(power production), D2 (startup) and D3 (shutdown)
    and sum them up for D_final to be put below: D_final is 9x3 matrix
D_final=D1+D2+D3;
D1=(D1./D_final)*100
D2=(D2./D_final)*100
D3=(D3./D_final)*100

else
     option
     part
     method
[N, D1, D2, D3]=Yaw_Error_Effect (obj,method,Stress_Factor,loadcase_hours
    );

D1
D2
D3

Yaw_zero_contribution=(D1./(D1+D2+D3))*100;
Yaw_positive_contribution=(D2./(D1+D2+D3))*100;
Yaw_negative_contribution=(D3./(D1+D2+D3))*100;

end % if condition of option ends here!


     %Create the diagram

   if (strcmpi(method, 'LGD'))

     [s_a, s_m] = LGD_plot (obj, eps_a_vec, eps_m_vec, n_matrix);
   elseif(strcmpi(method, 'sLGD'))

     [s_a, s_m] = shifted_LGD_plot (obj, eps_a_vec, eps_m_vec, n_matrix);
   elseif(strcmpi(method, 'CLD'))

     [s_a, s_m] = CLD_plot (obj, eps_a_vec, eps_m_vec, n_matrix);

   end
```

Bibliography

[1] P. Sharma, "Wind Energy: Renewable energy harnesses natural wind power," goo.gl/REAu2, 2008, [Online; accessed 16-June-2013].

[2] M. Hansen, "Aeroelastic instability problems for wind turbines," *Wind Energy*, vol. 1, p. 27, 2007.

[3] Wikipedia, "Renewable energy," http://en.wikipedia.org/wiki/Renewable_energy, 2013, [Online; accessed 26-May-2013].

[4] *WindTurbines- Part 1: Design Requirements*, IEC, Geneva, Switzerland Std. IEC 61 400-1, Rev. Edition 3.

[5] M. Rosemeier, "Non-linear ultimate limit state analysis of a wind turbine blade," Master's thesis, Denmark Technical University (DTU), 2013.

[6] D. J. Laino and A. C. Hansen, "User's guide to the wind turbine aerodynamics computer software aerodyn," Windward Engineering, LC, Tech. Rep., 2002.

[7] B. Jonkman, "Turbsim user's guide version 1.50," National Renewable Energy Laboratory (NREL), Tech. Rep., 2009.

[8] J. M. Jonkman and M. L. B. Jr., "Fast user's guide," National Renewable Energy Laboratory (NREL), Tech. Rep., 2005.

[9] N. Gupta, M. Strach, and A. Antoniou, "Loads analysis of the nrel 5-mw reference turbine for an onshore site," internship report as a part of fulfilment of MSc. in TU Delft, 2012.

[10] F. Vorpahl and A. Reuter, "Fully-coupled wind turbine simulation including substructuring of support structure components: Influence of newly developed modeling approach on fatigue loads for an offshore wind turbine on a tripod support structure," in *Proceedings of the Twenty-first (2011) International Offshore and Polar Engineering Conference*, 2011.

[11] R. Nijssen, "Fatigue life prediction and strength degradation of wind turbine rotor blade composites," Ph.D. dissertation, TU Delft, 2006.

[12] Nijssen, "Wmc 5 mw laminate lay-out of reference blade for wp 3," Knowledge Centre Wind turbine Materials and Constructions, Tech. Rep., 2007.

[13] T. P. Philippidis, A. E. Antoniou, T. A. Vaggelis, and A. Passipoularidis, "Static tests on the standard ob ud and md off-axis coupons main test phase 1," University of Patras, TU Delft, DLR, CRES, VUB, ECN, Tech. Rep. Optimat Blades TG 2, 2005.

[14] T. P. Philippidis, D. J. Lekou, and C. Baharoudis, "Assessment of failure probability under uni-axial and multi-axial static and fatigue load," University of Patras, TU Delft, DLR, CRES, VUB, ECN, Tech. Rep. Optimate Blades TG 2, 2006.

[15] *Guideline for the Certification of Wind Turbines*, Germanischer Lloyd (GL) Std., 2010.

[16] J. Jonkman, S. Butterfield, W. Musial, and G. Scott, "Definition of a 5-mw reference wind turbine for offshore system development," National Renewable Energy Laboratory (NREL), Tech. Rep., 2009.

[17] J. Manwell and J. McGowan, *Wind Energy Explained: Theory, Design and Application*, 2nd ed., A. Rogers, Ed. John Wiley and Sons, 2009.

[18] Ansys 14.0 help file. http://www.ansys.com.

[19] C. Lindenburg, "Programs for buckling strength prediction of rotor blades," Energy research Centre of the Netherlands, ECN, Tech. Rep., 1999.

[20] S. Miao, S. Donaldson, and E. Toubia, "Parametric study of sandwich panel buckling in composite wind turbine blades," Department of Civil and Environmental Engineering, University of Dayton, Tech. Rep., 2011.

[21] M. D. Banea and L. F. M. da Silva, Eds., *Adhesively bonded joints in composite materials: An overview*, Institution of Mechanical Engineers. Sage Publications, 2008.

[22] G. Schepers, W. Bierbooms, and J. Holierhoek. (2012) Strength and fatigue: Introduction to wind energy. Lecture Series in TU Eindhoven. ECN and TU Delft.

[23] A. Puck and H. Schuermann, "Failure analysi of frp laminates by means of physically based phenomenological models," *Elsevier*, vol. 1, p. 23, 1996.

[24] R. F. C. Jr., "High cycle tensile fatigue of unidirectional fiberglass composite tested at high frequency," Master's thesis, Montana State University, 1993.

[25] T. Westphal and R. Nijssen, Eds., *Blade Materials and Fatigue*, ser. TU Delft, no. Design and Manufacturing of Wind Turbine Rotor Blades. Knowledge Cnetre of WMC, 2012.

[26] J. Varandas. Gnu octave ver. 3.6.2. http://www.gnu.org/software/octave/.

[27] G. Freebury and W. Musial, "Determining equivalent damage loading for full-scale wind turbine blade fatigue tests," in *19th American Society of Mechanical Engineers (ASME) Wind Energy Symposium*. National Renewable Energy Laboratory (NREL), 2000.

[28] P. Ragan and L. Manuel, "Comparing estimates of wind turbine fatigue loads using time-domain and spectral methods," *Wind Engineering*, vol. 31, no. 2, p. 19, 2007.

Glossary

List of Acronyms

IEC	International Electro-technical Commission
FAST	Fatigue Aerodynamics Structural and Turbulence
GL	Germanischer Lloyd
DLC	Design Load Case/s
FE	Finite Element
FEA	Finite Element Analysis
FEM	Finite Element Model
DOF	Degree of Freedom
MPC	Multipoint Constraint
UD	Uni-Directional
DEL	Damage Equivalent Load
TE	Trailing Edge
SC	Spar Cap